NASA CR-152126

(NASA-CR-152126) A MACH LINE PANEL METHOD FOR COMPUTING THE LINEARIZED SUPERSONIC FLOW OVER PLANAR WINGS (Boeing Commercial Airplane Co., Seattle) 91 p HC A05/MF A01 CSCL 01A G3/02

N78-27087

Unclas 25873

A Mach Line Panel Method for Computing the Linearized Supersonic Flow Over Planar Wings

F. Edward Ehlers and Paul E. Rubbert

Boeing Commercial Airplane Company
Seattle, Washington

Prepared for
NASA Ames Research Center
under Contract NAS 2-7729

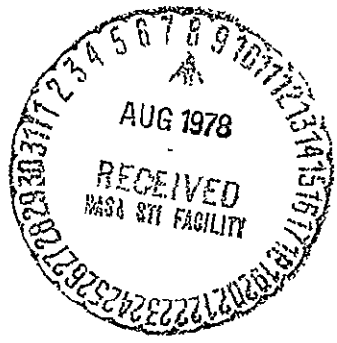

National Aeronautics and
Space Administration

1978

. TECHNICAL REPORT STANDARD TITLE PAGE

1. Report No NASA CR-152126	2. Government Accession No.	3. Recipient's Catalog No.
4 Title and Subtitle A Mach Line Panel Method for Computing the Linearized Supersonic Flow Over Planar Wings		5 Report Date May 1978 6. Performing Organization Code
7 Author(s) F. E. Ehlers and P. E. Rubbert		8. Performing Organization Report No. D6-46373
9. Performing Organization Name and Address The Boeing Commercial Airplane Company P. O. Box 3707 Seattle, Washington 98124		10. Work Unit No 11. Contract or Grant No NAS2-7729
12 Sponsoring Agency Name and Address National Aeronautics and Space Administration Washington, D.C.		13. Type of Report and Period Covered Contractor Report 14. Sponsoring Agency Code
15 Supplementary Notes		

16. Abstract

A method is described for solving the linearized supersonic flow over planar wings using panels bounded by two families of Mach lines. Polynomial distributions of source and doublet strength lead to simple, closed-form solutions for the aerodynamic influence coefficients, and a nearly triangular matrix yields rapid solutions for the singularity parameters.

The source method was found to be accurate and stable both for analysis and design boundary conditions. Similar results were obtained with the doublet method for analysis boundary conditions on the portion of the wing downstream of the supersonic leading edge, but instabilities in the solution occurred for the region containing a portion of the subsonic leading edge. Research on the method was discontinued before this difficulty was resolved.

17. Key Words	18. Distribution Statement
Linearized theory Subsonic flow Panel methods Aerodynamics	Unclassified-Unlimited

19. Security Classif. (of this report)	20. Security Classif. (of this page)	21. No of Pages	22. Price
Unclassified	Unclassified	86	

Form DOT F 1700.7 (8-69)

FIGURES

CONTENTS

CONTENTS (Concluded)

A MACH LINE PANEL METHOD FOR COMPUTING THE LINEARIZED SUPERSONIC FLOW OVER PLANAR WINGS

F.E. Ehlers and P.E. Rubbert
Boeing Commercial Airplane Company

1.0 SUMMARY

This report describes a study that was conducted in an attempt to develop advanced supersonic panel methods in linearized supersonic flow. This study centered around the use of panels bounded by the two families of Mach lines, a feature which appeared at the outset to offer significant advantages. Mach line paneling allows the accurate treatment of discontinuities in velocity and velocity gradient which occur along special Mach lines emanating from discontinuities in the wing planform. The use of Mach line coordinates also leads to simple, closed-form solutions for the aerodynamic influence coefficients. By ordering the panels along characteristic or Mach line strips a nearly triangular matrix results for the simultaneous equations to be solved for the flow parameters. The solution of the flow over the wing is, therefore, very rapid.

Both doublet and source panel formulations were implemented and evaluated. The doublet method was tested on a swept, parabolic-cambered wing, and the source method was tested on a swept wing with a symmetrical parabolic arc profile. The source method was accurate and stable both for analysis boundary conditions in which wing slope is prescribed and for design boundary conditions in which surface pressure is prescribed and wing slope is computed. Refining of the panel size improved the accuracy of the source method. Similar results for analysis boundary conditions with the doublet method were obtained for the portion of the wing bounded on the downstream side by two Mach lines which intersect at an interior point and inclose only the supersonic leading edge. However, instabilities in the solution occurred for the region containing a portion of the subsonic leading edge.

Research on the method was discontinued before the difficulty was resolved in favor of a method (ref. 1) that appeared to offer more promise in terms of its adaptability to general nonplanar configurations. This latter method subsequently underwent extensive development and will be reported in a forthcoming NASA contract report.

2.0 INTRODUCTION

Since wings in supersonic flow are usually thin and adequately described by linearized boundary conditions, it is natural to represent the wing by doublet and source distributions on a plane. In contract report NASA CR-2423, Mercer, Weber, and Lesferd (ref. 2) proposed a method utilizing Mach line paneling on a plane with linearized boundary conditions and presented some preliminary analysis and classification of panel forms which occur in a representative wing planform. This report describes the continued investigation into this method.

The approach appears to have several advantages:

1. The Mach lines are well defined on the mean plane on which thickness and camber can be described by source and doublet distributions.

2. As discontinuities in velocity and velocity gradient occur only across certain Mach lines, denoted here as "special Mach lines," the discontinuities can be conveniently taken into account in the influence coefficients by appropriate paneling.

3. With the two families of Mach lines as coordinates, the region of integration for the source and doublet integrals on the plane is easily described and leads to simple, closed-form expressions for the influence coefficients.

4. Solutions can be obtained extremely rapidly since the aerodynamic influence matrix can be placed in nearly triangular form by ordering the panels along characteristic strips on the wing planform.

In this report both the source and the doublet Mach line panel methods are described in detail. The source method for the thickness problem is very efficient and yields accurate results for both analysis and design type boundary conditions. The doublet method for the camber problem was successful in regions directly behind the supersonic leading edges but exhibited instabilities in regions downstream of subsonic leading edges. However, because of the success of the subsonic panel method of Johnson and Rubbert (ref. 1) and its greater applicability to a wide range of configurations and its apparent extendability to supersonic flow, the Mach line panel method described here was abandoned before the difficulty with the doublet method in the region behind subsonic leading edges could be resolved.

The method discussed here is based on linearized supersonic flow theory. The perturbation velocity potential ϕ is given by the Prandtl Glauert differential equation

$$(1 - M^2)\phi_{x_o x_o} + \phi_{y_o y_o} + \phi_{z_o z_o} = 0$$

where M is the freestream Mach number and x_0, y_0, z_0 are the Cartesian coordinates in the flow. The freestream is in the x_0 direction and the wing boundary conditions are applied on the $z_0 = 0$ plane.

3.0 SYMBOLS AND ABBREVIATIONS

a,b,c,d	Coefficients in polynomial distribution of doublet strength
B	$=\sqrt{M^2-1}$
C(x,y)	Correction function for Mach line strips with a portion of the subsonic leading edge in zone of dependence (sec. B9 of app. B)
C_{ik}	Contribution to pressure coefficient from the kth panel in the ith column
C_p	Pressure coefficient
$f_i(x,y)$	Basic functions for integrals over leading edge panel i = 1 to 3 for supersonic leading edge panels and i = 4 to 6 for subsonic leading edge panels
G(i,k,x,y)	Polynomial used in doublet strength for the kth panel in the ith column
$g_i(x,y)$	Downwash functions associated with the polynomial coefficients of doublet strength from supersonic leading edge panels; i = 1,2,3,4
$\overline{g}_j(x,y)$	Pressure functions associated with source strength polynomial coefficients for supersonic leading edge; j = 1,2,3,4
$h_i(x,y)$	Downwash functions associated with the polynomial coefficients of doublet strength from interior panels; i = 1,2,3,4
$\overline{h}(x,y)$	Pressure function associated with the single coefficient of interior source panel
H_0	$=\sqrt{(x-\xi)(y-n)}$ Hyperbolic distance on the plane z = 0 in Mach line coordinates
i or j	Column index
i_c	Column index for last column behind supersonic leading edge
k	Index for panel number in any column
M	Freestream Mach number
N(i,k,j)	Doublet parameter numbers for the kth panel in the ith column; j = 1,2,3,4
$N_p(i,k)$	$= i(i-1)/2 + k$, for $i \leqslant i_c$; panel number for the kth panel in the ith column; $N_p(i,k) = [i_c(i_c+1) + (3i_c - i + 2)(i - i_c - 1)]/2 + k$, $i > i_c$
s_1	Width of column in region behind supersonic leading edge
s_2	Width of column in region behind subsonic leading edge

$S_i(x,y)$	Downwash functions associated with the coefficients of the doublet strength in subsonic leading edge panels; i = 1,2,3,4
$\bar{S}_j(x,y)$	Pressure function associated with the coefficients of the source strength for subsonic leading edge panels; j = 1,2
x_0,y_0,z_0	Cartesian coordinates; x_0 aligned with the freestream
X_n	Doublet parameters consisting of the polynomial coefficients of the double strength for all panels
x,y,z	Mach line coordinate system defined in equation (3)
x,y	Denote differentiation with respect to the designated variable when used as a subscript
x_i	$x + i \epsilon s_1$; panel coordinate for panels in the ith row from y coordinate axis
y_j	$= y - js_1$, $j \leqslant i_c$; panel coordinate in jth column for $j \leqslant i_c$
y_j	$= y - i_c s_1 - (j - i_c + 1)\, s_2$; panel coordinate for jth column for $j > i_c$
w	Downwash
ϵ_1	Slope of supersonic leading edge defined by $x + \epsilon_1 y = 0$
ϵ_2	Slope of subsonic leading edge defined by $x - \epsilon_2 y = 0$
μ	Doublet strength
μ_{ik}	Total doublet strength in kth panel of ith column; equations (A27) and (A34)
σ	Source strength
σ_{ik}	Total source strength in kth panel of the ith column; equation (A64)
ϕ	Perturbation velocity potential

4.0 PLANAR MACH LINE DOUBLET PANEL METHOD WITH LINEARIZED BOUNDARY CONDITIONS

4.1 THEORETICAL DESCRIPTION OF THE METHOD

The camber of a three dimensional wing of small curvature can be simulated by a doublet distribution on a plane. In supersonic linearized theory, the perturbation velocity potential ϕ induced by such a doublet distribution is given by the integral

$$\phi(x_o, y_o, z_o) = \frac{1}{2\pi} \frac{\partial}{\partial z_o} \iint_{S_w} \frac{\mu(\xi,\eta)\, d\xi d\eta}{\sqrt{(x_o - \xi)^2 - B^2(y_o - \eta)^2 - B^2 z_o^2}} \tag{1}$$

where S_w is the portion of the wing cut by the upstream Mach cone from the point x_0,y_0,z_0 and $B = \sqrt{M^2-1}$. The velocity potential is normalized to the freestream velocity and the coordinates x,y,z to the wing chord. The doublet distribution μ is determined by satisfying the downwash boundary conditions on the plane $z_0 = 0$

$$\partial\phi/\partial z_o = f_{x_o}(x_o, y_o) \tag{2}$$

where $f_{x_o}(x_o,y_o)$ is the slope of the camber surface $z_0 = f(x_0,y_0)$. The Mach line panel method of solving the boundary value problem of equation (2) is facilitated by introducing Mach line coordinates defined by the transformation (see fig. 1).

$$\begin{aligned} z_0 &= z \\ x_0 - B y_0 &= 2Bx/M \\ x_0 + B y_0 &= 2By/M \end{aligned} \tag{3}$$

Since the Jacobian of the transformation in equation (3) is $2B/M^2$, the potential in equation (1) in the new variables takes the form

$$\phi = \frac{1}{2\pi M} \frac{\partial}{\partial z} \iint_{S_w} \frac{\mu(\xi,\eta)\, d\xi d\eta}{\sqrt{(x-\xi)(y-\eta) - M^2 z^2/4}}$$

Under the transformation in equation (3), the differential equation for ϕ becomes

$$\phi_{zz} - M^2 \phi_{xy} = 0$$

Differentiating the potential with respect to z and using the fact that the integral as well as ϕ itself satisfies the differential equation, we can replace the second derivative with respect to z by the second derivative with respect to x and y. With this change in derivatives, the evaluation of ϕ_z on the plane z = 0 may be found by setting z = 0 in the integrand without first performing the differentiation (ref. 3). Thus we obtain

$$\phi_z = \frac{M}{2\pi} \frac{\partial^2}{\partial x \partial y} \int_y^{y(x)} \int_x^{\ell(\eta)} \frac{\mu(\xi,\eta)\, d\xi d\eta}{\sqrt{(x-z)(y-\eta)}} \tag{4}$$

where $\xi = \ell(\eta)$ and $y = y(x)$ are the equations of the leading edge.

In this form the integration must be performed before differentiation because of the inverse square root singularity of the integrand. This problem is eliminated by introducing the new variables of integration

$$\xi' = \sqrt{x - \xi} \qquad \eta' = \sqrt{y - \eta} \tag{5}$$

which lead to

$$\phi_z = \frac{2M}{\pi} \frac{\partial^2}{\partial x \partial y} \int_0^{\sqrt{y - y(x)}} \int_0^{\sqrt{x - \ell(y - \eta^2)}} \mu(x - \xi^2, y - \eta^2)\, d\xi d\eta \tag{6}$$

where we have dropped the primes for convenience. Some simplification results from performing the differentiation before integration. When equation (6) is substituted into the boundary condition in equation (2), with the quantity $f_{x_o}(x_o, y_o)$ accordingly transformed into the Mach line coordinates in equation (3), an integral equation for the doublet distribution $\mu(x,y)$ results.

Once the doublet distribution on the plane has been solved, the pressure on the wing can be evaluated. From the relationship implicit in equation (1),

$$\lim_{z \to 0^+} \phi = -\mu/2$$

the pressure coefficient on the upper side of the wing is

$$\begin{aligned} C_p &= -2\, \phi_{x_o} = -\frac{M}{B} (\phi_x + \phi_y) \\ &= \left(\frac{M}{2B}\right)(\mu_x + \mu_y) \end{aligned} \tag{7}$$

The pressure coefficient on the lower side of the wing has the same magnitude, but opposite in sign.

The numerical approach to solving the integral equation using the Mach line panel method is to divide the wing planform into small panels by a grid system of the two families of Mach lines with x and y being constant, and then determine the doublet distribution on each panel by imposing the appropriate boundary conditions at certain discrete points on the planform. A typical paneled wing with $M = \sqrt{2}$ is shown in figure 2. The paneling is comprised of

parallelogram-shaped interior panels having edges bounded by two families of Mach lines and triangular panels adjacent to the leading and trailing edges. The doublet distribution on each panel is approximated by a polynomial with sufficient boundary and continuity conditions to establish the coefficients of the polynomial. The doublet strength must vanish along a leading and side edge and be continuous across panel edges. The downwash at certain points on the panels computed by summing the integrals of the form of equation (6) over all panels in the region of dependence must equal to the prescribed camber slope at these same points.

It is necessary that the doublet distribution be continuous over the planform as such discontinuities at panel edges introduce free vortex lines. For convenience of the discussion, we shall draw the paneling and wing planform in the oblique Mach line coordinate x,y system as if it were orthogonal (which is the case for a Mach number of $\sqrt{2}$). The interior panels are then rectangular.

In supersonic flow a rectangular panel influences the flow field in the region within the downstream Mach cone which emanates from the upstream vertex of the panel. With Mach line paneling, the panel edges coincide with the boundaries of this region as seen in figure 3. Continuity of the doublet strength is assured by choosing a polynomial which vanishes on the lines x = constant and y = constant defining the two upstream boundaries of the panel. In terms of local panel coordinates with the origin at the upstream vertex of the rectangular panel, the doublet strength μ must be proportional to x,y for rectangular panels within the planform; i.e.,

$$\mu = xy\, P(x,y)$$

where P(x,y) is a polynomial. If we further postulate that on the downstream panel edges that the doublet strength be quadratic, this restricts μ to the form

$$\mu = xy\,(a + bx + cy + dxy) \qquad (8)$$

The relation for μ is continued analytically along characteristic strips downstream of the panel trailing edges by its quadratic relation on the downstream boundaries: $x = \Delta x$ and $y = \Delta y$; where Δx and Δy are the panel length and width, respectively. Hence the contribution to μ in the two downstream characteristic strips containing the panel is quadratic in the Mach line variable running normal to the edge (see fig. 3). In the remaining portion of the domain of influence bounded by the two characteristics or Mach lines from the downstream vertex, the doublet strength μ is constant as indicated in figure 3. The range of integration for control points in the four distinct regions of influence of the panel is illustrated in figure 4 with the corresponding functional relations for the doublet strength described in equation (8).

The complete doublet distribution on a given interior panel consists of the function in equation (8) associated with that panel plus contributions from:

1. The quadratic doublet strengths at the downstream edges of those panels in the two characteristic strips running upstream of the panel as shown in figure 5.

2. The constant doublet strengths at the downstream corners of those panels within the region between the two upstream running characteristic strips.

Equation (8) for the doublet strength has four free parameters, which can be determined as follows.

Continuity of the normal derivative (in which Mach line variables) is applied at the downstream ends of the leading edges of the panel, leaving two parameters to be determined by the downwash boundary conditions at two control points on the panel, see figure 6. However, for an interior panel in which one of the leading edges is a special Mach line along which discontinuities in velocity or velocity gradient may occur, the requirement of the continuity of the doublet gradient is relaxed on this edge and is replaced by a downwash boundary condition. The formulas for the downwash induced by a doublet distribution on interior panels are derived in section A2 of appendix A. They are simple, rational algebraic expressions.

The treatment for a triangular panel adjacent to a supersonic leading edge is similar. Since the doublet strength must vanish on the leading edge of the wing, the doublet distribution must be of the form

$$\mu = (x + \epsilon_1 y)\ (a + bx + cy + dxy) \tag{9}$$

where $x + \epsilon_1 y = 0$ defines the portion of the leading edge covered by the panel and the origin is on the upstream corner of the panel illustrated in figure 7. It is easily seen that μ vanishes on the x and y Mach line boundaries of the zone of influence for the leading edge panel. In the same manner as for the interior panels, the value of doublet strength is continued along the two characteristic strips by the quadratic relations on its downstream boundaries. In the region defined by the two x and y Mach lines from the downstream vertex the doublet strength μ is constant. The range of integration for control points in the four distinct regions of influence of the panel is illustrated in figure 8. The four free parameters in equation (9) are determined as follows.

In order to ensure the continuity of the doublet gradient along all straight supersonic leading edges, we require the polynomial $(a + bx + cy + dxy)$ at the upstream corner to agree with the adjacent leading edge panel value as indicated in figure 6. The downwash boundary conditions at the upstream corner point, the middle of the panel leading edge, and near the downstream corner point furnish the rest of the conditions to render the four parameters determinate. The formulas for the downwash induced by a doublet distribution on supersonic leading edge panels are derived in section A1 of appendix A.

For the subsonic leading edge panels, we use a doublet distribution of the form given in equation (9) for the supersonic leading edge; namely,

$$\mu = (x - \epsilon_2 y)\ (a + bx + cy + dxy) \tag{10}$$

Here the origin is at the upstream corner of the panel and $x - \epsilon_2 y = 0$ defines the panel leading edge. The doublet distribution of equation (10) is continued along strips in the x direction by its value on the downstream boundary at $x = \epsilon_2 s_2$, and since μ vanishes on the leading edge, μ also vanishes for $y > s_2$ (see fig. 9). The range of integration for control points in the three distinct regions of influence of the panel is illustrated in figure 9. The four free parameters in equation (10) are determined by imposing the edge conditions and the downwash condition. With the choice of doublet distribution given in equation (10), the condition of vanishing doublet strength on the leading edge is automatically satisfied. The continuity of the doublet gradient across the downstream edge is enforced when determining the parameters for the interior panels. The continuity of the doublet strength along the upstream panel edge determines two parameters (a and b) in equation (10). One relation is to satisfy the continuity of the normal gradient of the doublet strength on the downstream corner of the same edge, leaving only a single parameter to be determined by the downwash condition at one control point, see figure 6. In case the upstream Mach line edge is a special Mach line, the continuity of the doublet normal gradient is relaxed and replaced by a downwash for the same reason described for the interior panels.

The derivation of the downwash from the subsonic leading edge panel is presented in section A3 of appendix A and in section B5 of appendix B and results are given by equations (A13) and (B19). The calculated downwash on the subsonic leading edge has a logarithmic singularity as seen from the function f_4 in equation (B5). Since μ is approximated by a polynomial, the tangential velocities are finite on the subsonic leading edge whereas analytical solutions for subsonic leading edge wings contain an inverse square root singularity in the tangential velocity at the leading edge. No wakes were included in the examples computed by the doublet Mach line panel, since there was no subsonic trailing edge. For all trailing edges, continuity of μ on the wing with the trailing vortex sheet must be maintained. From equation (7), we see that for continuity of pressure across the sheet, the doublet distribution on the wake must be of the form

$$\mu = P_n(x-y)$$

where P_n is a polynomial. From equation (9) the expression for μ on the panel adjacent to on either a supersonic or subsonic trailing edge of the form

$$x = \epsilon_3 y$$

is a polynomial of the fourth degree in x or y. Hence, P_n must also be a quartic in its argument $x-y$ and the coefficients must be chosen to make μ continuous at the trailing edge. For a subsonic trailing edge panel a downwash control point must be located on the trailing edge to satisfy the Kutta condition of smooth flow.

As seen from equations (8), (9), and (10) for the doublet distribution on a panel, there are four parameters to be determined by appropriate conditions on each panel. For supersonic leading edge panels we require the polynomials

$$a + bx + cy + dxy$$

to agree with adjacent leading edge panel values at all corners. This ensures continuity of the gradient along all straight supersonic leading edges and leaves three parameters to satisfy the downwash boundary conditions at three control points.

For interior panels, continuity of the normal derivative ($\partial/\partial x$ or $\partial/\partial y$) of the doublet strength is applied at the downstream ends of the two leading edges of the panel, leaving two parameters free to be determined by downwash boundary conditions at two control points on the panel. However, for interior panels in which one of the leading edges is a special Mach line along which discontinuities in velocity or velocity gradient may occur, the requirement of the continuity of the doublet gradient is relaxed on this edge and is replaced by a downwash control point (see fig. 6).

For subsonic leading edge panels, two relations are required to satisfy continuity of μ with the upstream Mach line edge. One relation is used to satisfy continuity of the normal gradient of the doublet on the downstream corner of the upstream Mach line edge, leaving only a single parameter to be determined by a downwash control point.

The control point locations and continuity conditions are illustrated in figure 6 for the wing planform used to test the method. Design type boundary conditions also are possible with the x_0 component of the perturbation velocity prescribed at the control points instead of the wing camber slopes.

4.2 DISCUSSION OF RESULTS FROM THE PLANAR MACH LINE DOUBLET PANEL METHOD

To test the method described in the foregoing discussion, a cambered swept wing of zero thickness having a parabolic arc profile was chosen. The camber is defined by the formula

$$z_1 = 2t\left(1 - Cy_1\right)\left(x_1 - x_1^2\right) \tag{11}$$

where the y_1 axis is along the leading edge and the x_1 axis perpendicular to the y_1 axis. A closed form exact solution of the linearized differential equation was derived to check against the panel method for the portion of the wing planform described in figure 6.

For the region downstream of the supersonic leading edge and upstream of the special Mach line, the panel method yields results in close agreement with the exact solution from linearized theory for $C = 0.3$ and a wing sweep of 30° at a Mach number $\sqrt{2}$ as shown in figure 10. The pressure distribution normalized to maximum camber was fairly insensitive to location of the control points in the panels. For the supersonic leading edge triangular panel, best results were obtained for the interior control point located at the downstream corner. Increasing the panel density improved the pressure distribution.

In the region behind the subsonic leading edge (or free edge aligned with the freestream), the predicted pressure distribution was poor. Increasing the panel density only served to increase the deviation from the closed form solution. A typical pressure distribution along a line close to and parallel to the special Mach line emanating downstream from the corner is shown in figure 11. The difference between calculated downwash distribution and wing slope follows a similar oscillating behavior in figure 12. The zero downwash difference values occur at control points where the boundary conditions were applied.

Continuity of the normal derivative of the doublet distribution at corners ensures the continuity of the pressure at corners. The pressure distribution on both sides of a row of panel edges as shown in figure 13 demonstrates that this condition was properly applied in the solution. The greatest discontinuity in pressure appears at the middle of the panel edge.

To test whether the difficulty stemmed from the corner where the subsonic and supersonic leading edges join, the flat plate conical flow solution was added to the panel method to eliminate the singularity along the special Mach line. The pressure distributions along Mach lines in the region behind the free edge are shown in figures 14 through 17. Considerable improvement resulted and the match with the exact solution in first column of panels downstream of the special Mach line is excellent. Away from the corner, the pressure distribution appears to oscillate about the exact solution. From the form of the oscillations if would appear that they are induced by the triangular subsonic leading edge panels, which for this case is a free edge.

A few attempts were made to alleviate this difficulty. An additional control point was added to the triangular leading edge by adding to the doublet distribution the term

$$\mu = cx\ [(y/x) - \epsilon_2(y/x)^2] \tag{12}$$

which corresponds to a conical flow pressure distribution. This failed to improve the pressure distribution.

Adding control points in the panels downstream of the special Mach line and applying mean square solution techniques to the set of simultaneous solution had a small effect in smoothing the result. However, as the condition of the continuity of normal derivative at panel corners was relaxed, the discontinuities of pressure along the panel edges become larger and also affect the solution in the region behind the supersonic leading edge.

5.0 PLANAR MACH LINE SOURCE PANEL METHOD WITH LINEARIZED BOUNDARY CONDITIONS

5.1 THEORETICAL DESCRIPTION OF THE METHOD

To solve the thickness problem for a planar wing, we use a source distribution over the wing planform. The velocity potential in terms of Mach line coordinates of equation (3) may be written down by appropriately dropping the z derivative in the expression for the doublet potential. Thus, we have

$$\phi = -\frac{1}{2\pi M} \iint_{S_W} \frac{\sigma(\xi,\eta)\, d\xi d\eta}{\sqrt{(x-\xi)(y-\eta) - M^2 z^2/4}} \tag{13}$$

This integral has the property that

$$\phi_z \Big|_{z=\pm 0} = \pm\sigma\ (x, y)/2 = \left(dz/dx_o\right)_{z=\pm 0}$$

where dz/dx_0 is the wing thickness slope. Dropping the factor 2 relates σ directly to the wing upper slope. The pressure on the wing is given by

$$C_p = -2\,\phi_{x_o} = -M\,(\phi_x + \phi_y)/B\Big|_{z=0} \tag{14}$$

Since we are interested in the flow properties on the wing, it is convenient to set z = 0 in equation (13) before differentiating with respect to x and y. Thus on the plane z = 0,

$$\phi = -\frac{1}{\pi M} \int_{y}^{y(x)} \int_{x}^{\ell(\eta)} \frac{\sigma(\xi,\eta)\, d\xi d\eta}{\sqrt{(x-\xi)(y-\eta)}}$$

$$= -\frac{4}{\pi M} \int_{0}^{\sqrt{y-y(x)}} \int_{0}^{\sqrt{x-\ell(y-\eta^2)}} \sigma\left(x-\xi^2, y-\eta^2\right) d\xi d\eta \tag{15}$$

where $x = \ell(y)$ or $y = y(x)$ describes the wing (or panel) leading edge.

The source panel method follows essentially the same procedure as the doublet panel method and we will use the same wing planform paneling to illustrate the method (see fig. 18). For supersonic leading edge panels, a quadratic source distribution in the following form is used:

$$\sigma = a + bx + cy + dxy \tag{16}$$

where the origin is at the upstream corner of the panel. One parameter is fixed by requiring σ to be continuous along the leading edge. The other three parameters are determined from tangency conditions at three control points. The source strength σ is continued outside the panel along characteristic strips by its linear values on the downstream panel edges in the same manner as described for the doublet strength.

Continuity of source strength with interior panels is maintained by defining the source strength on interior panels by a relation of the form

$$\sigma = dxy \tag{17}$$

where the origin of coordinates is at the upstream corner of the panel. Since there is only one parameter d, it is determined by a single downwash control point (or pressure) at the panel center. The source strength of the interior panel is continued by its linear relation on its downstream boundaries in a manner similar to the doublet strength distribution.

For subsonic leading edge panels, the source distribution is given by

$$\sigma = cy + dxy \tag{18}$$

where the two parameters are determined by imposing the tangency condition at two distinct points shown in figure 18. Unlike the doublet panels, the value of σ on the upstream characteristic strip is continued into the subsonic edge panel since σ does not necessarily vanish on wing edges, either subsonic or supersonic.

For the planform in figure 18, the relation for σ on a given panel is derived in appendix A and appendix B along with formulas for the pressure coefficient. The same basic functions appear in the pressure coefficient for the source as in the formulas for the doublet downwash.

Either analysis (i.e., upper surface slope) boundary conditions or design (i.e., pressure coefficient) boundary conditions may be applied. The location of control points is shown in figure 18. Since C_p has a logarithmic singularity on the subsonic leading edge, the control point must be moved off the edge of the subsonic leading edge panel for design boundary conditions.

5.2 DISCUSSION OF RESULTS FROM THE PLANAR MACH LINE SOURCE PANEL METHOD

To test the source panel method, a wing with a symmetric parabolic arc profile was chosen which has the same spanwise and chordwise variation in slope for the upper surface as the cambered zero thickness wing used to test the doublet method (eq. (11)). The angle of sweep is 30°, and the freestream Mach number is $\sqrt{2}$. The subsonic leading edge angle was selected to make an isosceles triangle with the downstream Mach line boundary as shown in figure 19. The exact linearized solution is easily obtained in closed form and was used as a comparison with the panel method results.

Figure 19 shows a plot of the pressure distribution from the panel method using six panels. The agreement with the exact solution is very close. Although the results of the panel method is indicated by circled points, the distribution is continuous in the whole region. Figure 20 shows a comparison of source distribution from the panel method with the wing slopes along the lines shown in the planform in the figure. This indicates that the boundary conditions are appropriately satisfied.

The design mode was also tested using the same wing. In this case the applied boundary condition was the theoretical pressure distribution from the exact linearized solution and the coefficients of the source distribution were solved for. The resulting source distribution is seen to be in close agreement with the wing slopes as indicated in figure 21.

6.0 CONCLUSION

The source panel method yielded very accurate results when either analysis (downwash) or design (pressure) boundary conditions were applied. The doublet method gave accurate results for analysis boundary conditions on regions behind a supersonic leading edge. Both methods were very stable and showed little sensitivity with variation in the location of control points on the panel. Refining the paneling improved the accuracy.

However, when the portion of the wing behind the subsonic leading edge was included in the solution, the doublet method became unstable and sensitive to control point location. Refinement of the paneling did not improve the accuracy but increased the oscillations in the panel solution and its departure from the exact linearized solution. The difficulty appears to lie in an unsuitable treatment of triangular panels occurring along the subsonic leading edges.

Research was discontinued on this method before the difficulty on the subsonic leading edge was resolved. The success and stability of the subsonic method for nonplanar surfaces developed by Johnson and Rubbert (ref. 1) suggested that it would also be suitable for supersonic flow. Such an approach also has the advantage of producing methods for both subsonic and supersonic flow which are compatible with respect to paneling and control point location.

APPENDIX A
DERIVATION OF BASIC FORMULAS FOR THE PLANAR MACH LINE PANEL METHODS

A1 FORMULAS FOR THE DOWNWASH FROM SUPERSONIC LEADING EDGE DOUBLET PANELS

We shall now develop the basic formulas for the downwash from the panels located at three different regions on the planform using the doublet distributions presented in section 4.1. Consider first the downwash induced by a supersonic leading edge panel. Since the doublet strength is continued on Mach line strips by its value on panel edges, the range of integration for points on and off the panel is illustrated in figure 8.

For simplicity we shall consider cases b and d only. The other cases can be easily obtained by dropping some of the terms. Thus, we have from equation (4) for case b when $x < 0$, $y > s_1$

$$w = \frac{M}{2\pi} \frac{\partial^2}{\partial x \partial y} \left\{ \int_{s_1}^{-x/\epsilon_1} \int_{x}^{-\epsilon_1 \eta} \mu(\xi, n) d\zeta d\eta / H_o + \int_{y}^{s_1} \int_{x}^{-\epsilon_1 s_1} \mu(\xi, s_1) \, d\zeta d\eta / H_o \right\} \quad (A1)$$

and for case d when $x > 0$, $y > s_1$

$$w = \frac{M}{2\pi} \frac{\partial^2}{\partial x \partial y} \left\{ \int_{s_1}^{0} \left[\int_{0}^{-\epsilon_1 \eta} \frac{\mu(\xi,\eta)}{H_o} \, d\xi + \int_{x}^{0} \frac{\mu(0,\eta)}{H_o} \, d\xi \right] d\eta \right.$$

$$\left. + \int_{y}^{s_1} \left[\int_{0}^{-\epsilon_1 s_1} \frac{\mu(\xi,s_1)}{H_o} d\xi + \int_{x}^{0} \frac{\mu(0,s_1)}{H_o} d\xi \right] d\eta \right\} \quad (A2)$$

where

$$H_o = \sqrt{(x-\xi)(y-\eta)}$$

With the integrals in their present form, the integration must be performed before the differentiation. When the variables of integration are changed to

$$\xi' = \sqrt{x-\xi} \quad , \quad \eta' = \sqrt{y-\eta} \quad (A3)$$

the differentiation may be performed first. The integral equation (A1) then takes the form for case b when $x < 0$, $y > s_1$

$$W = \frac{2M}{\pi} \frac{\partial^2}{\partial x \partial y} \left\{ \int_{\sqrt{y - s_1}}^{\sqrt{y + x/\epsilon_1}} \int_0^{\sqrt{x + \epsilon_1 (y - \eta^2)}} \mu\left(x - \xi^2, y - \eta^2\right) d\xi d\eta \right.$$

$$\left. + \int_0^{\sqrt{y - s_1}} \int_0^{\sqrt{x + \epsilon_1 s_1}} \mu\left(x - \xi^2, x_1\right) d\xi d\eta \right\}$$

Performing the differentiation and noting that μ vanishes on the leading edge; i.e., $\mu(-\epsilon_1 y, y) = 0$ leads to

$$W = \frac{2M}{\pi} \left\{ \int_{\sqrt{y - s_1}}^{\sqrt{y + x/\epsilon_1}} \mu_y\left(-\epsilon_1 \left(y - \eta^2\right), y - \eta^2\right) d\eta / 2\sqrt{x + \epsilon_1 \left(y - \eta^2\right)} \right.$$

$$\left. + \int_{\sqrt{y - s_1}}^{\sqrt{y + x/\epsilon_1}} \int_0^{\sqrt{x + \epsilon_1 \left(y - \eta^2\right)}} \mu_{x_y}\left(x - \xi^2, y - \eta^2\right) d\xi d\eta \right\} \qquad \text{(A4)}$$

for case b in which $x < 0$ and $y > s_1$. Similarly, equation (A2) becomes

$$W = \frac{2M}{\pi} \left\{ \int_{\sqrt{y - s_1}}^{\sqrt{y}} \mu_y\left(-\epsilon_1 \left(y - \eta^2\right), y - \eta^2\right) d\eta / 2\sqrt{x + \epsilon_1 \left(y - \eta^2\right)} \right.$$

$$\left. + \int_{\sqrt{y - s_1}}^{\sqrt{y}} \int_{\sqrt{x}}^{\sqrt{x + \epsilon_1 \left(y - \eta^2\right)}} \mu_{xy}\left(x - \xi^2, y - \eta^2\right) d\xi d\eta \right\} \qquad \text{(A5)}$$

for case d in which $x > 0$, $y > s_1$

The cases a and c in figure 8 easily result from the preceding equations by setting $\sqrt{y - s_1} = 0$ whenever $y < s_1$.

Evaluating the integrals using equation (9) for μ leads to the downwash in the form

$$W = \left(M\sqrt{\epsilon_1}/\pi\right)\left[a\, g_1(x,y) + b\, g_2(x,y) + c g_3(x,y) + d\, g_4(x,y)\right] \qquad \text{(A6)}$$

The functions g_i are presented in section B3 of appendix B.

A2 FORMULAS FOR THE DOWNWASH FROM INTERIOR DOUBLET PANELS

For the interior panel, the regions of integration are depicted in figure 4. We shall consider the case $y > s_1$ and $x > \epsilon_1 s_1$. The downwash integral then becomes

$$W = \frac{M}{2\pi} \frac{\partial^2}{\partial x \partial y} \left\{ \int_{s_1}^{0} \int_{\epsilon_1 s_1}^{0} \mu(\xi,\eta)\, d\xi d\eta / H_o \right.$$

$$+ \int_{y}^{s_1} \left[\int_{x}^{\epsilon_1 s_1} \frac{\mu\left(\epsilon_1 s_1, s_1\right)}{H_o} d\xi + \int_{\epsilon_1 s_1}^{0} \frac{\mu\left(\xi, s_1\right)}{H_o} d\xi \right] d\eta$$

$$\left. + \int_{s_1}^{0} \int_{x}^{\epsilon_1 s_1} \mu\left(\epsilon_1 s_1, \eta\right) d\xi d\eta / H_o \right\} \qquad \text{(A7)}$$

In terms of the variables in equation (A3), we obtain, after performing the differentiation,

$$W = \frac{2M}{\pi} \int_{\sqrt{y - s_1}}^{\sqrt{y}} \int_{\sqrt{x - \epsilon_1 s_1}}^{\sqrt{x}} \mu_{x_y}\left(x - \xi^2, y - \eta^2\right) d\xi d\eta \qquad \text{(A8)}$$

since $\mu\left(0, s_1\right) = \mu\left(\epsilon_1 s_1, 0\right) = \mu_y\left(0, s_1\right) = 0.$

The remaining cases a, b, and c in figure 4 follow by setting $\sqrt{y - s_1}$ equal to zero for $y < s_1$ and $\sqrt{x - \epsilon_1 s_1} = 0$ for $x < \epsilon_1 s_1$. Substituting equation (8) for μ yields the following relation for the downwash

$$W = \left(M\sqrt{\epsilon_1}/\pi\right)\left[a\, h_1(x, y) + b\, h_2(x, y) + c\, h_3(x, y) + d\, h_4(x, y)\right] \qquad \text{(A9)}$$

where the functions h_i are derived in section B4 of appendix B.

A3 FORMULAS FOR THE DOWNWASH FROM SUBSONIC LEADING EDGE DOUBLET PANELS

For the subsonic leading edge panels, we use a doublet distribution of the form of equation (10); i.e.,

$$\mu = \left(x - \epsilon_2 y\right)(a + bx + cy + dxy) \tag{A10}$$

where the origin is at the upstream corner of the panel. The doublet distribution of equation (A10) is continued along strips in the x direction by its value on the boundary $x = \epsilon_2 s_2$ and vanishes for $y > s_2$. The special cases for the regions of integration are illustrated in figure 9. The most general case c yields the downwash formula

$$W = \frac{M}{2\pi}\frac{\partial^2}{\partial x \partial y}\left\{\int_{s_2}^{0}\left[\int_{\epsilon_2 s_2}^{\epsilon_2 \eta}\frac{\mu(\xi,\eta)}{H_o}\,d\zeta + \int_{x}^{\epsilon_2 s_2}\frac{\mu\left(\epsilon_2 s_2, \eta\right)}{H_o}\,d\xi\right]d\eta\right\} \tag{A11}$$

In terms of the variables in equation (A3), these integrals become, after differentiation,

$$W = \frac{2M}{\pi}\left\{\int_{\sqrt{y - s_2}}^{\sqrt{y}}\mu_y\left(\epsilon_2\left(y - \eta^2\right), y - \eta^2\right)d\eta / 2\sqrt{x - \epsilon_2\left(y - \eta^2\right)}\right.$$

$$\left. + \int_{\sqrt{y - s_2}}^{\sqrt{y}}\int_{\sqrt{x - \epsilon_2 s_2}}^{\sqrt{x - \epsilon_2\left(y - \eta^2\right)}}\mu_{x_y}\left(x - \xi^2, y - \eta^2\right)d\xi d\eta\right\} \tag{A12}$$

The cases a and b are easily derived from equation (A12) by setting $\sqrt{y - s_2}$ equal to zero whenever $y < s_2$ and similarly $\sqrt{x - \epsilon_2 s_2}$ equal to zero for $x < \epsilon_2 s_2$. Substituting equation (A10) for μ in equation (A12) and integrating yields the following form for the downwash

$$W = \left(M\sqrt{\epsilon_2}/\pi\right)\left[aS_1(x, y) + bS_2(x, y) + cS_3(x, y) + dS_4(x, y)\right] \tag{A13}$$

where the S_j (j = 1 to 4) functions are derived in section B5 of appendix B.

A4 DESCRIPTION OF PANEL AND PARAMETER NUMBERING SYSTEM

To test the method, we choose a wing planform consisting of a straight supersonic leading edge followed by a straight subsonic leading edge and consider the region bounded by the two leading edges and a Mach line which intersects the two edges as shown in figure 22. The planform in figure 22 is divided into two regions by the special Mach line from the corner which in turn are divided by the other family of Mach lines into rectangular and triangular panels. The panel numbering follows the sequence as shown in figure 22. The ith column has i panels for $i \leqslant i_c$. Summing the previous panels, we see that the panel number N_p for the kth panel in the ith column is

$$N_p(i,k) = i(i-1)/2 + k, k = 1 \text{ to } i. \tag{A14}$$

Since there are four parameters (a,b,c,d) associated with each panel, the parameter numbers associated with the kth panel of the ith column is given by

$$N(i,k,j) = 2i(i-1) + 4(k-1) + j, j = 1 \text{ to } 4. \tag{A15}$$

Since the doublet distribution in each panel is referred to the origin of coordinates at the upstream corners of each panel, we define panel variables x_i, y_j by

$$x_i = x + i\epsilon_1 s_1, i = 1, 2, \ldots \tag{A16}$$

$$y_j = y - js_1, j \leqslant i_c, j = 1, 2, \ldots \tag{A17}$$

where s_1 is the column width behind the supersonic leading edge.

For $j > i_c$, we have

$$y_j = y - i_c s_1 - (j - i_c + 1)s_2 \tag{A18}$$

where s_2 is the width of the subsonic Mach line columns. Since $\epsilon_1 s_1 = \epsilon_2 s_2$, the definition of x_i for $i > i_c$ remains the same.

A5 THE DOUBLET DISTRIBUTION FOR PANELS IN COLUMNS BEHIND THE SUPERSONIC LEADING EDGE $(i < i_c)$

It is convenient to define the function

$$G(i, k, x, y) = X_{N(i, k, 1)} + x\, X_{N(i, k, 2)} + y\, X_{N(i, k, 3)} + x\, y X_{N(i, k, 4)} \tag{A19}$$

where the X_N correspond to the parameters (a,b,c,d) in equations (8) through (10) and N(i,k,j) is defined in equation (A15).

Then the contribution to the doublet distribution from variables related to the kth panel in the ith column is, for $i < i_c$,

$$\mu = x_{i-k+1}\, y_{i-1}\, G\left(i, k, x_{i-k+1}, y_{i-1}\right) \tag{A20}$$

for $i \geqslant k > 2$ for interior panels and

$$\mu = \left(x_{i-1} + \epsilon_1\, y_{i-1}\right) G\left(i, 1, x_{i-1}, y_{i-1}\right) \tag{A21}$$

for supersonic leading edge panels.

We shall now construct μ in the kth panel of the ith column for columns behind the supersonic leading edge. The upstream panels in the same row as the kth panel of the ith column are

$$N_p\ (i-j,\ k-j) \text{ for } j = 1,2,3, \ldots, k-1 \tag{A22}$$

These panels contribute to the x variation in the form

$$x_{i-k+1}\, G\left(i-k+1,\ 1,\ x_{i-k},\ s_1\right) + \sum_{j=1}^{k-2} x_{i-k+1}\, s_1\, G\left(i-j,\ k-j,\ x_{i-k+1},\ s_1\right) \tag{A23}$$

Similarly, the upstream panel numbers in the same column are

$$N_p(i,k-j),\ j = 1,2,3, \ldots, k-1$$

and they contribute to the variation with y in the form

$$\epsilon_1\, y_{i-1}\, G\left(i,\ 1,\ 0,\ y_{i-1}\right) + \sum_{j=2}^{k-1} \epsilon_1 s_1\, y_{i-1}\, G\left(i, j, \epsilon_1 s_1, y_{i-1}\right) \tag{A24}$$

The corner values from the remaining upstream supersonic leading edge panels contribute a constant term of the form

$$\sum_{j=2}^{k-1} \epsilon_1 s_1\, G\left(i-j+1,\ 1,\ 0,\ s_1\right) \tag{A25}$$

Contribution to the constant from the interior panels upstream of the k – 1 row from panels numbered

$$N_p(i-j,k-j-1),\ j = 1,2,3, \ldots, k-3$$

is

$$\sum_{j=1}^{k-3} \epsilon_1 s_1^2 \, G\left(i-j,\, k-1-j,\, \epsilon_1 s_1,\, s_1\right).$$

Contribution to the constant from upstream k – 2 row is

$$\sum_{j=1}^{k-4} \epsilon_1 s_1^2 \, G\left(i-j,\, k-2-j,\, \epsilon_1,\, s_1,\, s_1\right)$$

and the total contributions to the constant from all upstream interior panels are

$$\sum_{n=1}^{k-3} \sum_{j=1}^{k-2-n} \epsilon_1 s_1^2 \, G\left(i-j,\, k-n-j,\, \epsilon_1 s_1,\, s_1\right) \tag{A26}$$

Combining equations (A23), (A24), (A25), and (A26) with the panel function itself yields the following value of μ_{ik} for the kth panel in the ith column

$$\begin{aligned}
\mu_{ik} = {} & x_{i-k+1}\, y_{i-1}\, G\left(i,\, k,\, x_{i-k+1},\, y_{i-1}\right) + x_{i-k+1}\, G\left(i-k+1,\, 1,\, x_{i-k},\, s_1\right) \\
& + s_1 \sum_{j=1}^{k-2} x_{i-k+1}\, G\left(i-j,\, k-j,\, x_{i-k+1},\, s_1\right) + \epsilon_1 y_{i-1}\, G\left(i,\, 1,\, 0,\, y_{i-1}\right) \\
& + \sum_{j=2}^{k-1} \epsilon_1 s_1\, y_{i-1}\, G\left(i,\, j,\, \epsilon_1 s_1,\, y_{i-1}\right) + \sum_{j=2}^{k-1} \epsilon_1 s_1\, G\left(i-j+1,\, 1,\, 0,\, s_1\right) \\
& + \sum_{n=1}^{k-3} \sum_{j=1}^{k-2-\eta} \epsilon_1 s_1^2 \, G\left(i-j,\, k-n-j,\, \epsilon_1 s_1,\, s_1\right)
\end{aligned} \tag{A27}$$

Equation (A27) holds for $k \geq 2$, if those summations are dropped for the particular values of k in which the upper limits are less than the lower limits.

A6 DOUBLET DISTRIBUTION FOR PANELS IN COLUMNS BEHIND THE SUBSONIC LEADING EDGE ($i > i_c$)

Let i_c be the last column for which the leading edge is supersonic. The total number of panels in the region to the left of the special Mach line is

$$i_c(i_c + 1)/2$$

The number of panels for $i > i_c$ in the ith column is

$$i_c - (i - i_c - 1) = 2i_c - i + 1$$

By summing the panels in the columns up to the ith column, we find that the panel number for the kth panel in the ith column is

$$N_p(i,k) = \left[i_c(i_c + 1) + (3i_c - i + 2)(i - i_c - 1) \right] /2 + k \tag{A28}$$

The numbers corresponding to the parameters in the panel are

$$N(i,k,j) = 4N_p(i,k) - 4 + j, \; j = 1,2,3,4. \tag{A29}$$

For the subsonic leading edge panel we have

$$\mu_{i1} = \left(x_{2i_c - i + 1} - \epsilon_2 \, y_{i-1} \right) G\left(i,1,x_{2i_c - i + 1}, y_{i-1}\right) \tag{A30}$$

The doublet distribution cannot be made continuous by analytically continuing the distribution from the upstream panel downstream into the subsonic leading edge panel, since μ must vanish on the leading edge. Thus μ must be matched in the subsonic leading edge panel on the upstream edge by two relations obtained by equating the two coefficients of the x variable.

Consider the kth panel in the ith column for $i > i_c$. Then the panel numbers for the panels in the same row for $i > i_c$ are

$$N_p(i - j, k + j), \; j = 1,2,3, \ldots, i - i_c - 1$$

The remaining interior panels upstream of the special Mach line in the same row are

$$N_p(i_c + 1 - j, k + i - i_c - j), \text{ for } j = 1, 2, 3, 4, \ldots, k + i - i_c - 2$$

where $N_p(i,k) = i(i-1)/2 + k$ for $i < i_c$.

The supersonic leading edge panel in the same row as the kth panel in the ith row is

$$N_p\ (2i_c-i-k+2,1)$$

Contributions to the x variable alone in μ for the kth panel of the ith column are given by

$$\sum_{j=1}^{i-i_c-1} x_{2i_c-i+2-k}\ s_2\ G\left(i-j,\ k+j,\ x_{2i_c-i+2-k},\ s_2\right)$$

$$+\sum_{j=1}^{k+1-i_c-2} x_{2i_c-i+2-k}\ s_1\ G\left(i_c+1-j,\ k+i-i_c-j,\ x_{2i_c-i+2-k},\ s_1\right)$$

$$+\ x_{2i_c-i+2-k}\ G\left(2i_c-i-k+2,\ 1,\ x_{2i_c-i-k+1},\ s_1\right) \qquad \text{(A31)}$$

Contributions to the y variable in μ for the kth panel of the ith column are

$$\sum_{j=1}^{k-2} \epsilon_2 s_2\ y_{i-1}\ G\left(i,\ k-j,\ \epsilon_2 s_2,\ y_{i-1}\right)$$

$$-\epsilon_2\ y_i\ G\left(i,\ 1,\ \epsilon_2 s_2,\ y_{i-1}\right)$$

$$+\ x_{2i_c-i+2-k}\ y_{i-1}\ G\left(i,\ k,\ x_{2i_c-i+2-k},\ y_{i-1}\right) \qquad \text{(A32)}$$

Except for a constant, μ_{ik} is given by the sum of equations (A31) and (A32). For k = 2, this constant will be zero since μ_{il} vanishes for $y_{i-1} = s_2$ and $x_{2i_c-i-1} = \epsilon_2 s_2$, a point on the leading edge.

To make μ continuous on the upstream edge of the first panel in the ith column, we set k = 2 and replace i by i-1 in equations (A31) and (A32).

Combining the results for $y_{i-1} = 0$, and equating to μ defined by equation (A30) for $y_{i-1} = 0$, we obtain

$$x_{2i_c-i+1}\, G\left(i,\ 1,\ x_{2i_c-i+1},\ 0\right)$$

$$= \sum_{j=0}^{i-i_c-2} x_{2i_c-i+1}\, s_2\, G\left(i-j-1,\ 2+j,\ x_{2i_c-i+1},\ s_2\right)$$

$$+ \sum_{i=1}^{i-i_c-1} x_{2i_c-i+1}\, s_1\, G\left(i_c+1-j,\ i-i_c+1-j,\ x_{2i_c-i+1},\ s_1\right)$$

$$+ x_{2i_c-i+1}\, G\left(2i_c-i+1,\ 1,\ x_{2i_c-i},\ s_1\right) \qquad \text{(A33)}$$

For the corner panel $i = i_c + 1$, equation (A33), takes the form

$$x_{i_c}\, G\left(i_c+1,\ 1,\ x_{i_c},\ 0\right) = x_{i_c}\, G\left(i_c,\ 1,\ x_{i_c-1},\ s_1\right)$$

Using the relation $x_{2i_c-i-1} = x_{2i_c-i} - \epsilon_1 s_1$, combining coefficients of x_{2i_c-i} and $x^2{}_{2i_c-i}$, and setting the coefficients in equation (A33) equal to zero yields two relations which reduce the free parameters of the subsonic leading edge panel to two.

To determine the constants resulting from the upstream panel corners for the columns $i > i_c$, we note that the constants from the panel corners are incorporated into the subsonic leading edge by means of the continuity conditions in equation (A33). Hence, for the kth panel in the ith column, the contributions to the constant term in μ_{ik} occur only for the rows k – 1 to 2. Since the constant term itself does not affect the pressure distribution it will not be written down. Accordingly, the doublet distribution for $i > i_c$ takes the form

$$\mu_{ik} = x_{2i_c-i+2-k}\, y_{i-1}\, G\left(i,\ k,\ x_{2i_c-i+2-k},\ y_{i-1}\right)$$

$$+ \sum_{j=1}^{i-i_c-1} x_{2i_c-i+2-k}\, s_2\, G\left(i-j,\ k+j,\ x_{2i_c-i+2-k},\ s_2\right)$$

$$+ \sum_{j=1}^{k+i-i_c-2} x_{2i_c-i+2-k}\, s_1\, G\left(i_c+1-j,\ k+i-i_c-j,\ x_{2i_c-i+2-k},\ s_1\right)$$

$$+ x_{2i_c-i+2-k}\, G\left(2i_c-i-k+2,\ 1,\ x_{2i_c-i-k+1},\ s_1\right)$$

$$+ \sum_{j=1}^{k-2} \epsilon_2 s_2\, y_{i-1}\, G\left(i,\ k-j,\ \epsilon_2 s_2,\ y_{i-1}\right)$$

$$- \epsilon_2\, y_{i-2}\, G\left(i,\ 1,\ \epsilon_2 s_2,\ y_{i-1}\right) + \text{constant} \qquad \text{(A34)}$$

A7 FORMULAS FOR THE DOWNWASH IN COLUMNS BEHIND SUPERSONIC LEADING EDGE ($i < i_c$)

Let W_{ik} be the contribution to the downwash $\partial\phi/\partial z$ from the panel variables in the kth panel of the ith column. For $i < i_c$, W_{ik} is defined in equation (A6) for a supersonic leading edge panel (k = 1), in equation (A9) for interior panels and by equation (A13) for subsonic leading edge panels. For the total downwash at the point on the kth panel of the ith column we add the contributions from all the panels upstream of the kth panel in the ith column. The contributions from the same row are

$$\sum_{m=0}^{k-1} W_{i-m,k-m}$$

The contributions from the row above the kth panel are

$$\sum_{m=0}^{k-2} W_{i-m,k-m-1}$$

and finally from all panels upstream of the kth panel of the ith column we have

$$W = \sum_{n=0}^{k-1} \sum_{m=0}^{k-n-1} W_{i-m,\,k-m-n}$$

Since the downwash W is computed from a different formula for the supersonic leading edge panels than for the interior panels it is convenient to separate them, thus we write

$$W = \sum_{m=0}^{k-1} W_{i-m,1} + \sum_{n=0}^{k-2} \sum_{m=0}^{k-n-2} W_{i-m,k-m-n} \qquad \text{(A35)}$$

Substituting equations (A6) and (A9) into equation (A35) yields

$$\pi W/M\sqrt{\epsilon} = \sum_{j=1}^{4} \sum_{m=0}^{k-1} X_{N(i-m,1,j)}\, g_j\left(x_{i-m-1}, y_{i-m-1}\right)$$

$$+ \sum_{j=1}^{4} \sum_{n=0}^{k-2} \sum_{m=0}^{k-n-2} X_{N(i-m,\,k-m-n,\,j)}\, h_j\left(x_{i-k+n+1}, y_{i-m-1}\right) \qquad \text{(A36)}$$

where $N(i,k,j) = 2i(i-1) + 4k + j - 4$.

A8 FORMULAS FOR THE DOWNWASH IN COLUMNS BEHIND SUBSONIC LEADING EDGE $(i > i_c)$

We consider the downwash in the kth panel of the ith column where now $i > i_c$. The panel number in the i_c column in the same row as the $N_p(i,k)$ panel is

$$N_p\left(i_c, i-i_c+k-1\right)$$

The contribution to W for all the panels in columns behind the supersonic leading edge is found from equation (A35) by setting $i = i_c$ and replacing k by $i-i_c + k-1$ or

$$\sum_{m=0}^{i-i_c+k-2} W_{i_c-m,1} + \sum_{n=0}^{i-i_c+k-3} \sum_{m=0}^{i-i_c+k-3-n} W_{i_c-m,i-i_c+k-1-m-n}$$

The contributions of the downwash to the kth panel of the ith column from panels in the columns whose numbers are greater than i_c and in the same or k row are

$$\sum_{m=0}^{i-i_c-1} W_{i-m,k+m}$$

Similarly for the k-1 row

$$\sum_{m=0}^{i-i_c-1} W_{i-m,k+m-1}$$

and for all k-2 rows

$$\sum_{n=0}^{k-2} \sum_{m=0}^{i-i_c-1} W_{i-m,\,k+m-n}$$

The contributions from the subsonic leading edge panels are

$$\sum_{m=0}^{i-i_c-1} W_{i-m,1}$$

and from the remaining interior panels

$$\sum_{n=0}^{i-i_c-2} \sum_{m=0}^{i-i_c-2-n} W_{i-m-n-1,2+m}$$

The total downwash for a point on the kth panel of the ith column for $i > i_c$ is, finally,

$$W = \sum_{m=0}^{i-i_c+k-2} W_{i_c-m,1} + \sum_{n=0}^{i-i_c+k-3} \sum_{m=0}^{i-i_c+k-3-n} W_{i_c-m,i-i_c+k-1-m-n}$$

$$+ \sum_{m=0}^{i-i_c-1} W_{i-m,1} + \sum_{n=0}^{k-2} \sum_{m=0}^{i-i_c-1} W_{i-m,k+m-n}$$

$$+ \sum_{n=0}^{i-i_c-2} \sum_{m=0}^{i-i_c-2-n} W_{i-m-n-1,2+m} \qquad \text{(A37)}$$

For the supersonic leading edge we have

$$\pi W_{i_c-m,1}/M\sqrt{\epsilon_1}$$

$$= \sum_{j=1}^{4} X_{N(i_c-m,1,j)} g_j \left(x_{i_c-m-1}, y_{i_c-m-1}\right) \qquad \text{(A38)}$$

for the subsonic leading edge

$$\pi W_{i-m,1}/M\sqrt{\epsilon_2}$$

$$= \sum_{j=1}^{4} X_{N(i-m,1,j)} S_j \left(x_{2i_c-i+m-1}, y_{i-m-1}\right) \qquad \text{(A39)}$$

and for the interior panels in columns $i > i_c$

$$\pi W_{i,k}/M\sqrt{\epsilon_2} = \sum_{j=1}^{4} X_{N(i,k,j)} h_j \left(x_{2i_c-i-k+2}, y_{i-1}\right) \qquad \text{(A40)}$$

and for interior panels in columns $i < i_c$

$$\pi W_{ik}/M\sqrt{\epsilon_1} = \sum_{j=1}^{4} X_{N(i,k,j)}\, h_j \left(x_{i-k+1}, y_{i-1}\right) \tag{A41}$$

Note that for $i < i_c$,

$$\begin{aligned} y_{i-1} &= y - (i-1)s_1 \\ N(i,k,j) &= 2i(i-1) + 4(k-1) + j \end{aligned} \tag{A42}$$

while for $i > i_c$

$$\begin{aligned} y_{i-1} &= y - i_c s_1 - (i_c - i + 2)\, s_2 \\ N(i,k,j) &= 2i_c(i_c+1) + 2(3i_c - i + 2)\,(i - i_c - 1) + 4(k-1) + j \end{aligned} \tag{A43}$$

Continuity of downwash along the supersonic leading edge at panel corners requires continuity of the derivatives of μ at panel corners. For the point between the i and i+1 columns, this becomes

$$X_{N(i+1,1,1)} = X_{N(i,1,1)} - \epsilon_1 s_1\, X_{N(i,1,2)} + s_1\, X_{N(i,1,3)} - \epsilon_1 s_1^2\, X_{N(i,1,4)} \tag{A44}$$

A9 MATRIX EQUATIONS FOR THE DOUBLET PANEL METHOD

At each panel both equations (A36) and (A37) for the downwash reduce to an equation of the form

$$\sum_{n=1}^{N} A_n X_n = W$$

where W is the local camber slope dz/dx_0 for the wing at a selected control point of the panel. Four such equations are needed for each panel since there are four variables to be defined at each panel. For subsonic leading panels two of these equations are provided by the condition that μ be continuous with the upstream panels by matching the coefficients of x and x^2 in equation (A33). Another condition is the continuity of the normal gradient of μ at a point on the upstream boundary of the panel. This condition is relaxed for panels bordering a special Mach line where pressure or pressure gradients may be discontinuous. The designation of downwash control points is indicated by dots and continuity of normal derivatives of μ at panel boundaries is indicated by arrows in figure 6 with the arrow heads lying in the panels in which the conditions apply. These continuity conditions are prescribed at the supersonic leading edge panel corners at

$$x = 0,\ y = s_1$$

for interior panels at

$$x = 0, y = s_1$$

$$x = \epsilon_1 s_1, y = 0$$

and for subsonic leading edge panels at

$$x = \epsilon_1 s_1 = \epsilon_2 s_2, y = 0,$$

when expressed in local panel coordinates. Noting that

$$\left.\begin{aligned} \frac{\partial}{\partial x}\left[x_\ell\, y_m\, G\left(\alpha, \beta, x_\ell, y_m\right)\right] &= y_m\, G\left(\alpha, \beta, 2x_\ell, y_m\right) \\ \text{and} \\ \frac{\partial}{\partial y}\left[x_\ell\, y_m\, G\left(\alpha, \beta, x_\ell, y_m\right)\right] &= x_\ell\, G\left(\alpha, \beta, x_\ell, 2y_m\right) \end{aligned}\right\} \quad \text{(A45)}$$

the conditions that $\partial\mu/\partial x$ is continuous at $x_{i-k+1} = \epsilon_1 s_1$ and $y_{i-1} = 0$ for the kth panel in the ith column is

$$\frac{\partial}{\partial y}\ \mu_{i,k}\ \Big|_{\epsilon_1 s_1, 0} = \frac{\partial}{\partial y}\ \mu_{i-1,k-1}\ \Big|_{\epsilon_1 s_1, s_1} \quad \text{(A46)}$$

From equation (A27) with the aid of equation (A45), equation (A46) becomes

$$\begin{aligned} s_1\, G\left(i, k, \epsilon_1 s_1, 0\right) + G\left(i, 1, 0, 0\right) + s_1 \sum_{i=2}^{k-1} G\left(i, j, \epsilon_1 s_1, 0\right) \\ = s_1\, G\left(i-1, k-1, \epsilon_1 s_1, 2\, s_1\right) + G\left(i-1, 1, 0, 2\, s_1\right) \\ + s_1 \sum_{j=2}^{k-2} G\left(i-1, j, \epsilon_2 s_1, 2\, s_1\right) \end{aligned} \quad \text{(A47)}$$

This leads to homogeneous equations of the form

$$\sum_{n=1}^{N} A_n X_n = 0$$

The other continuity condition

$$\frac{\partial}{\partial x}\ \mu_{i,k}\ \Big|_{0, s_1} = \frac{\partial}{\partial x}\ \mu_{i,k-1}\ \Big|_{\epsilon_1 s_1, s_1} \quad \text{(A48)}$$

with the aid of equations (A27) and (A45) leads to

$$s_1\, G(i, k, 0, s_1) + X_{N(i-k+1,\,1,\,1)} - \epsilon_1 s_1\, X_{N(i-k+1,\,1,\,2)}$$

$$+ s_1\left[X_{N(i-k+1,\,1,\,3)} - \epsilon_1 s_1\, X_{N(i-k+1,\,1,\,4)}\right] + s_1 \sum_{j=1}^{k-2} G\left(i-j, k-j, 0, s_1\right)$$

$$= s_1\, G\left(i, k-1, 2\,\epsilon_1 s_1, s_1\right) + X_{N(i-k+2,\,1,\,1)} + \epsilon_1 s_1\, X_{N(i-k+2,\,1,\,2)}$$

$$+ s_1\left[X_{N(i-k+2,\,1,\,3)} + \epsilon_1 s_1\, X_{N(i-k+2,\,1,\,4)}\right]$$

$$+ s_1 \sum_{j=1}^{k-3} G\left(i-j, k-1-j, 2\,\epsilon_1 s_1, s_1\right) \tag{A49}$$

The case for which k = 2, must be treated separately. Equation (A46) yields

$$\frac{\partial}{\partial y}\left[x_{i-1}\, y_{i-1}\, G\left(i, 2, x_{i-1}, y_{i-1}\right) + \epsilon_1\, y_{i-1}\, G\left(i, 1, 0, y_{i-1}\right)\right] \epsilon_1 s_1, 0$$

$$= \frac{\partial}{\partial y}\left[\left(x_{i-2} + \epsilon_1\, y_{1-2}\right) G\left(i-1, 1, x_{i-2}, y_{1-2}\right)\right]_{0,\, s_1} \tag{A50}$$

or

$$s_1\, G\left(i, 2, \epsilon_1 s_1, 0\right) + G\left(i, 1, 0, 0\right) = G\left(i-1, 1, 0, 2\, s_1\right) \tag{A51}$$

Similarly, equation (A48) yields

$$\frac{\partial}{\partial x}\left[x_{i-1}\, y_{i-1}\, G\left(i, 2, x_{i-1}, y_{i-1}\right) + x_{i-1}\, G\left(i-1, 1, x_{i-2}, s_1\right)\right]_{0,\, s_1}$$

$$= \frac{\partial}{\partial x}\left[\left(x_{i-1} + \epsilon_1\, y_{i-1}\right) G\left(i, 1, x_{i-1}, y_{i-1}\right)\right]_{0,\, s_1} \tag{A52}$$

or

$$s_1\, G\left(i, 2, 0, s_1\right) + G\left(i-1, 1-\epsilon_1 s_1, s_1\right)$$

$$= \epsilon_1 s_1\left[X_{N(i,\,1,\,2)} + s_1\, X_{N(i,\,1,\,4)}\right] + G\left(i, 1, 0, s_1\right) \tag{A53}$$

Continuity of $\partial\mu/\partial y$ on the upstream boundary of the subsonic leading edge panel of the ith column is found by setting k = 2, replacing i by i – 1 in equation (A34), and differentiating. Thus with equation (A30), we have

$$\frac{\partial}{\partial y}\Big[\, x_{2i_c-i+1}\, y_{i-2}\, G\Big(i-1,\, 2,\, x_{2i_c-i-1},\, y_{i-2}\Big) - \epsilon_2\, y_{i-3}\, G\Big(i-1,\, 1,\, \epsilon_2 s_2,\, y_{i-2}\Big)\Big]_{\epsilon_2 s_2,\, s_2}$$

$$= \frac{\partial}{\partial y}\Big[\Big(x_{2i_c-i+1} - \epsilon_2\, y_{i-1}\Big)\, G\Big(i,\, 1,\, x_{2i_c-i+1},\, y_{i-1}\Big)\Big]_{\epsilon_2 s_2,\, 0}$$

or

$$s_2\, G\Big(i-1,\, 2,\, \epsilon_2 s_2,\, 2\, s_2\Big) - G\Big(i-1,\, 1,\, \epsilon_2 s_2,\, 2\, s_2\Big)$$

$$= s_2\, \Big[\, X_{N(i,1,3)} + \epsilon_2 s_2\, X_{N(i,\,1,\,4)}\Big] - G\Big(i,\, 1,\, \epsilon_2 s_2,\, 0\Big)$$

Equations corresponding to equations (A47) and (A49) for interior panels for $i > i_c$ can be derived in a similar manner using equation (A34) for μ_{ik}.

A10 SOURCE DISTRIBUTION FOR COLUMNS BEHIND SUPERSONIC LEADING EDGE

The source panel method follows essentially the same procedure as the doublet method, and we use the same wing planform to test the method. For supersonic leading edge panels, a quadratic source distribution in the following form is used:

$$\sigma = a + bx + cy + dxy \tag{A54}$$

where the origin is at the upstream corner of the panel. One parameter is fixed by requiring σ to be continuous along the leading edge. For the supersonic leading edge panels denoted by subscripts 1 and 2 and numbered 1 and 2 in figure 22, the continuity conditions take the form

$$a_2 = a_1 - b\epsilon_1 s_1 + cs_1 - d\epsilon_1 s_1^{\,2} \tag{A55}$$

for a leading edge of the form $x + \epsilon_1 y = 0$. Here s_1 is the panel width (y direction).

For interior panels, we associate a single free parameter and modify the source distribution by

$$\sigma = d\, xy \tag{A56}$$

where the origin of x and y is at the upstream leading edge corner of the panel. Since it vanishes on the leading edges, it preserves continuity when σ is continued downstream along Mach line strips by the value on the panel trailing edge in the same manner as the doublet panel method.

To construct the value of the source at some kth interior panel in column i we consider the same wing as in the doublet method. From figure 22 we define σ in the leading edge panels as

$$\sigma_1 = a_1 + b_1 + c_1 y + d_1 xy$$

$$\sigma_2 = a_2 + b_2 x_1 + c_2 y_1 + d_2 x_1 y_1$$

$$\sigma_4 = a_4 + b_4 x_2 + c_4 y_2 + d_4 x_2 y_2 \qquad \text{(A57)}$$

where x_i, y_j has the same meaning as in the doublet paneling. To preserve continuity the source distribution in panel 3 takes the form

$$\sigma_3 = \sigma_1 (x, s_1) + \sigma_2 (0, y_1) - \sigma_2 (0, 0) + d_3 x_1 y_1 \qquad \text{(A58)}$$

Since $a_2 = a_1 - b\,\epsilon_1 s_1 + c s_1 - d\,\epsilon_1 s_1^2$ from equation (A55) we have

$$\sigma_1 (x, s_1) - \sigma_2 (0, 0) = (b_1 + d_1 s_1)\ (x + \epsilon_1 s_1)$$

$$= (b_1 + d_1 s_1)\ x_1$$

from which

$$\sigma_3 = (b_1 + d_1 s_1)\ x_1 + a_2 + c_2 y_1 + d_3 x_1 y_1 \qquad \text{(A59)}$$

and similarly

$$\sigma_5 = (b_2 + d_2 s_1)\ x_2 + a_4 + c_4 y_2 + d_5 x_2 y_2 \qquad \text{(A60)}$$

To find σ_6 we write

$$\sigma_6 = \sigma_3 (x_1, s_1) + \sigma_5 (\epsilon_1 s_1, y_2) - \sigma_5 (\epsilon_1 s_1, 0) + d_6 x y_2 \qquad \text{(A61)}$$

or

$$\sigma_6 = (b_1 + d_1 s_1)\ x_1 + d_3 s_1 x_1 + d_5 \epsilon_1 s_1 y_2 + d_6 + y_2$$

$$+ a_4 + c_4 y_2 + (b_2 + d_2 s_1)\ \epsilon_1 s_1 \qquad \text{(A62)}$$

We note that the supersonic leading edge panels are continued in the y characteristic strip in the form

$$(b_1 + d_1 s_1) x_1$$

and the constant term, a, only enters for the leading edge panel of the same column as the panel under consideration.

The panel numbering system for the source panel method is identical to that used in the doublet panel method. The panel number for $i < i_c$ for the kth panel in the ith column is then given by

$$N_p = i(i-1)/2 + k \quad , \quad k = 1, 2, \ldots, i$$

For k=1, the leading edge panel has four associated parameters while for all other k there is only one associated parameter. The variable (or parameter) number in the kth panel ($k > 1$) is

$$N(i,k) = i(i-1)/2 + k + 3i = i(i+5)/2 + k, \; k > 1 \tag{A63}$$

For k = 1, the variable numbers are.

$$N_1(i,j) = i(i+5)/2 + j - 3 \quad , \quad j = 1,2,3,4$$

The pattern in equation (A62) can be generalized and for the kth panel in the ith column we have

$$\begin{aligned}
\sigma_{ik} = & \left(X_{N_1(i-k+1,2)} + s_1 X_{N_1(i-k+1,4)} \right) x_{i-k+1} \\
& + s_1 \sum_{j=1}^{k-2} X_{N(i-j,k-j)} x_{i-k+1} \\
& + \epsilon_1 s_1 \sum_{j=1}^{k-2} X_{N(i,k-j)} y_{i-1} \\
& + X_{N_1(i,1)} + X_{N_1(i,3)} y_{i-1} + X_{N(i,k)} x_{i-k+1} y_{i-1} \\
& + \sum_{j=1}^{k-2} \left(X_{N_1(i-j,2)} + s_1 X_{N_1(i-j,4)} \right) \epsilon_1 s_1 \\
& + \epsilon_1 s_1^2 \sum_{n=1}^{k-3} \sum_{m=1}^{k-2-n} X_{N(i-n,k-m-n)}
\end{aligned} \tag{A64}$$

where N(i,k) denotes the variable number for the kth panel defined for $k > 1$ in equation (A63), and $N_1(i,j)$ denotes the variable numbers for the first panel of the ith column given by the equation following equation (A63).

A11 PRESSURE COEFFICIENT FROM THE SUPERSONIC LEADING EDGE PANELS AND FROM THE INTERIOR PANELS

The velocity potential resulting from a leading edge panel for points in the panel is seen from equation (15) to be

$$\phi = -\frac{4}{\pi M} \int_0^{\sqrt{y+x/\epsilon_1}} \int_0^{\sqrt{x+\epsilon_1 (y-\eta^2)}} \sigma\left(x-\xi^2, y-\eta^2\right) d\xi d\eta \tag{A65}$$

where $x + \epsilon_1 y = 0$ defines the leading edge.

For points outside the panel, $x < 0$, $y > s_1$, we have

$$\phi = -\frac{4}{\pi M} \left\{ \int_{\sqrt{y-s_1}}^{\sqrt{y+x/\epsilon_1}} \int_0^{\sqrt{x+\epsilon_1(y-\eta^2)}} \sigma\left(x-\xi^2, y-\eta^2\right) d\xi d\eta \right.$$
$$\left. + \int_0^{\sqrt{y-s_1}} \int_0^{\sqrt{x+\epsilon_1 s_1}} \sigma\left(x-\xi^2, s_1\right) d\xi d\eta \right\} \tag{A66}$$

For $x > 0$, $y < s_1$, we obtain

$$\phi = -\frac{4}{\pi M} \left\{ \int_0^{\sqrt{y}} \int_{\sqrt{x}}^{\sqrt{x+\epsilon_1 \left(y-\zeta^2\right)}} \sigma\left(x-\xi^2, y-\eta^2\right) d\xi d\eta \right.$$
$$\left. + \int_0^{\sqrt{y}} \int_0^{\sqrt{x}} \sigma\left(0, y-\eta^2\right) d\xi d\eta \right\} \tag{A67}$$

Similarly, for $x > 0$, $y > s_1$,

$$\phi = -\frac{4}{\pi M}\left\{\int_{\sqrt{y-s_1}}^{\sqrt{y}}\int_{\sqrt{x}}^{\sqrt{x+c_1\left(y-\eta^2\right)}}\sigma\left(x-\xi^2, y-\eta^2\right)d\xi d\eta\right.$$

$$+\int_{\sqrt{y-s_1}}^{\sqrt{y}}\int_{0}^{\sqrt{x}}\sigma\left(0, y-\eta^2\right)d\xi d\eta$$

$$+\int_{0}^{\sqrt{y-s_1}}\int_{\sqrt{x}}^{\sqrt{x+\epsilon_1 s_1}}\sigma\left(x-\xi^2, s_1\right)d\xi d\eta$$

$$\left.+\int_{0}^{\sqrt{y-s_1}}\int_{0}^{\sqrt{x}}\sigma\left(0, s_1\right)d\xi d\eta\right\} \qquad \text{(A68)}$$

Only equations (A66) and (A68) need be considered, since the other two cases result from setting $\sqrt{y-s_1} = 0$ when $y < s_1$ and $\sqrt{x} = 0$ when $x < 0$. From equation (A66) the pressure coefficient becomes

$$C_p = -\frac{M}{B}\left(\phi_x + \phi_y\right) = \frac{4}{\pi B}\left\{\left(1+\epsilon_1\right)\int_{\sqrt{y-s_1}}^{\sqrt{y+x/\epsilon_1}}\frac{\sigma\left(-\epsilon_1\left(y-\eta^2\right), y-\eta^2\right)d\eta}{2\sqrt{x^2+\epsilon_1\left(y-\eta^2\right)}}\right.$$

$$+\int_{\sqrt{y-s_1}}^{\sqrt{y+x/\epsilon_1}}\int_{0}^{\sqrt{x+\epsilon_1\left(y-\eta^2\right)}}\left[\sigma_x\left(x-\xi^2, y-\eta^2\right)+\sigma_y\left(x-\xi^2, y-\eta^2, y\right)\right]d\xi d\eta$$

$$\left.+\int_{0}^{\sqrt{y-s_1}}\int_{0}^{\sqrt{x+\epsilon_1 s_1}}\sigma_x\left(x-\xi^2, s_1\right)d\xi d\eta\right\}$$

where the term $\int_{0}^{\sqrt{y-s_1}}\frac{\sigma\left(-\epsilon_1 s_1, s_1\right)d\eta}{2\sqrt{x+\epsilon_1 s_1}}$ is dropped because of continuity of σ at panel corners.

Equation (A68) yields

$$C_p = \frac{4}{\pi B}\left\{ (1+\epsilon_1) \int_{\sqrt{y-s_1}}^{\sqrt{y}} \frac{\sigma\left(-\epsilon_1\left(y-\eta^2\right), y-\eta^2\right) d\eta}{2\sqrt{x+\epsilon_1\left(y-\eta^2\right)}} \right.$$

$$+ \int_{\sqrt{y-s_1}}^{\sqrt{y}} \int_{\sqrt{x}}^{\sqrt{x+\epsilon_1 (y-\eta^2)}} \left[\sigma_x\left(x-\xi^2, y-\eta^2\right) + \sigma_y\left(x-\xi^2, y-\eta^2\right)\right] d\xi d\eta$$

$$+ \int_{\sqrt{y-s_1}}^{\sqrt{y}} \int_{0}^{\sqrt{x}} \sigma_y\left(0, y-\eta^2\right) d\xi d\eta$$

$$\left. + \int_{0}^{\sqrt{y-s_1}} \int_{\sqrt{x}}^{\sqrt{x+\epsilon_1 s_1}} \sigma_x\left(x-\xi^2, s_1\right) d\xi d\eta \right\} \qquad \text{(A69)}$$

where we have neglected the terms

$$\frac{1}{2\sqrt{y}} \int_0^{\sqrt{x}} \sigma\,(0,0)\, d\xi \quad \text{and} \quad \frac{1}{2\sqrt{x+\epsilon_1 s_1}} \int_0^{\sqrt{y-s_1}} \sigma\left(-\epsilon_1 s_1, s_1\right) d\eta$$

which are cancelled because of the continuity of σ at panel corners.

Choosing $\sigma(x,y) = a + bx + cy + dxy$ and integrating yields C_p in the form

$$C_p = \left(\sqrt{\epsilon_1}/\pi B\right)\left[a\,\bar{g}_1\,(x,y) + b\,\bar{g}_2\,(x,y) + c\,\bar{g}_3\,(x,y) + d\,\bar{g}_4(x,y)\right] \qquad \text{(A70)}$$

where the $\bar{g}$ functions are derived in section B6 of appendix B.

For interior panels, we use a source distribution of the form

$$\sigma = d\,x\,y \qquad \text{(A71)}$$

with the origin of the coordinates at the upstream corner. The velocity potential for interior panels is given by

$$\phi = -\frac{4}{\pi M} \int_0^{\sqrt{y}} \int_0^{\sqrt{x}} \sigma\left(x-\xi^2, y-\eta^2\right) d\xi d\eta \qquad \text{(A72)}$$

for $x < \epsilon_1 s_1$, $y < s_1$. For $x > \epsilon_1 s_1$ and $y > s_1$, we have

$$\phi = -\frac{4}{\pi M}\left\{\int_{\sqrt{y-s_1}}^{\sqrt{y}}\int_{\sqrt{x-\epsilon_1 s_1}}^{\sqrt{x}} \sigma\left(x-\xi^2, y-\eta^2\right) d\xi d\eta + \int_{\sqrt{y-s_1}}^{\sqrt{y}}\int_{0}^{\sqrt{x-\epsilon_1 s_1}} \sigma\left(\epsilon_1 s_1, y-\eta^2\right) d\xi d\eta\right.$$

$$\left. + \int_{0}^{\sqrt{y-s_1}}\int_{0}^{\sqrt{x-\epsilon_1 s_1}} \sigma\left(\epsilon_1 s_1, s_1\right) d\xi d\eta + \int_{0}^{\sqrt{y-s_1}}\int_{\sqrt{x-\epsilon_1 s_1}}^{\sqrt{x}} \sigma\left(x-\xi^2, s_1\right) d\xi d\eta\right\} \qquad \text{(A73)}$$

The pressure coefficient from equation (A73) becomes

$$C_p = \frac{4}{\pi B}\left\{\int_{\sqrt{y-s_1}}^{\sqrt{y}}\int_{\sqrt{x-\epsilon_1 s_1}}^{\sqrt{x}} \left[\sigma_x\left(x-\xi^2, y-\eta^2\right) + \sigma_y\left(x-\xi^2, y-\eta^2\right)\right] d\xi d\eta\right.$$

$$+ \int_{\sqrt{y-s_1}}^{\sqrt{y}}\int_{0}^{\sqrt{x-\epsilon_1 s_1}} \sigma_y\left(\epsilon_1 s_1, y-\eta^2\right) d\xi d\eta$$

$$\left. + \int_{0}^{\sqrt{y-s_1}}\int_{\sqrt{x-\epsilon_1 s_1}}^{\sqrt{x}} \sigma_x\left(x-\xi^2, s_1\right) d\xi d\eta\right\} \qquad \text{(A74)}$$

where we have used the condition $\sigma(0,y) = \sigma(x,0) = 0$. Integration yields

$$C_p = (4/\pi B)\, d\,\bar{h}\,(x,y) \qquad \text{(A75)}$$

where $\bar{h}(x,y)$ is given in section B7 of appendix B.

A12 PRESSURE COEFFICIENT FROM THE SUBSONIC LEADING EDGE PANELS

The contribution to the source distribution from subsonic leading edge panels is simpler than that from supersonic leading edges. With the origin of the panel coordinates at the upstream corner, the source distribution from parameters associated with the panel is given by

$$\sigma = cy + dxy \tag{A76}$$

Unlike the doublet panels, the value of σ on the upstream panel edge is continued into the subsonic leading edge panel since σ need not vanish on the subsonic leading edge as the doublet must. For points in the panel, $x < \epsilon_2 s_2$, $y < s_2$, we have

$$\phi = -\frac{4}{\pi M} \int_0^{\sqrt{y}} \int_0^{\sqrt{x - \epsilon_2 (y - \eta^2)}} \sigma\left(x - \xi^2, y - \eta^2\right) d\xi d\eta \tag{A77}$$

For points outside the panel in which $x > \epsilon_2 s_2$ and $y < s_2$, we have

$$\phi = -\frac{4}{\pi M} \int_0^{\sqrt{y}} \left[\int_{\sqrt{x - \epsilon_2 s_2}}^{\sqrt{x - \epsilon_2 (y - \eta^2)}} \sigma\left(x - \xi^2, y - \eta^2\right) d\xi + \int_0^{\sqrt{x - \epsilon_2 s_2}} \sigma\left(\epsilon_2 s_2, y - \eta^2\right) d\xi \right] d\eta \tag{A78}$$

Similarly, for $x > \epsilon_2 s_2$ and $y > s_2$, we obtain

$$\phi = -\frac{4}{\pi M} \left\{ \int_{\sqrt{y - s_2}}^{\sqrt{y}} \left[\int_{\sqrt{x - \epsilon_2 s_1}}^{\sqrt{x - \epsilon_2 (y - \eta^2)}} \sigma\left(x - \xi^2, y - \eta^2\right) d\xi + \int_0^{\sqrt{x - \epsilon_2 s_2}} \sigma\left(\epsilon_2 s_2, y - \eta^2\right) d\xi \right] d\eta \right.$$
$$\left. + \int_0^{\sqrt{y - s_2}} \int_0^{\sqrt{x - \epsilon_2 (y - \eta^2)}} \sigma\left(\epsilon_2 s_2, s_2\right) d\xi d\eta \right\} \tag{A79}$$

With ϕ defined by equation (A79) the pressure coefficient becomes

$$C_p = \frac{4}{\pi B}\left\{(1-\epsilon_2)\left[\int_{\sqrt{y-s_2}}^{\sqrt{y}} \frac{\sigma\left(\epsilon_2\left(y-\eta^2\right), y-\eta^2\right)d\eta}{2\sqrt{x-\epsilon_2\left(y-\eta^2\right)}} + \int_0^{\sqrt{y-s_2}} \frac{\sigma\left(\epsilon_2 s_2, s_2\right)d\eta}{2\sqrt{x-\epsilon_2\left(y-\eta^2\right)}}\right]\right.$$

$$+ \int_{\sqrt{y-s_2}}^{\sqrt{y}} \int_{\sqrt{x-\epsilon_2 s_2}}^{\sqrt{x-\epsilon_2\left(y-\eta^2\right)}} \left[\sigma_x\left(x-\zeta^2, y-\eta^2\right) + \sigma_y\left(x-\zeta^2, y-\eta^2\right)\right] d\zeta d\eta$$

$$\left. + \int_{\sqrt{y-s_2}}^{\sqrt{y}} \int_0^{\sqrt{x-\epsilon_2 s_2}} \sigma_y\left(\epsilon_2 s_2, y-\eta^2\right) d\zeta d\eta \right\} \qquad \text{(A80)}$$

Substituting equation (A76) for σ into equations (A80) yields a relation of the form

$$C_p = \left(2\sqrt{\epsilon_2}/\pi B\right)\left[c\bar{S}_1\,(x,y) + d\bar{S}_2\,(x,y)\right] \qquad \text{(A81)}$$

where $\bar{S}_1$ and $\bar{S}_2$ are derived in section B8 of appendix B.

A13 CORRECTION TO THE PRESSURE COEFFICIENT FROM SUPERSONIC LEADING EDGE PANELS AND FROM INTERIOR PANELS WHEN THE SUBSONIC LEADING EDGE PANEL OF THE SAME ROW IS IN THE ZONE OF DEPENDENCE OF THE CONTROL POINT

The formulas developed in sections A11 and A12 for supersonic leading edge and interior rectangular panels were derived on the assumption that the characteristic strip in which they lie extended all the way to the Mach lines through the control point x,y as indicated in figures 4 and 8. These formulas must be corrected when the Mach line cuts the subsonic leading edge at the end of the row as shown in figures 23 and 24. There will be an additional contribution from the line integral of σ along the subsonic leading edge and an area integral subtracted from the results in sections A11 and A12 because of the termination of the characteristic strip by the subsonic leading edge panel.

We consider a point (x,y) as shown in figure 23 and compute the pressure resulting from the contribution of the supersonic leading edge panel. The value of σ on the downstream side of the triangular panel on the supersonic edge is carried on in the strip downstream of the panel edge by its value on the panel edge, or, as shown in section A10,

$$\sigma = \left(b + ds_1\right) x_1$$

where the origin of x_1 is on the upstream edge of the subsonic leading edge panel.

To find the correction to the pressure coefficient for the panel due to the subsonic leading edge in the zone of dependence of the point, we need to subtract the contribution from the area bounded by the lines $\xi = \sqrt{x}$, $\eta = \sqrt{y}$, and the subsonic edge. This integral takes the form

$$\Delta C_{p_a} = -\frac{4}{\pi B}\left(b + ds_1\right) \int_0^{\sqrt{y}} \frac{\int^{\sqrt{x}} d\xi d\eta}{\sqrt{x - \epsilon_2\left(y - \eta^2\right)}}$$

and the contribution from the integral along the segment of subsonic leading edge is

$$\Delta C_{p_\ell} = \frac{2}{\pi B}\left(b + d\,s_1\right) \int_0^{\sqrt{y}} \frac{\epsilon_2\left(1-\epsilon_2\right)\left(y - \eta^2\right) d\eta}{\sqrt{x - \epsilon_2\left(y - \eta^2\right)}} \tag{A82}$$

for points $y < s_2$. For $y > s_2$ we have, instead,

$$\Delta C_{p_a} = -\frac{4}{\pi B}\left(b + d\,s_1\right)\left[\int_{\sqrt{y - s_2}}^{\sqrt{y}} \frac{\int^{\sqrt{x}} d\xi d\eta}{\sqrt{x - \epsilon_2\left(y - \eta^2\right)}} + \int_0^{\sqrt{y-s}} \frac{\int^{\sqrt{x}} d\xi d\eta}{\sqrt{x - \epsilon_2 s_2}}\right] \tag{A83}$$

and

$$\Delta C_{p_\ell} = \frac{2}{\pi B}\,\epsilon_2\left(1 - \epsilon_2\right)\left(b + d\,s_1\right)\left[\int_{\sqrt{y - s_2}}^{\sqrt{y}} \frac{\left(y - \eta^2\right) d\eta}{\sqrt{x - \epsilon_2\left(y - \eta^2\right)}} + s_2 \int_0^{\sqrt{y-s}} \frac{d\eta}{\sqrt{x - \epsilon_2\left(y - \eta^2\right)}}\right] \tag{A84}$$

The evaluation of these integrals yields a relation of the form

$$\Delta C_p = \frac{2}{\pi B}\left(b + d\,s_1\right)\sqrt{\epsilon_2}\; C\,(x,y) \tag{A85}$$

where C(x,y) is derived in section B9 of appendix B. Note that the origin of coordinates for C(x,y) is that for the subsonic leading edge panel on the same row as the supersonic leading edge panel being considered. The correction to the pressure coefficient for rectangular panels is found from equation (A85) with b set equal to zero.

There is required a correction due to the constant value of σ which is obtained from the first subsonic leading edge panel. In this panel the value of σ contributed from the adjacent supersonic leading edge panel is

$$\begin{aligned}\sigma &= a + cs_1 + ds_1 x + bx \\ &= a - b\,\epsilon_1 s_1 + cs_1 - d\,\epsilon_1 s_1^{\,2} + \left(b + ds_1\right)\left(x + \epsilon_1 s_1\right)\end{aligned}$$

This is seen to differ from that in figure 23 by the terms

$$a - b\,\epsilon_1 s_1 + cs_1 - d\,\epsilon_1 s_1^{\,2}$$

The correction to C_p from these terms from the last supersonic leading edge panel for points downstream of the special Mach line from the corner is given by

$$\Delta C_p = \frac{2}{\pi B}\left(a - b\,\epsilon_1 s_1 + c s_1 - d\,\epsilon_1 s_1^2\right) \int_0^{\sqrt{y}} \frac{\left(1-\epsilon_2\right) d\eta}{\sqrt{x-\epsilon_2\left(y-\eta^2\right)}}$$

$$= \frac{2}{\pi B}\sqrt{\epsilon_2}\,\frac{\left(1-\epsilon_2\right)}{\epsilon_2} f_4(x,y)\left(a - b\,\epsilon_1 s_1 + c s_1 - d\,\epsilon_1 s_1^2\right) \qquad \text{(A86)}$$

for a point in the subsonic leading edge region. The function $f_4(x,y)$ is given in equation (B5) of appendix B.

We now consider the subsonic leading edge correction to the pressure from panels. In figure 24 we see that the contribution from the integral along the subsonic leading edge has the same form as σ for the supersonic leading edge panels except that b = 0 and hence the correction to C_p contains the same function C(x,y).

A14 SOURCE DISTRIBUTION FOR PANELS IN COLUMNS BEHIND THE SUBSONIC LEADING EDGE

To define the source distribution in the kth panel for the ith column where $i > i_c$, i_c being the last column with a supersonic leading edge panel, we consider the variable numbering for columns adjoining the subsonic leading edge. The subsonic leading edge panel has two variables while each interior panel has only one. In numbering the variables, we start with the total number of variables in the columns adjoining the supersonic leading edge; i.e.,

$$i_c\left(i_c+5\right)/2 + i_c$$

The variable in the kth panel of the $i_c + 1$ column is then seen to be

$$N\left(i_c+1,k\right) = i_c\left(i_c+5\right)/2 + i_c + k + 1 \text{ for } k > 1$$

Each successive column (i increasing) has one less panel and hence one less variable. For the ith column and kth panel, we have for the variable number

$$N(i,k) = i_c\left(i_c+5\right)/2 + i_c + \sum_{n=1}^{i-i_c-1}\left(i_c+2-n\right) + k + 1$$

Forming the summation and simplifying yields

$$N(i,k) = i_c\left(i_c+5\right)/2 + \left(3i_c - i + 5\right)\left(i-i_c\right)/2 + k - 1$$

for $k > 1$.

The variable numbers for the leading edge panels are

$$N_1(i,j) = i_c\left(i_c+5\right)/2 + \left(3i_c - i + 5\right)\left(i-i_c\right)/2 - 2 + j$$

$$j = 1,2$$

We now find σ_{ik} by combining the contributions from all upstream columns and rows For the kth panel in the ith column, the panel number in the same row and the i_c or $i_c + 1$ column is

$$i - i_c + k - 1$$

The contribution to the x variable from panels in the columns behind the subsonic leading edge is seen to be

$$s_2 \sum_{j=1}^{i-i_c-1} X_{N(i-j,k+j)}\, x_{2i_c-i-k+2} \equiv \Sigma_1\, x_{2i_c-i-k+2} \tag{A87}$$

Contribution to the y variable in the kth panel of the ith column is

$$\epsilon_2 s_2 \sum_{j=1}^{k-2} X_{N(i,k-j)}\, y_{i-1} + \left(X_{N_1(i,1)} + \epsilon_2 s_2\, X_{N_1(i,2)}\right) y_{i-1} \equiv \Sigma_2\, y_{i-1} \tag{A88}$$

The constant terms resulting from the corner values of σ for the rectangular panels in subsonic columns is

$$\Sigma_3 \equiv \epsilon_2 s_2^2 \sum_{n=1}^{i-i_c-2} \sum_{j=1}^{n} X_{N\left(i_c+j,n-j+2\right)}$$

$$+ \sum_{n=1}^{k-1} \sum_{j=1}^{i-i_c-1} \epsilon_2 s_2^2\, X_{N\left(i_c+j,i-i_c+k-n-j\right)} \tag{A89}$$

The contribution to the constant from the subsonic leading edge panels is

$$\Sigma_4 \equiv s_2 \sum_{j=1}^{i-i_c-1} \left[\epsilon_2 s_2\, X_{N_1\left(i_c+j,1\right)} + X_{N_1\left(i_c+j,2\right)}\right] \tag{A90}$$

The contribution to the x variable and to the constant from the supersonic leading edge columns is found by setting $i = i_c$ in equation (A64) and replacing k by $i - i_c + k - 1$ and then substituting $y_{i-1} = s_1$. This yields

$$\left(X_{N_1}(2i_c-i-k+2,2) + s_1\, X_{N_1}(2i_c-i-k+2,4)\right) x_{2i_c-i-k+2}$$

$$+ s_1 \sum_{j=1}^{i-i_c+k-3} X_{N(i_c-j,i-i_c+k-1-j)}\, x_{2i_c-i-k+2}$$

$$+ \epsilon_1 s_1^2 \sum_{j=1}^{i-i_c+k-3} X_{N(i_c,i-i_c+k-1-j)} + X_{N_1}(i_c,1) + X_{N_1}(i_c,3)\, s_1$$

$$+ X_{N(i_c,i-i_c+k-1)}\, s_1\, x_{2i_c-i-k+2} + \sum_{j=1}^{i-i_c+k-3} \left(X_{N_1}(i_c-j,2) + s_1\, X_{N_1}(i_c-j,4)\right) \epsilon_1 s_1$$

$$+ \epsilon_1 s_1^2 \sum_{h=1}^{i-i_c+k-4} \sum_{m=1}^{i-i_c+k-3-\eta} X_{N(i_c-\eta,i-i_c+k-1-m-n)}$$

$$\equiv \Sigma_5\, x_{2i_c-i-k+2} + \Sigma_6 \tag{A91}$$

The source distribution σ_{ik} for the kth panel in the ith column is found by combining equations (A87) and (A91) or

$$\sigma_{ik} = \left(\Sigma_1 + \Sigma_5 + X_{N(i,k)}\, y_{i-1} \right) x_{2i_c-i-k+2}$$

$$+ \Sigma_2\, y_{i-1} + \Sigma_3 + \Sigma_4 + \Sigma_6 \qquad \text{(A92)}$$

Equation (A92) can be interpreted to hold for all i,k, and $i > i_c$ if those summations are dropped for which the upper limits are less than the lower limit or terms in which negative column or panel numbers occur. One exception is the first panel in the $i_c + 1$ column which must be treated separately. Thus,

$$\sigma_{i_c+1,1} = X_{N_1}(i_c,1) - \epsilon_1 s_1\, X_{N_1}(i_c,2) + s_1\, X_{N_1}(i_c,3) - \epsilon_1 s_1^2\, X_{N_1}(i_c,4)$$

$$+ \left[X_{N_1}(i_c,2) + s_1\, X_{N_1}(i_c,4) \right] x_{i_c}$$

$$+ X_{N_1}(i_c+1,1)\, y_{i_c} + X_{N_1}(i_c+1,2)\, x_{i_c}\, y_{i_c}$$

Evaluating equation (A92) for $i = i_c + 1$ and $k = 1$ reveals that we must add the term

$$- \epsilon_1 s_1 \left[X_{N_1}(i_c+1,2) + s\, X_{N_1}(i_{xc}+1,4) \right] \qquad \text{(A93)}$$

to equation (A92) for this particular panel.

For analysis boundary conditions in which the wing shape is given and the pressure is to be found, either equation (A92) or (A64) is set equal to the slope of the wing at the control point of the panel. These equations together with the homogeneous equations involving continuity of σ at panel corners on the supersonic leading edge yield a set of equations to be solved for the x_n variables.

A15 COMPLETE PRESSURE COEFFICIENT FROM THE SOURCE PANELS

The contribution to the pressure coefficient from each panel is summed in the same way as downwash is computed from the doublet panels. From equation (A35), we write for the pressure in the kth panel of the ith column for $i < i_c$

$$C_p = \sum_{m=0}^{k-1} C_{i-m,1} + \sum_{n=0}^{k-2} \sum_{m=0}^{k-\eta-2} C_{i-m,k-m-n} \tag{A94}$$

where the first subscript denotes the column and the second subscript the panel number in the column. For the first sum, we use equation (A70) and obtain

$$C_{i-m,1} = \frac{\sqrt{\epsilon_1}}{\pi B} \sum_{j=1}^{4} X_{N_1(i-m,j)} \bar{g}_j \left(x_{i-m-1}, y_{i-m-1}\right) \tag{A95}$$

and for the second sum, we use equation (A75) and obtain

$$C_{i-m,k-m-n} = \frac{4}{\pi B} X_{N(i-m,k-m-n)} \bar{h}\left(x_{i-k+n-1}, y_{i-m-1}\right) \tag{A96}$$

where N(i,k) and $N_1(i,j)$ are defined in equation (A63) and the following equation. The variable subscripts were found from equation (A20) with i–m replacing i and k–m–n replacing k.

For $i > i_c$, we obtain from equation (A37)

$$\begin{aligned} C_p = {} & \sum_{m=0}^{i-i_c+k-2} C_{i_c-m,1} + \sum_{n=0}^{i-i_c+k-3} \sum_{m=0}^{i-i_c+k-3-n} C_{i_c-m,i-i_c+k-1-m-n} \\ & + \sum_{m=0}^{i-i_c-1} C_{i-m,1} + \sum_{n=0}^{k-2} \sum_{m=0}^{i-i_c-1} C_{i-m,k+m-n} \\ & + \sum_{n=0}^{i-i_c-2} \sum_{m=0}^{i-i_c-2-n} C_{i-m-n-1,2+m} \end{aligned} \tag{A97}$$

In the first two sums, the $C_{j,k}$ terms are computed according to equations (A95) and (A96), respectively, for those panels lying in rows which terminate in a subsonic leading edge panel outside the zone of influence of the kth panel in the ith column. Separating these panels yields

$$C_p = \left\{ \sum_{m=i-i_c}^{i-i_c+k-2} C_{i_c-m,1} + \sum_{n=0}^{k-2} \sum_{m=0}^{i-i_c+k-3-n} C_{i_c-m,i-i_c+k-1-m-n} \right.$$

$$\left. + \sum_{m=0}^{i-i_c-1} C_{i-m,1} + \sum_{n=0}^{k-2} \sum_{m=0}^{i-i_c-1} C_{i-m,k+m-n} \right\}$$

$$+ \sum_{m=0}^{i-i_c-1} C_{i_c-m,1} + \sum_{n=k-1}^{i-i_c+k-3} \sum_{m=0}^{i-i_c+k-3-n} C_{i_c-m,i-i_c+k-1-m-n}$$

$$+ \sum_{n=0}^{i-i_c-2} \sum_{m=0}^{i-i_c-2-n} C_{i-m-n-1,2+m} \qquad \text{(A98)}$$

where the quantities outside the curly brackets require correction terms from subsonic leading edge panels.

The pressure coefficient contribution for the first sum is computed from equation (A95) with i set equation equal to i_c. For the second term we use equation (A75) and obtain

$$C_{i_c-m,i-i_c+k-1-m-n} = \frac{4}{\pi B} X_{N(i_c-m,i-i_c+k-1-m-n)} \bar{h}\left(x_{2i_c-i-k+n+2},\ y_{i_c-m-1}\right) \qquad \text{(A99)}$$

where the variable subscripts were obtained from equation (A20) with i replaced by i_c-m and k by $i-i_c+k-1-m-n$. For the third term, we obtain from equations (A30) and (A81)

$$C_{i-m,1} = \frac{2\sqrt{\epsilon_2}}{\pi B} \sum_{j=1}^{2} X_{N_1(i-m,j)} \bar{s}_j \left(x_{2i_c-i+m-1},\ y_{i-m-1}\right) \qquad \text{(A100)}$$

For $i - i_c > m > 0$, we must add the correction given in equation (A85). Hence, we obtain

$$C_{i_c-m,1} = \frac{\sqrt{\epsilon_1}}{B} \sum_{n=1}^{4} X_{N_1(i_c-m,n)} \bar{g}_n\left(x_{i_c-m-1},\ y_{i_c-m-1}\right)$$

$$+ \frac{2}{\pi B}\left[X_{N_1(i_c-m,2)} + s_1\ X_{N_1(i_c-m,4)}\right] C\left(x_{i_c-m},\ y_{i_c-m}\right) \qquad \text{(A101)}$$

For m = 0, we also must include the correction in equation (A86). We obtain

$$C_{i_c,1} = \frac{2\left(1-\epsilon_2\right)}{\pi B\sqrt{\epsilon_2}}\ f_4\left(x_{i_c}, y_{i_c}\right)\Big[X_{N_1}(i_c,1) - \epsilon_1 s_1\ X_{N_1}(i_c,2) + s_1\ X_{N_1}(i_c,3)$$

$$- \epsilon_1 s_1^2\ X_{N_1}(i_c,4)\Big] + \frac{\sqrt{\epsilon_1}}{B}\ \sum_{n=1}^{4}\ X_{N_1}(i_c,n)\,\bar{g}_n\left(x_{i_c-1}, y_{i_c-1}\right)$$

$$+\ \frac{2}{\pi B}\left[X_{N_1}(i_c,2) + s_1\ X_{N_1}(i_c,4)\right] C\left(x_{i_c},\ y_{i_c}\right) \qquad \text{(A102)}$$

for $i - i_c > m > 0$, $n \geq k-1$, we add the correction given in equation (A85). This yields

$$C_{i_c-m,i-i_c+k-1-m-n} =$$

$$\frac{4}{\pi B}\ X_{N(i_c-m,i-i_c+k-1-m-n)}\Big[\bar{h}\left(x_{2i_c-i-k+2+n},\right.$$

$$\left.y_{i_c-m-1}\right) + \left(s_1/2\right) C\left(x_{2i_c-1-k+2+n},\ y_{i-i_c+k+2+n}\right)\Big] \qquad \text{(A103)}$$

APPENDIX B
INTEGRATION OF THE AERODYNAMIC INFLUENCE COEFFICIENTS FOR THE PLANAR MACH LINE PANELS

B1 BASIC INTEGRALS FOR SUPERSONIC LEADING EDGE PANELS

For the basic integrals of the supersonic leading edge panels, we consider the following three integrals: designated by f_1, f_2, f_3:

$$f_1(x,y) = \int_0^{\sqrt{y}} \frac{d\eta}{\sqrt{x/\epsilon_1 + (y-\eta^2)}} = \int_0^{\sqrt{y/(x/\epsilon_1 + y)}} \frac{dt}{\sqrt{1-t^2}}$$

$$= \mathrm{SIN}^{-1}\left(\sqrt{\frac{y}{x/\epsilon_1 + y}}\right)$$

$$= f_1(x,y) \tag{B1}$$

Since $(x + \epsilon_1 s_1)/\epsilon_1 + (y - s_1) = x/\epsilon_1 + y$, we also have

$$\int_{\sqrt{y-s_1}}^{\sqrt{y}} \frac{d\eta}{\sqrt{x/\epsilon_1 + y - \eta^2}} = f_1(x,y) - f_1(x + \epsilon_1 s_1, y - s_1) \tag{B2}$$

Similarly, for the second integral we write

$$f_2(x,y) = \int_0^{\sqrt{y}} \frac{\eta^2 d\eta}{\sqrt{x/\epsilon_1 + y - \eta^2}} = -\frac{\sqrt{yx/\epsilon_1}}{2} + \frac{x/\epsilon_1 + y}{2} f_1(x,y) \tag{B3}$$

and finally, for the third, we use

$$f_3(x,y) = \int_0^{\sqrt{y}} \eta^2 \sqrt{x/\epsilon_1 + y - \eta^2}\, d\eta$$

$$= \frac{y\sqrt{yx/\epsilon_1}}{4} + \frac{(x/\epsilon_1 + y)}{4} f_2(x,y) \tag{B4}$$

The functions $f_2(x,y)$ and $f_3(x,y)$ have the same property as shown for $f_1(x,y)$ in equation (B2). We also require the following limits on the integration:

$$\int_0^{\sqrt{x/\epsilon_1 + y}} \frac{d\eta}{\sqrt{x/\epsilon_1 + y - \eta^2}} = \int^1 \frac{dt}{\sqrt{1-t^2}} = \frac{\pi}{2}$$

$$\int_0^{\sqrt{x/\epsilon_1 + y}} \frac{\eta^2\, d\eta}{\sqrt{x/\epsilon_1 + y - \eta^2}} = \frac{\pi\,(x/\epsilon_1 + y)}{4}$$

$$\int_0^{\sqrt{x/\epsilon_1 + y}} \eta^2 \sqrt{x/\epsilon_1 + y - \eta^2}\, d\eta = \frac{\pi\,(x/\epsilon_1 + y)^2}{16}$$

This is also interpreted as

$$f_1(x,y) = \pi/2 \quad , \quad x < 0$$

$$f_2(x,y) = \pi(x/\epsilon_1 + y)/4 \quad , \quad x < 0$$

$$f_3(x,y) = \pi(x/\epsilon_1 + y)^2/16 \quad , \quad x < 0$$

B2 BASIC INTEGRALS FOR SUBSONIC LEADING EDGE PANELS

For the subsonic leading edge, we consider the following three basic integrals:

$$f_4(x,y) = \int_0^{\sqrt{y}} \frac{d\eta}{\sqrt{x/\epsilon_2 - y + \eta^2}} = \log\left(\frac{\sqrt{y} + \sqrt{x/\epsilon_2}}{\sqrt{x/\epsilon_2 - y}}\right) \tag{B5}$$

$$f_5(x,y) = \int_0^{\sqrt{y}} \sqrt{x/\epsilon_2 - y + \eta^2}\, d\eta = \frac{\sqrt{yx/\epsilon_2}}{2} + \frac{(x/\epsilon_2 - y)}{2} f_4(x,y) \tag{B6}$$

$$f_6(x,y) = \int_0^{\sqrt{y}} \eta^2 \sqrt{x/\epsilon_2 - y + \eta^2} = \frac{x\sqrt{yx/\epsilon_2}}{4\epsilon_2} - \frac{(x/\epsilon_2 - y)}{4} f_5(x,y) \tag{B7}$$

since $(x/\epsilon_2 - s) - (y - s) = x/\epsilon_2 - y$, we obtain for the limits $\sqrt{y - s_2}$ to $\sqrt{y}$.

$$f_6(x,y) - f_6(x - \epsilon_2 s_2, y - s_2)$$

Similar relations hold for f_4 and f_5.

B3 AERODYNAMIC INFLUENCE COEFFICIENTS FOR SUPERSONIC LEADING EDGE DOUBLET PANELS

Consider now the downwash at points for which $x > 0$, $y > s_1$. In the panel the doublet distribution is of the form

$$\mu(x,y) = (x+\epsilon_1 y)\ (a + bx + cy + dxy)$$

and the derivative with respect to y is

$$\mu_y = (x+\epsilon_1 y)\ (c + dx) + \epsilon_1\ (a + bx + cy + dxy)$$

On the leading edge $x = -\epsilon_1 y$ we obtain

$$\mu_y = \epsilon_1 \left[a + (c - \epsilon_1 b)\, y - d\, \epsilon_1\, y^2 \right] \tag{B8}$$

Also

$$\mu_{xy} = (c + \epsilon_1\, b) + 2d\,(x + \epsilon_1 y) \tag{B9}$$

Substituting equations (B8) and (B9) into equation (A5) and using the expression for the downwash.

$$W = \left(M\sqrt{\epsilon_1}/\pi \right) \left[a\, g_1\,(x,y) + b\, g_2\,(x,y) + c\, g_3\,(x,y) + d\, g_4\,(x,y) \right] \tag{B10}$$

leads to

$$W = \frac{M\sqrt{\epsilon_1}}{\pi} \left\{ \int_{\sqrt{y - s_1}}^{\sqrt{y}} \left[a + (c - \epsilon_1\, b)(y - \eta^2) - d\epsilon_1\, (y - \eta^2)^2 \right] d\eta \,/\, \sqrt{x/\epsilon_1 + (y - \eta^2)} \right.$$

$$+ 2 \int_{\sqrt{y - s_1}}^{\sqrt{y}} \left[c + \epsilon_1\, b + 4\, d\, (x + \epsilon_1\, y - \epsilon_1 \eta^2)/3 \right] \sqrt{x/\epsilon_1 + (y - \eta^2)}\, d\eta$$

$$\left. - 2\sqrt{x/\epsilon_1} \int_{\sqrt{y - s_1}}^{\sqrt{y}} \left[c + \epsilon_1\, b + \frac{4dx}{3} + 2\, \epsilon_1\, d\,(y - \eta^2) \right] d\eta \right\}$$

Applying the identities

$$\sqrt{x/\epsilon_1 + y - \eta^2} \equiv \frac{(x/\epsilon_1 + y) - \eta^2}{\sqrt{x/\epsilon_1 + y - \eta^2}}$$

$$\frac{\eta^4}{\sqrt{x/\epsilon_1 + y - \eta^2}} \equiv -\eta^2 \sqrt{x/\epsilon_1 + y - \eta^2} + \frac{(x/\epsilon_1 + y)\,\eta^2}{\sqrt{x/\epsilon_1 + y - \eta^2}}$$

yields

$$W = \frac{M\sqrt{\epsilon_1}}{\pi}\left\{\int_{\sqrt{y-s_1}}^{\sqrt{y}}\left[a+(c-\epsilon_1 b)\,y-d\epsilon_1 y^2\right]d\eta/\sqrt{x/\epsilon_1+y-\eta^2}\right.$$

$$-\int_{\sqrt{y-s_1}}^{\sqrt{y}}(c-\epsilon_1 b-2d\,\epsilon_1 y)\,\eta^2/\sqrt{x/\epsilon_1+y-\eta^2}$$

$$+2\int_{\sqrt{y-s_1}}^{\sqrt{y}}\left[c+\epsilon_1 b+4d\,(x+\epsilon_1 y)/3\right]\left[(x/\epsilon_1+y)-\eta^2\right]d\eta/\sqrt{x/\epsilon_1+y-\eta^2}$$

$$+d\,\epsilon_1\left[\int_{\sqrt{y-s_1}}^{\sqrt{y}}\eta^2\sqrt{x/\epsilon_1+y-\eta^2}\,d\eta-(x/\epsilon_1+y)\int_{\sqrt{y-s_1}}^{\sqrt{y}}\eta^2\,d\eta/\sqrt{x/\epsilon_1+y-\eta^2}\right]$$

$$-2\sqrt{x/\epsilon_1}\left[c+\epsilon_1 b+4d\,(x+\epsilon_1 y)/3\right]\left(\sqrt{y}-\sqrt{y-s_1}\right)+4d\,\epsilon_1 s_1\sqrt{(x/\epsilon_1)(y-s_1)}/3$$

$$\left.-\frac{8\epsilon_1 d}{3}\int_{\sqrt{y-s_1}}^{\sqrt{y}}\eta^2\sqrt{x/\epsilon_1+y-\eta^2}\,d\eta\right\} \qquad \text{(B11)}$$

The result can be simplified even more by noting that, since $x/\epsilon_1 + y = (x/\epsilon_1 + s_1) + (y-s_1)$,

$$(x/\epsilon_1+y)\int_{\sqrt{y-s_1}}^{\sqrt{y}}d\eta/\sqrt{x/\epsilon_1+y-\eta^2}=(x/\epsilon_1+y)\left[f_1(x,y)-f_1(x+\epsilon_1 s_1,\,y-s_1)\right]$$

$$=2\left[f_2(x,y)-f_2(x+\epsilon_1 s_1,\,y-s_1)\right]$$

$$+\sqrt{yx/\epsilon_1}-\sqrt{(y-s_1)\,(x/\epsilon_1+s_1)}$$

Separating the g_i functions according to equation (B10) yields

$$g_1(x,y)=f_1(x,y)-f_1(x+\epsilon_1 s_1,\,y-s_1) \qquad \text{(B12)}$$

$$g_2(x,y) = \epsilon_1 \left\{ -y\left[f_1(x,y) - f_1\left(x+\epsilon_1 s_1, y-s_1\right)\right] \right.$$
$$+3\left[f_2(x,y) - f_2\left(x+\epsilon_1 s_1, y-s_1\right)\right]$$
$$\left. +2\sqrt{y-s_1}\left[\sqrt{x/\epsilon_1} - \sqrt{x/\epsilon_1 + s_1}\right]\right\} \qquad \text{(B13)}$$

$$g_3(x,y) = y\left[f_1(x,y) - f_1\left(x+\epsilon_1 s_1, y-s_1\right)\right]$$
$$+ f_2(x,y) - f_2\left(x+\epsilon_1 s_1, y-s_1\right)$$
$$+2\sqrt{y-s_1}\left(\sqrt{x/\epsilon_1} - \sqrt{x/\epsilon_1 + s_1}\right) \qquad \text{(B14)}$$

$$g_4(x,y) = \epsilon_1 \left\{ -y^2\left[f_1(x,y) - f_1\left(x+\epsilon_1 s_1, y-s_1\right)\right] \right.$$
$$-\left(x/\epsilon_1 - y\right)\left[f_2(x,y) - f_2\left(x+\epsilon_1 s_1, y-s_1\right)\right]$$
$$+8\left(x/\epsilon_1 + y\right)\left[f_2(x,y) - f_2\left(x+\epsilon_1 s_1, y-s_1\right)\right.$$
$$\left. +\sqrt{y-s_1}\left(\sqrt{x/\epsilon_1} - \sqrt{x/\epsilon_1 + s_1}\right)\right] /3$$
$$-5\left[f_3(x,y) - f_3\left(x+\epsilon_1 s_1, y-s_1\right)\right] /3$$
$$\left. +4s_1\sqrt{(y-s_1)x/\epsilon_1} / 3\right\} \qquad \text{(B15)}$$

Equations (B12), (B13), (B14), and (B15) hold when $x > 0$ and $y > s_1$. Similar equations for $x < 0$, $y < s_1$; $x < 0$, $y > s_1$; and $x > 0$, $y < s_1$ can be written down by setting the terms which become imaginary equal to zero and by assigning to $f_1(x,y)$ for $x < 0$ the limiting value as x goes to zero: i.e., $\pi/2$. Terms like

$$\sqrt{\left(x/\epsilon_1\right)\left(y-s_1\right)}$$

which are real for $x < 0$ and $y < s_1$ must be discarded also, because they represent solutions in the wrong nappe of the Mach cone.

B4 AERODYNAMIC INFLUENCE COEFFICIENTS FOR INTERIOR DOUBLET PANELS

From equations (A8) and (B8) we obtain

$$W = \frac{2M}{\pi} \int_{\sqrt{y - s_1}}^{\sqrt{y}} \int_{\sqrt{x - \epsilon_1 s_1}}^{\sqrt{x}} \Big[a + 2b(x - \xi^2) + 2c(y - \eta^2) + 4d(x - \xi^2)(y - \eta^2) \Big] d\xi d\eta$$

Integration yields

$$\begin{aligned} W = \frac{2M}{\pi} \Big\{ & \Big[a + 4bx/3 + 4cy/3 + \frac{16}{9} dxy \Big] \Big(\sqrt{x} - \sqrt{x - \epsilon_1 s_1} \Big) \Big(\sqrt{y} - \sqrt{y - s_1} \Big) \\ & - 2 s_1 (c + 4dx/3) \sqrt{y - s_1} \Big(\sqrt{x} - \sqrt{x - \epsilon_1 s_1} \Big) /3 \\ & - 2 \epsilon_1 s_1 (b + 4dy/3) \sqrt{x - \epsilon_1 s_1} \Big(\sqrt{y} - \sqrt{y - s_1} \Big) /3 \\ & + 4 d \epsilon_1 s_1^2 \sqrt{(x - \epsilon_1 s_1)(y - s_1)} /9 \Big\} \end{aligned}$$

Defining the h_i functions according to equation (A9) leads to

$$\begin{aligned} h_1(x,y) &= 2 \Big(\sqrt{x/\epsilon_1} - \sqrt{x/\epsilon_1 - s_1} \Big) \Big(\sqrt{y} - \sqrt{y - s_1} \Big) \\ h_2(x,y) &= 4x h_1(x,y)/3 - 4\epsilon_1 s_1 \sqrt{x/\epsilon_1 - s_1} \Big(\sqrt{y} - \sqrt{y - s_1} \Big) /3 \\ h_3(x,y) &= 4y h_1(x,y)/3 - 4 s_1 \sqrt{y - s_1} \Big(\sqrt{x/\epsilon_1} - \sqrt{x/\epsilon_1 - s_1} \Big) /3 \\ h_4(x,y) &= (16/9) \Big[xy h_1(x,y) - x s_1 \sqrt{(y - s_1) x/\epsilon_1} - \epsilon_1 s_1 y \sqrt{y (x/\epsilon_1 - s_1)} \\ &\quad + s_1 (x + \epsilon_1 y + \epsilon_1 s_1/2) \sqrt{(y - s_1)(x/\epsilon_1 - s_1)} \Big] \end{aligned} \qquad \text{(B16)}$$

Equation (B16) holds for $x > \epsilon_1 s_1$ and $y > s_1$. The functions can easily be found for other ranges of x and y by taking the real part, except when both $y < s_1$ and $x < \epsilon_1 s_1$. The terms like

$$\sqrt{(y - s_1)(x/\epsilon_1 - s_1)}$$

although real, must also be discarded since they are on the wrong side of the Mach cone.

B5 AERODYNAMIC INFLUENCE COEFFICIENTS FOR SUBSONIC LEADING EDGE DOUBLET PANELS

Substituting equation (A10) into equation (A12) yields

$$W = \left(M\sqrt{\epsilon_2}/\pi\right)\left\{ \int_{\sqrt{y-s_2}}^{\sqrt{y}} \left[a + (c + \epsilon_2 b)(y-\eta^2) + d\epsilon_2 (y-\eta^2)^2 \right] d\eta / \sqrt{x/\epsilon_2 - y + \eta^2} \right.$$

$$\left. + \left(2/\sqrt{\epsilon_2}\right) \int_{\sqrt{y-s_2}}^{\sqrt{y}} \int_{\sqrt{x-\epsilon_2 s_2}}^{\sqrt{x-\epsilon_2(y-\eta^2)}} \left[c - \epsilon_2 b + 2d\,(x - \epsilon_2 y + \epsilon_2\eta^2 - \xi^2) \right] d\xi d\eta \right. \qquad \text{(B17)}$$

This may be written, after one integration,

$$W = \frac{M\sqrt{\epsilon_2}}{\pi}\left\{ - \int_{\sqrt{y-s_2}}^{\sqrt{y}} \left[a + (c + \epsilon_2 b)(x/\epsilon_2) + dx^2/\epsilon_2 \right] d\eta \,/\sqrt{x/\epsilon_2 - y + \eta^2} \right.$$

$$+ \int_{\sqrt{y-s_2}}^{\sqrt{y}} \left[c + \epsilon_2 b + d\,(x + \epsilon_2 y) \right] \sqrt{x/\epsilon_2 - y + \eta^2}\; d\eta$$

$$- d\,\epsilon_2 \int_{\sqrt{y-s_2}}^{\sqrt{y}} \eta^2 \sqrt{x/\epsilon_2 - y + \eta^2}\; d\eta$$

$$+ 2 \int_{\sqrt{y-s_2}}^{\sqrt{y}} \left[c - \epsilon_2 b + 4d\,(x - \epsilon_2 y + \epsilon_2 \eta^2)/3 \right] \sqrt{x/\epsilon_2 - y + \eta^2}\; d\eta$$

$$\left. - 2 \int_{\sqrt{y-s^2}}^{\sqrt{y}} \left[c - \epsilon_2 b + 2d\left(\frac{2x + \epsilon_2 s_2}{3} - \epsilon_2 y + \epsilon_2 \eta^2 \right) \right] \sqrt{x/\epsilon_2 - s_2}\; d\eta \right\} \qquad \text{(B18)}$$

Here we have made use of the identities

$$\frac{y-\eta^2}{\sqrt{x/\epsilon_2 - y + \eta^2}} = \frac{x/\epsilon_2}{\sqrt{x/\epsilon_2 - y + \eta^2}} - \sqrt{x/\epsilon_2 - y + \eta^2}$$

$$\frac{(y-\eta^2)^2}{\sqrt{x/\epsilon_2 - y + \eta^2}} = \frac{(x/\epsilon_2)^2}{\sqrt{x/\epsilon_2 - y + \eta^2}} - (x/\epsilon_2 + y - \eta^2)\sqrt{x/\epsilon_2 - y + \eta^2}$$

Following the pattern of equation (A13) and equating coefficients of equation (B18) yields for the S_i functions

$$S_1(x,y) = -f_4(x,y) + f_4\left(x - \epsilon_2 s_2, y - s_2\right)$$

$$S_2(x,y) = x S_1(x,y) - \epsilon_2\left[f_5(x,y) - f_5\left(x - \epsilon_2 s_2, y - s_2\right)\right]$$

$$+ 2\epsilon_2\sqrt{x/\epsilon_2 - s_2}\left(\sqrt{y} - \sqrt{y - s_2}\right)$$

$$S_3(x,y) = x S_1(x,y)/\epsilon_2 + 3\left[f_5(x,y) - f_5\left(x - \epsilon_2 s_2, y - s_2\right)\right]$$

$$- 2\sqrt{x/\epsilon_2 - s_2}\left(\sqrt{y} - \sqrt{y - s_2}\right)$$

$$S_4(x,y) = x^2 S_1(x,y)/\epsilon_2$$

$$+\left(11x - 5\epsilon_2 y\right)\left[f_5(x,y) - f_5\left(x - \epsilon_2 s_2, y - s_2\right)\right]$$

$$+ (5\epsilon_2/3)\left[f_6(x,y) - f_6\left(x - \epsilon_2 s_2, y - s_2\right)\right]$$

$$+\frac{8}{3}\left(x - \epsilon_2 y\right)\sqrt{x/\epsilon_2 - s_2}\left(\sqrt{y - s_2} - \sqrt{y}\right)$$

$$-\frac{4\epsilon_2 s_2}{3}\sqrt{y\,(x/\epsilon_2 - s_2)} \qquad \text{(B19)}$$

Equation (B19) holds for $x < \epsilon_2 s_2$ and $y > s_2$. For other ranges of the variables the relations are found by setting f_4, f_5, f_6 equal to zero when one of the arguments is negative and dropping all radicals with negative arguments. The terms like

$$\sqrt{(x/\epsilon_2 - s_2)(y - s_2)}$$

also must be discarded when $x < \epsilon_2 s_2$ and $y < s_2$ as discussed in the previous sections.

B6 AERODYNAMIC INFLUENCE COEFFICIENTS FOR SUPERSONIC LEADING EDGE SOURCE PANELS

Substituting

$$\sigma(x,y) = a+bx+cy+dxy$$

into equation (A69) yields

$$C_p = \frac{2}{\pi B}\left\{ (1+\epsilon_1) \int_{\sqrt{y-s_1}}^{\sqrt{y}} \left[a + (c-\epsilon_1 b)(y-\eta^2) - \epsilon_1 d (y-\eta^2)^2 \right] d\eta \Big/ \sqrt{x+\epsilon_1 (y-\eta^2)} \right.$$

$$+ 2 \int_{\sqrt{y-s_1}}^{\sqrt{y}} \int_{\sqrt{x}}^{\sqrt{x+\epsilon_1(y-\eta^2)}} \left[b + c + d (x-\xi^2+y-\eta^2) \right] d\xi d\eta$$

$$\left. + 2c\sqrt{x}\left(\sqrt{y}-\sqrt{y-s_1}\right) + 2(b+d s_1)\sqrt{y-s_1}\left(\sqrt{x+\epsilon_1 s_1}-\sqrt{x}\right) \right\}$$

or

$$C_p = \frac{2\sqrt{\epsilon_1}}{\pi B}\left\{ \left(\frac{1+\epsilon_1}{\epsilon_1}\right) \int_{\sqrt{y-s_1}}^{\sqrt{y}} \left[a + (c-\epsilon_1 b)(y-\eta^2) - \epsilon_1 d (y-\eta^2)^2 \right] d\eta \Big/ \sqrt{x/\epsilon_1 + y - \eta^2} \right.$$

$$+ 2 \int_{\sqrt{y-s_1}}^{\sqrt{y}} \sqrt{x/\epsilon_1 + y - \eta^2} \left[b + c + d \left(\frac{2x - \epsilon_1 (y-\eta^2)}{3} + y - \eta^2 \right) \right] d\eta$$

$$- 2 \int_{\sqrt{y-s_1}}^{\sqrt{y}} \sqrt{x/\epsilon_1} \left[b + d (2x/3 + y - \eta^2) \right] d\eta$$

$$\left. + 2(b+d s_1)\sqrt{y-s_1}\left(\sqrt{x/\epsilon_1 + s_1} - \sqrt{x/\epsilon_1}\right) \right\}$$

With the aid of the identities

$$\int \frac{\eta^4\, d\eta}{\sqrt{x/\epsilon_1 + y - \eta^2}} = \int \left[-\eta^2 \sqrt{x/\epsilon_1 + y - \eta^2} + \frac{(x/\epsilon_1 + y)\,\eta^2}{\sqrt{x/\epsilon_1 + y - \eta^2}} \right] d\eta$$

$$= -f_3(x,y) + (x/\epsilon_1 + y)\, f_2(x,y)$$

$$\int \sqrt{x/\epsilon_1 + y - \eta^2}\, d\eta = \int \frac{(x/\epsilon_1 + y)\, d\eta}{\sqrt{x/\epsilon_1 + y - \eta^2}} - \int \frac{\eta^2\, d\eta}{\sqrt{x/\epsilon_1 + y - \eta^2}}$$

$$= f_2(x,y) + \sqrt{(x/\epsilon_1)\, y}$$

the preceding integrals can be expressed in terms of the basic integrals f_1, f_2, and f_3 defined in equations (B1), (B3), and (B4), respectively. Defining the functions $\bar{g}_1$, $\bar{g}_2$, $\bar{g}_3$, and $\bar{g}_4$ by means of equations (A70), we obtain

$$\bar{g}_1(x,y) = 2\left(\frac{1+\epsilon_1}{\epsilon_1}\right)\left[f_1(x,y) - f_1(x + \epsilon_1 s_1, y - s_1)\right]$$

$$\bar{g}_2(x,y) = \epsilon_1\, y\, \bar{g}_1(x,y) + 2(3+\epsilon_1)\left[f_2(x,y) - f_2(x + \epsilon_1 s_1, y - s_1)\right]$$

$$\bar{g}_3(x,y) = y\, \bar{g}_1(x,y) - 2\left\{\left(\frac{1-\epsilon_1}{\epsilon_1}\right)\left[f_2(x,y) - f_2(x + \epsilon_1 s_1, y - s_1)\right]\right.$$

$$\left. - 2\sqrt{y\, x/\epsilon_1} + 2\sqrt{(y - s_1)(x/\epsilon_1 + s_1)}\right\}$$

$$\bar{g}_4(x,y) = -\epsilon_1\, y^2\, \bar{g}_1(x,y) + 2\left\{-\left[(3-\epsilon_1)\, x/\epsilon_1 - (9+\epsilon_1)\, y\right]\left[f_2(x,y)\right.\right.$$

$$\left. - f_2(x + \epsilon_1 s_1, y - s_1)\right] + (5\epsilon_1 - 3)\left[f_3(x,y) - f_3(x + \epsilon_1 s_1, y - s_1)\right]$$

$$+ 2y(1-\epsilon_1)\sqrt{y\, x/\epsilon_1}$$

$$\left. + 4(x + y - s_1)\sqrt{(y - s_1)\, x/\epsilon_1} - 2(2x - \epsilon_1 y + 3y - 3s_1)\sqrt{(y - s_1)(x/\epsilon_1 + s_1)}\right\} /3$$

(B20)

The preceding formulae hold for $x > 0$ and $y > s_1$. Formulae for other regions of the flow may easily be written down by noting that

$$f_i = 0 \text{ for } y < 0, \quad i > 1$$

and

$$f_1(x,y) = \lim_{x \to 0} f_1(x,y) = \pi/2 \text{ when } x < 0$$

and by discarding all radicals with negative radicands, including double radicals like

$$\sqrt{xy/\epsilon_1}$$

when x and y both less than 0, even though they are real.

B7 AERODYNAMIC INFLUENCE COEFFICIENTS FOR RECTANGULAR INTERIOR SOURCE PANELS

For $x > \epsilon_2 s_2$ and $y > s_2$, substituting

$$\sigma(x,y) = dxy$$

into equation (A74) and using equation (A75) yields the following integrals to be evaluated for determining h(x,y) in equation (A75)

$$\bar{h}(x,y) = \int_{\sqrt{y-s_1}}^{\sqrt{y}} \int_{\sqrt{x-\epsilon_1 s_1}}^{\sqrt{x}} \left[x - \xi^2 + y - \eta^2\right] d\xi d\eta$$

$$+ \int_{\sqrt{y-s_1}}^{\sqrt{y}} \int_{0}^{\sqrt{x-\epsilon_1 s_1}} \epsilon_1 s_1 \, d\xi d\eta + \int_{0}^{\sqrt{y-s_1}} \int_{\sqrt{x-\epsilon_1 s_1}}^{\sqrt{x}} s_1 \, d\xi d\eta$$

This immediately integrates to

$$\bar{h}(x,y) = \frac{2}{3}\Big[(x+y)\sqrt{xy} - (x+y-s_1)\sqrt{x(y-s_1)}$$

$$- (x+y-\epsilon_1 s_1)\sqrt{y(x-\epsilon_1 s_1)}$$

$$+ (x+y-\epsilon_1 s_1 - s_1)\sqrt{(y-s_1)(x-\epsilon_1 s_1)}\Big] \qquad \text{(B21)}$$

The preceding equations hold for $y > s_2$, $x > \epsilon_2 s_2$. It may be applied to other regions of the wing by discarding all imaginary terms. As in the other influence coefficients terms like

$$\sqrt{xy}$$

when $x < 0$ and $y < 0$ are also discarded.

B8 AERODYNAMIC INFLUENCE COEFFICIENTS FOR SUBSONIC LEADING EDGE SOURCE PANELS

Substituting equation (A76) into equation (A80) yields the following relation for C_p from the subsonic leading edge panel

$$C_p = \frac{4}{\pi B}\left\{(1-\epsilon_2)\left[\int_{\sqrt{y-s_2}}^{\sqrt{y}} \frac{c(y-\eta^2)+\epsilon_2 d(y-\eta^2)}{2\sqrt{x-\epsilon_2(y-\eta^2)}}\,d\eta + \int_0^{\sqrt{y-s_2}} \frac{c s_2 + d\,\epsilon_2 s_2^2}{2\sqrt{x-\epsilon_2(y-\eta^2)}}\,d\eta\right]\right.$$

$$+\int_{\sqrt{y-s_2}}^{\sqrt{y}}\int_{\sqrt{x-\epsilon_2 s_2}}^{\sqrt{x-\epsilon_2(y-\eta^2)}}\left[d\left(x-\xi^2+y-\eta^2\right)+c\right]d\xi d\eta$$

$$\left.+(d\,\epsilon_2 s_2 + c)\int_{\sqrt{y-s_2}}^{\sqrt{y}}\int_0^{\sqrt{x-\epsilon_2 s_2}} d\xi d\eta\right\}$$

Expressing C_p in the form of equation (A81) yields, for the functions s_1 and s_2

$$\bar{S}_1(x,y) = \left(\frac{1-\epsilon_2}{\epsilon_2}\right)\left[\int_{\sqrt{y-s_2}}^{\sqrt{y}} \frac{(y-\eta^2)\,d\eta}{\sqrt{x/\epsilon_2 - y+\eta^2}} + s_2\int_0^{\sqrt{y-s_2}} \frac{d\eta}{\sqrt{x/\epsilon_2 - y+\eta^2}}\right]$$

$$+2\int_{\sqrt{y-s_2}}^{\sqrt{y}} \sqrt{x/\epsilon_2 - y+\eta^2}\,d\eta$$

$$\bar{S}_2(x,y) = (1-\epsilon_2)\left[\int_{\sqrt{y-s_2}}^{\sqrt{y}} \frac{(y-\eta^2)^2 d\eta}{\sqrt{x/\epsilon_2 - y+\eta^2}} + s_2^2\int_0^{\sqrt{y-s_2}} \frac{d\eta}{\sqrt{x/\epsilon_2 - y+\eta^2}}\right]$$

$$+\frac{2}{\sqrt{\epsilon_2}}\int_{\sqrt{y-s_2}}^{\sqrt{y}}\int_{\sqrt{x-\epsilon_2 s_2}}^{\sqrt{x-\epsilon_2(y-\eta^2)}} \left(x-\xi^2+y-\eta^2\right)d\xi d\eta$$

$$+2\,\epsilon_2 s_2\sqrt{x/\epsilon_2} - s_2\left(\sqrt{y}-\sqrt{y-s_2}\right)$$

By using the relations

$$\frac{y-\eta^2}{\sqrt{x/\epsilon_2 - y + \eta^2}} = \frac{x/\epsilon_2}{\sqrt{x/\epsilon_2 - y + \eta^2}} - \sqrt{x/\epsilon_2 - y + \eta^2}$$

$$\frac{(y-\eta^2)^2}{\sqrt{x/\epsilon_2 - y + \eta^2}} = \frac{(x/\epsilon_2)^2}{\sqrt{x/\epsilon_2 - y + \eta^2}} - (x/\epsilon_2 + y - \eta^2)\sqrt{x/\epsilon_2 - y + \eta^2}$$

the results of the integration may be expressed in terms of the functions f_4, f_5, and f_6 defined in equations (B5), (B6), and (B7), respectively. This leads to

$$S_1(x,y) = \left(\frac{1-\epsilon_2}{\epsilon_2}\right)\left[(x/\epsilon_2)\, f_4(x,y) - (x/\epsilon_2 - s_2) f_4(x - \epsilon_2 s_2, y - s_2)\right]$$

$$+\left(\frac{3\epsilon_2 - 1}{\epsilon_2}\right)\left[f_5(x,y) - f_5(x - \epsilon_2 s_2, y - s_2)\right]$$

$$S_2(x,y) = (1-\epsilon_2)(x^2/\epsilon^2_2)\left[f_4(x,y) - f_4(x - \epsilon_2 s_2, y - s_2)\right]$$

$$+\left[(7\epsilon_2 - 3)\, x/\epsilon_2 + (5\epsilon_2 + 3)\, y\right]\left[f_5(x,y) - f_5(x - \epsilon_2 s_2, y - s_2)\right]/3$$

$$-(5\epsilon_2 + 3)\left[f_6(x,y) - f_6(x - \epsilon_2 s_2, y - s_2)\right]/3 + (1-\epsilon_2)\, s_2^2\, f_4(x - \epsilon_2 s_2, y - s_2)$$

$$-4(x + y - \epsilon_2 s_2)\sqrt{y(x/\epsilon_2 - s_2)}\,/3$$

$$+4(x + y - \epsilon_2 s_2 + s_2/2)\sqrt{(y - s_2)(x/\epsilon_2 - s_2)}/3 \qquad \text{(B22)}$$

The preceding equations hold for $y > s_2$ and $x > \epsilon_2 s_2$. Similar relations may be written down for other regions of the flow by following the rules in section B5 of appendix B.

B9 SUBSONIC LEADING EDGE CORRECTION TO THE AERODYNAMIC INFLUENCE COEFFICIENTS FOR SUPERSONIC LEADING EDGE SOURCE PANELS AND INTERIOR SOURCE PANELS

Combining equations (A83) and (A84) and considering equation (A85), we see that the correction to $\bar{g}_2$, $\bar{g}_4$, and $\bar{h}$ from the panel in those rows containing a subsonic leading edge in the zone of dependence of the point x,y is given by

$$C(x,y) = (1-\epsilon_2)\left[\int_{\sqrt{y-\epsilon_2 s_2}}^{\sqrt{y}} \frac{(y-\eta^2)\,d\eta}{\sqrt{x/\epsilon_2 - y + \eta^2}} + s_2 \int_0^{\sqrt{y-s_2}} \frac{d\eta}{\sqrt{x/\epsilon_2 - y + \eta^2}}\right]$$

$$-(2/\sqrt{\epsilon_2}) \int_{\sqrt{y-s_2}}^{\sqrt{y}} \frac{\int_{\epsilon_2(y-\eta^2)}^{x} d\xi\, d\eta}{\sqrt{x-\epsilon_2(y-\eta^2)}}$$

$$-(2/\sqrt{\epsilon_2}) \int_0^{\sqrt{y-s_2}} \frac{\int_{\epsilon_2 s_2}^{x} d\xi\, d\eta}{\sqrt{x-\epsilon_2 s_2}}$$

Performing the integration yields, after some simplification,

$$C(x,y) = (1-\epsilon_2)\left[(x/\epsilon_2)\, f_4(x,y) - (x/\epsilon - s_2)\, f_4(x-\epsilon_2 s_2,\ y-s_2)\right]$$

$$+(1+\epsilon_2)\left[f_5(x,y) - f_5(x-\epsilon_2 s_2,\ y-s_2)\right]$$

$$-2\sqrt{(x/\epsilon_2)\,y} + 2\sqrt{(x/\epsilon_2 - s_2)\,(y-s_2)} \qquad \text{(B23)}$$

This relation holds for $x > \epsilon_2 s_2$ and $y > s_2$. The expressions for other ranges of x and y are easily found by following the same procedure as for S_1 and S_2 in section B5 of appendix B. The origin of the preceding equations corresponds to that for the subsonic leading edge panel in the same row as the panel for which the correction is to be applied.

REFERENCES

1. Johnson, F.T. and Rubbert, P.E.: "Advanced Panel-Type Influence Coefficient Methods Applied to Subsonic Flows," AIAA paper 75-50, January 1975.

2. Mercer, J.E., Weber, J.A., and Lesferd, E.P.: *Aerodynamic Influence Coefficient Method Using Singularity Splines*, NASA CR-2423, 1974.

3. Smith, J.H.B., Beasley, J.A., Short, D. and Walkden, F: "The Calculation of the Warp to Produce a Given Load and the Pressures due to a Given Thickness on Thin Slender Wings in Supersonic Flow," British A.R.C., R&M 3471, 1965.

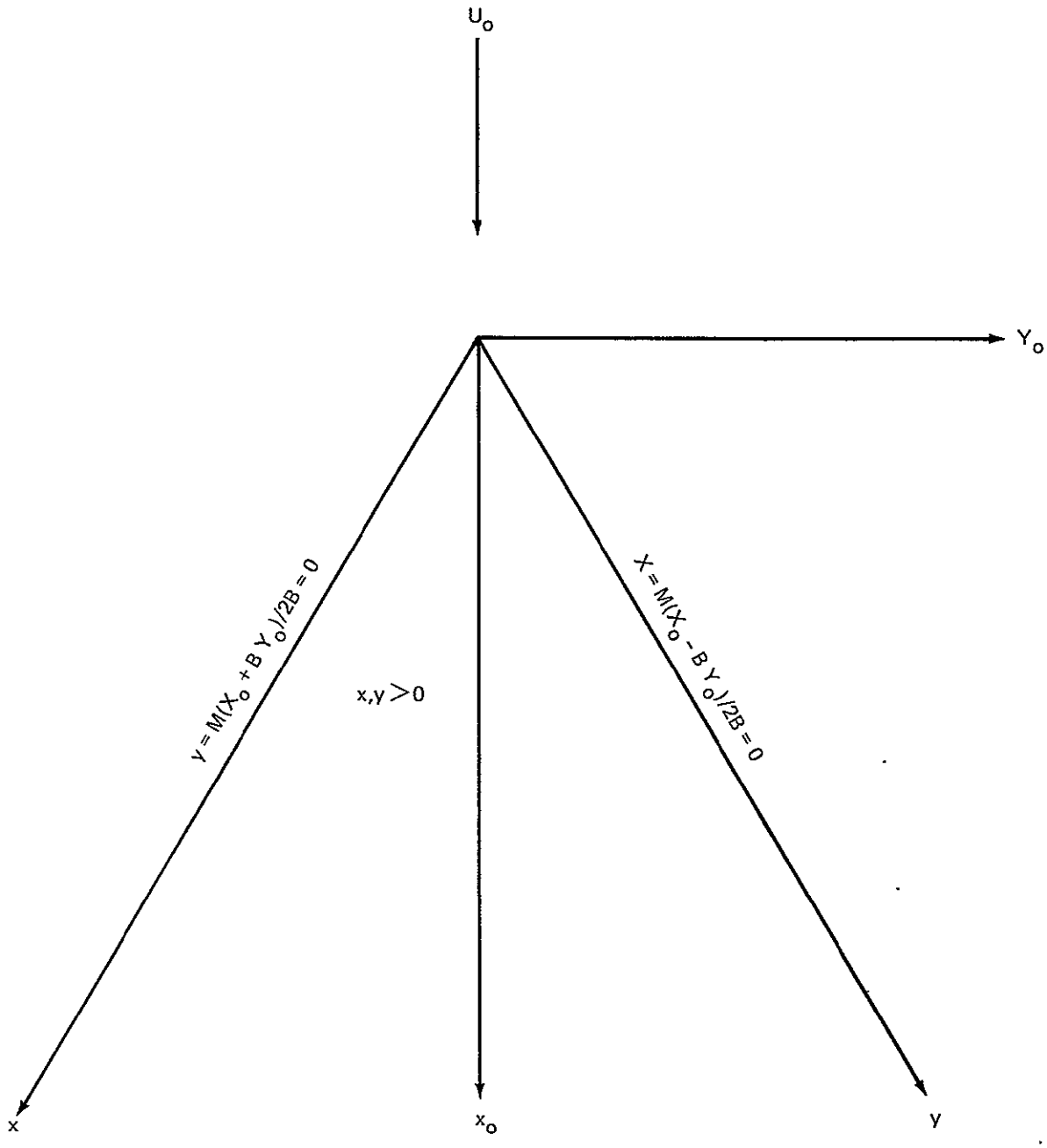

Figure 1.—Mach Line Coordinates x,y

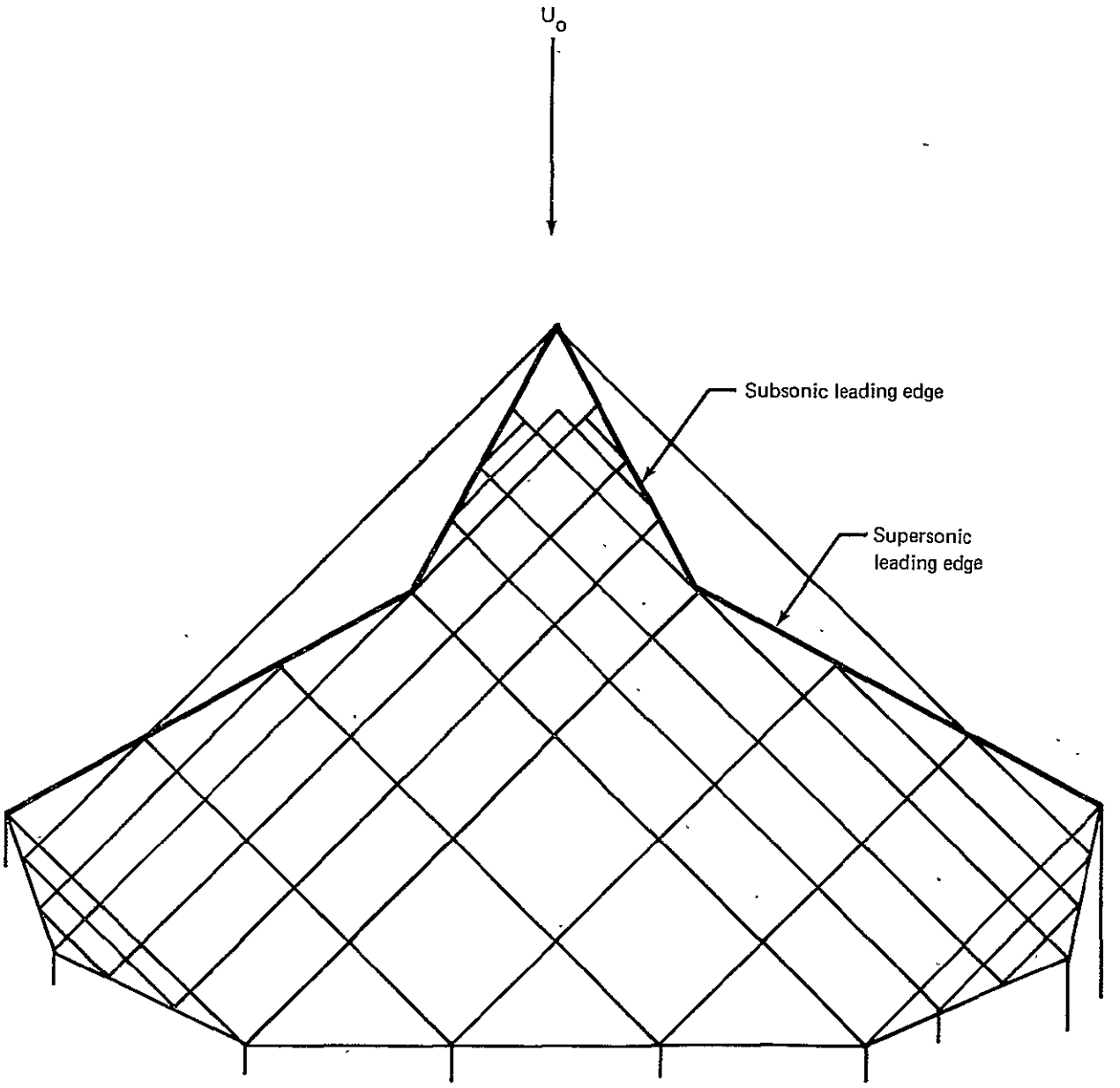

Figure 2.—Mach Line Paneling on Planar Wing at $M = \sqrt{2}$

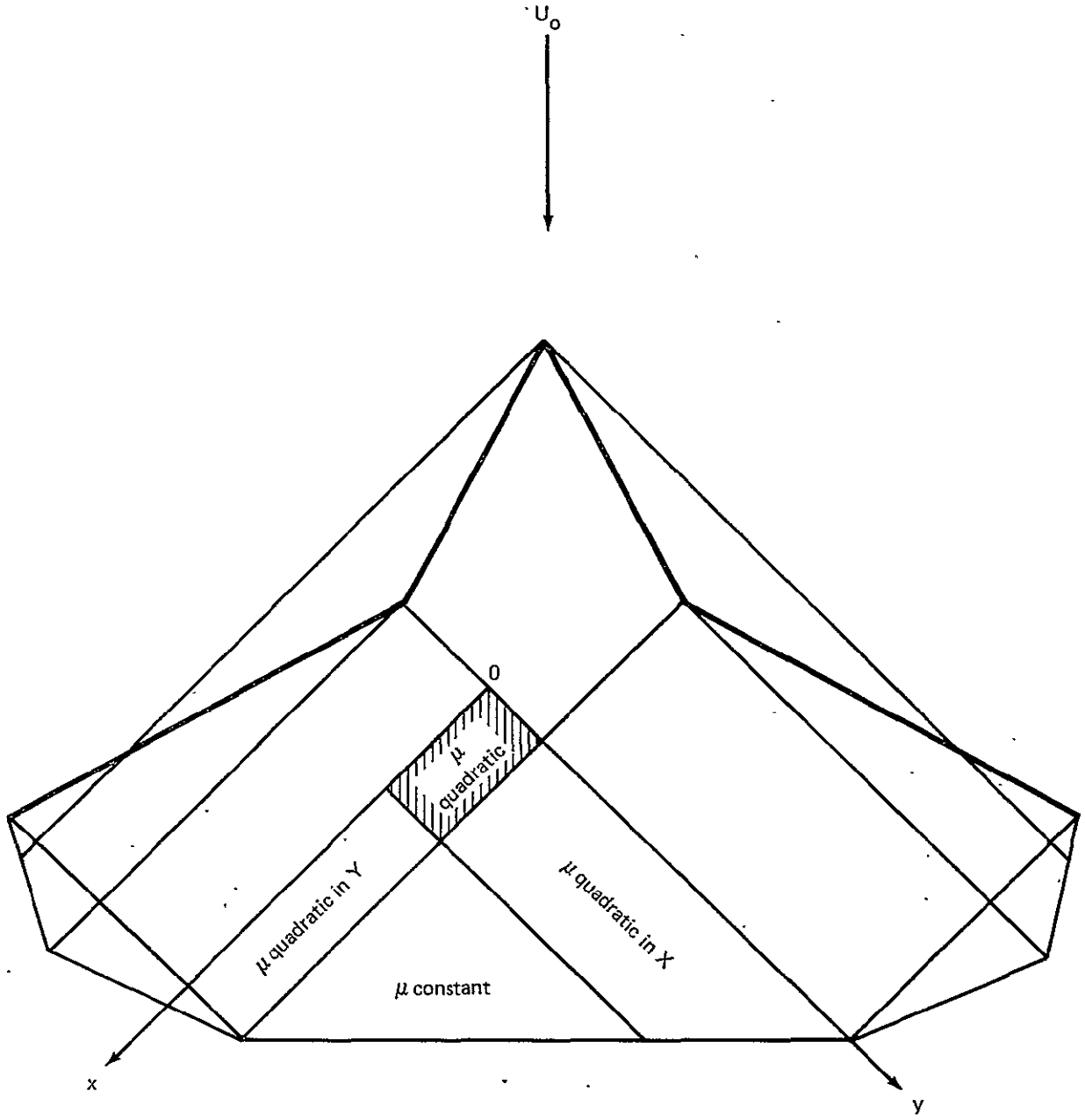

Figure 3.—Analytic Continuation of the Doublet Distribution on the Wing Associated With an Interior Mach Line Panel at $M = \sqrt{2}$

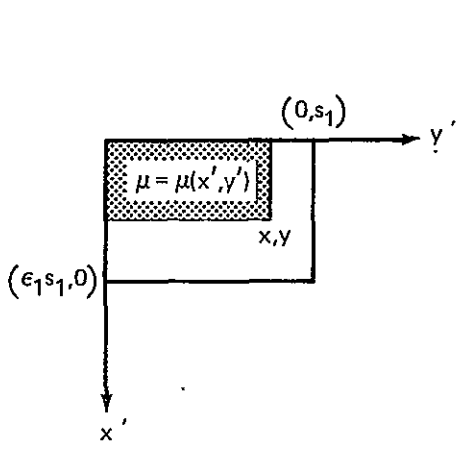

(a) Control Point x,y Inside the Panel

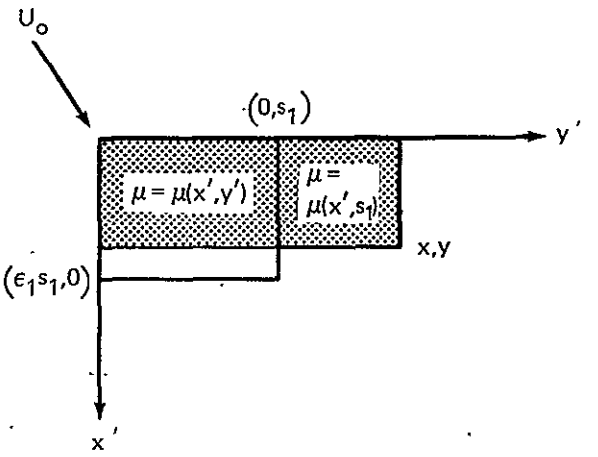

(b) Control Point x,y Outside the Panel and on y Characteristic Strip

x,y Fixed point
x',y' Variables of integration

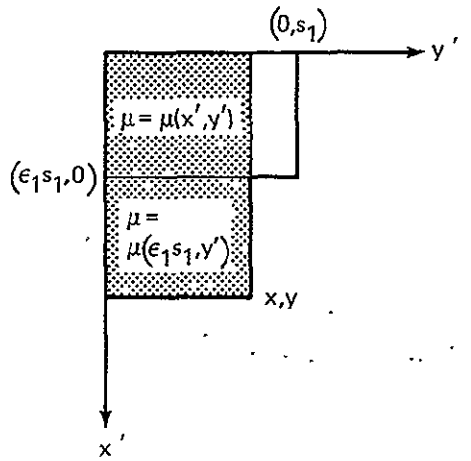

(c) Control Point x,y Outside the Panel and on x Characteristic Strip

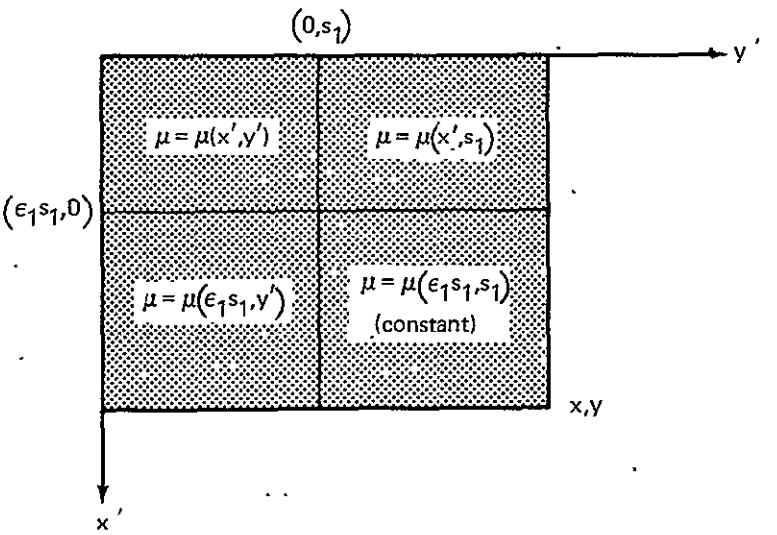

(d) Control Point x,y Outside the Panel and Between Characteristic Strips

Figure 4.—Range of Integration for Interior Mach Line Panel and Analytic Continuation of Doublet Strength Outside of the Panel

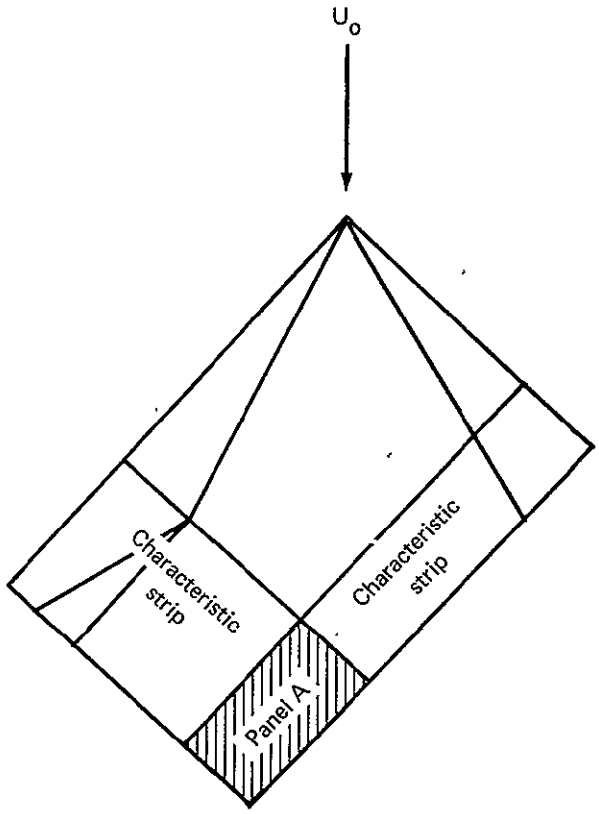

Figure 5.—Domain of Dependence of an Interior Panel With Illustration of Upstream Characteristic Strips

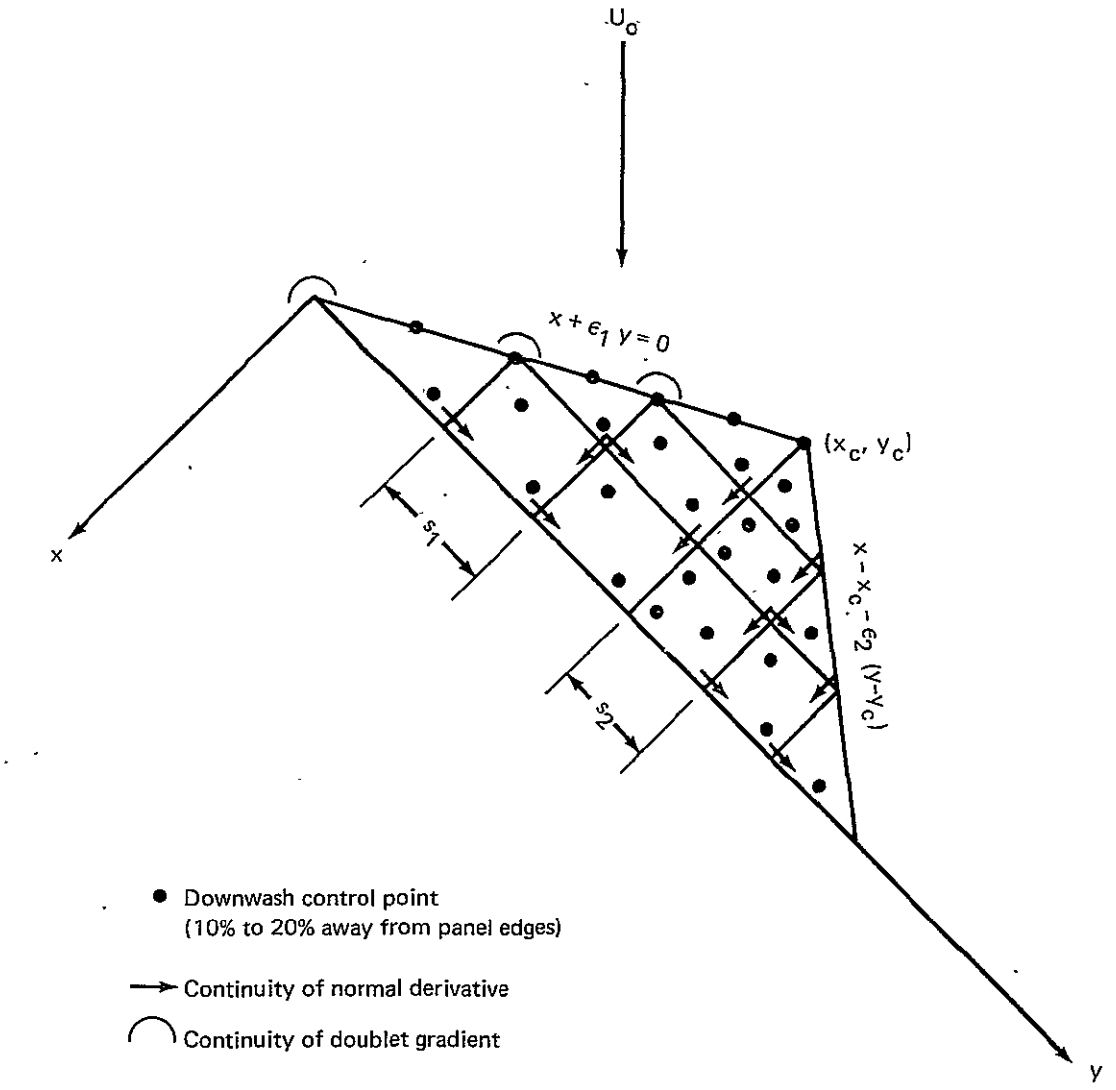

Figure 6.—Control Point Locations and Continuity Conditions for Doublet Mach Line Paneling

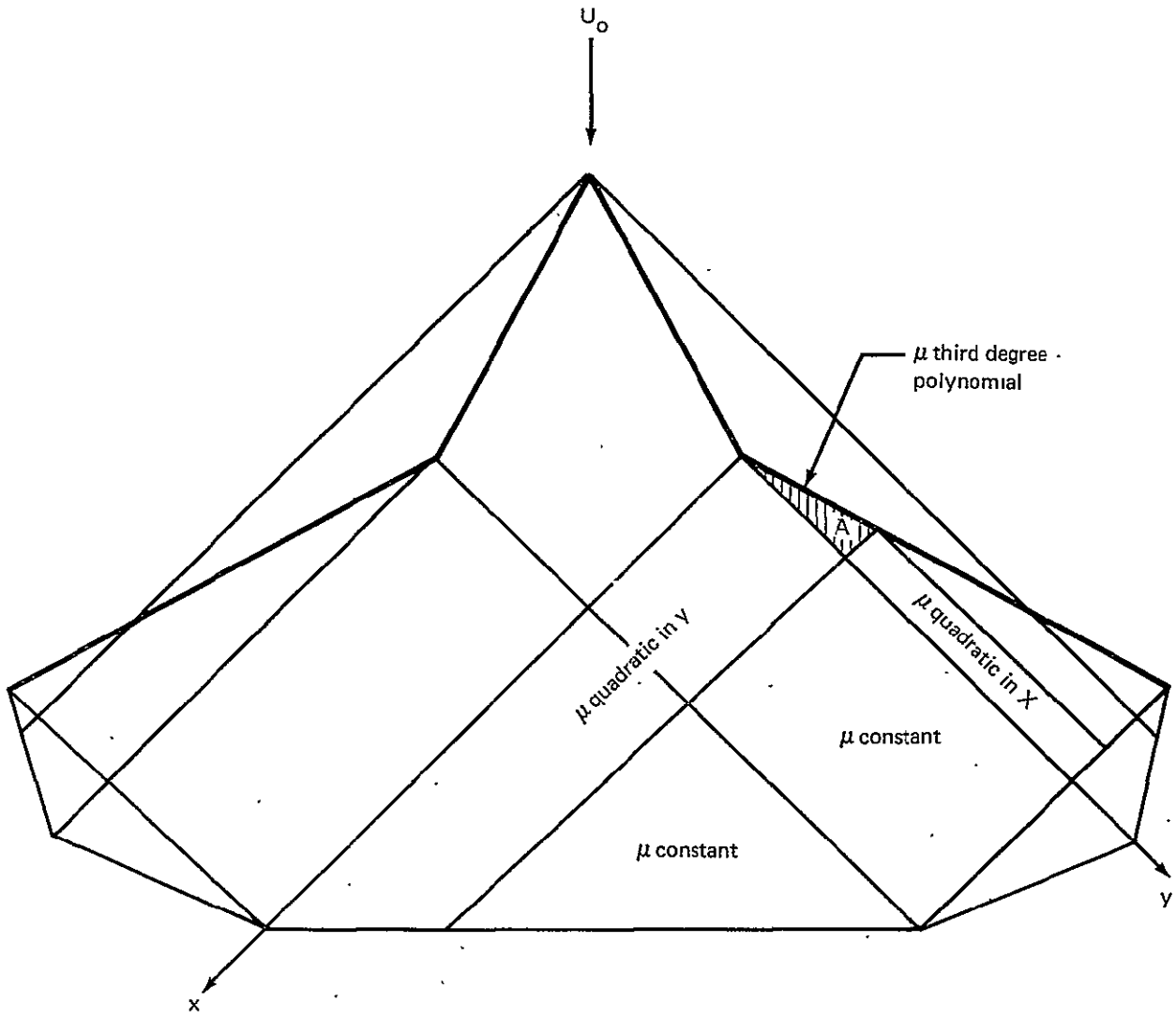

Figure 7.—Analytic Continuation of the Doublet Distribution on the Wing Associated With a Mach Line Panel Adjacent to Supersonic Leading Edge at $M = \sqrt{2}$

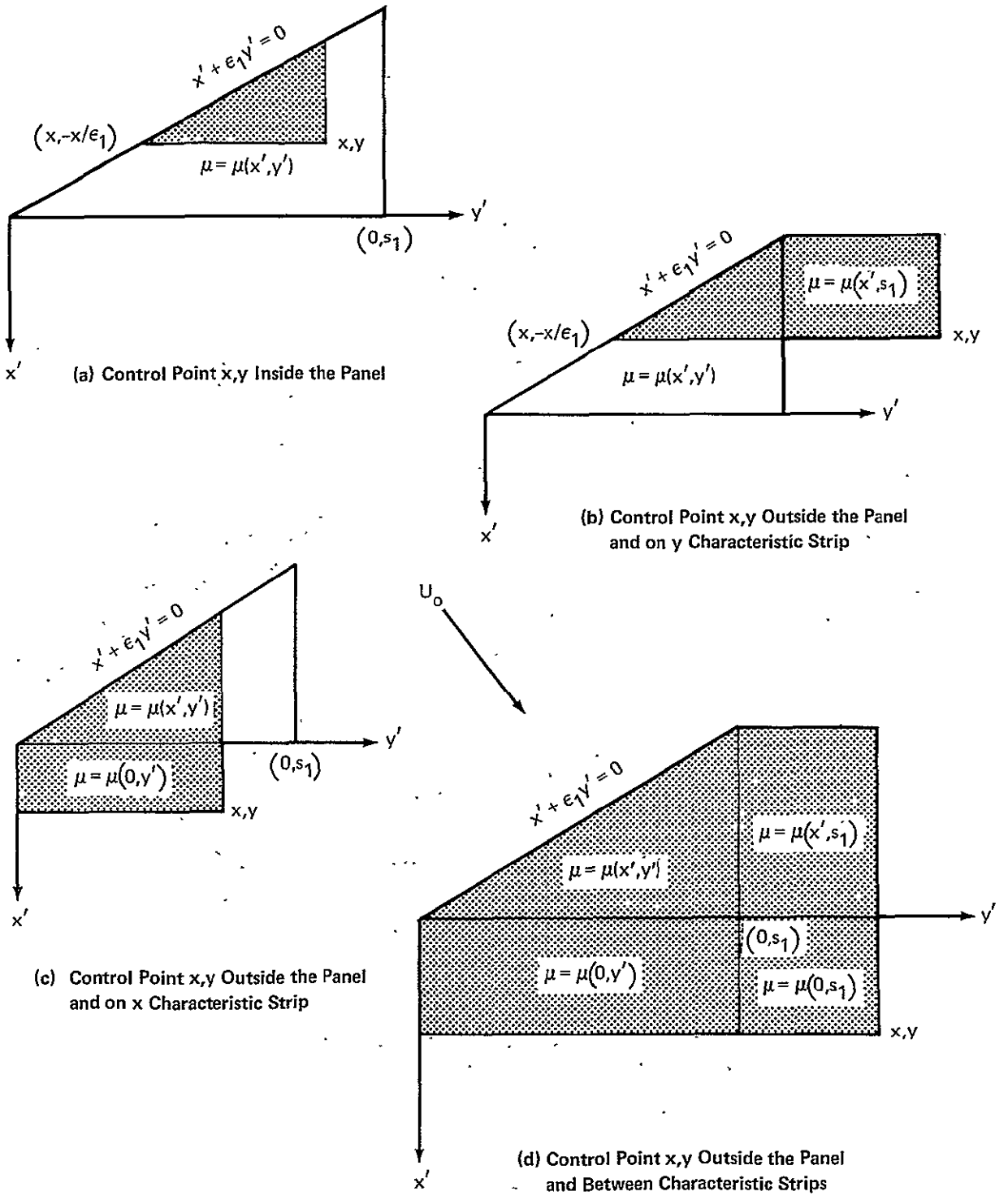

Figure 8.—Range of Integration for Supersonic Leading Edge Mach Line Panel Analytic Continuation of Doublet Strength Outside of the Panel

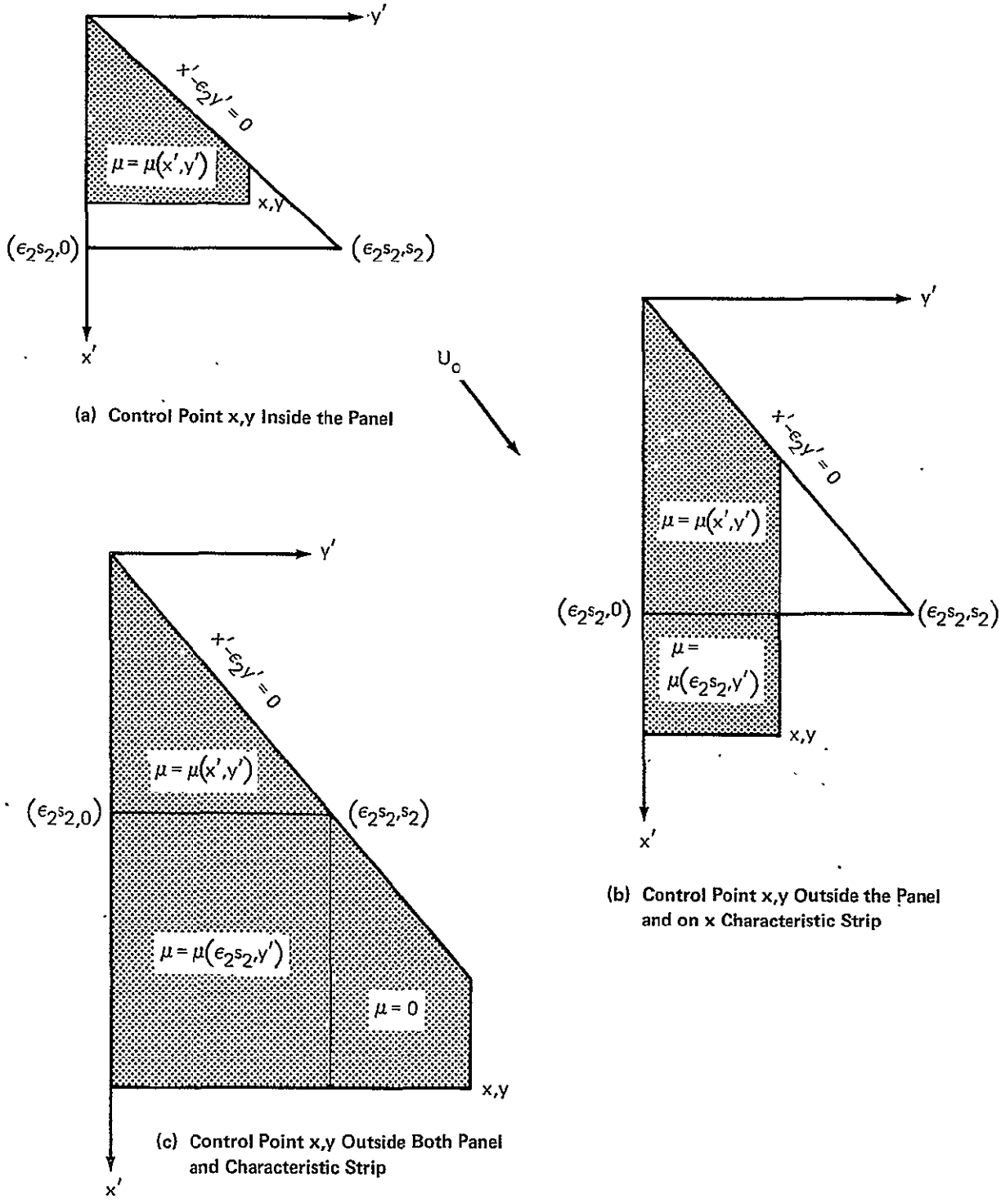

Figure 9.—Range of Integration for Subsonic Leading Edge Mach Line Panel and Analytic Continuation of Doublet Strength Outside of the Panel

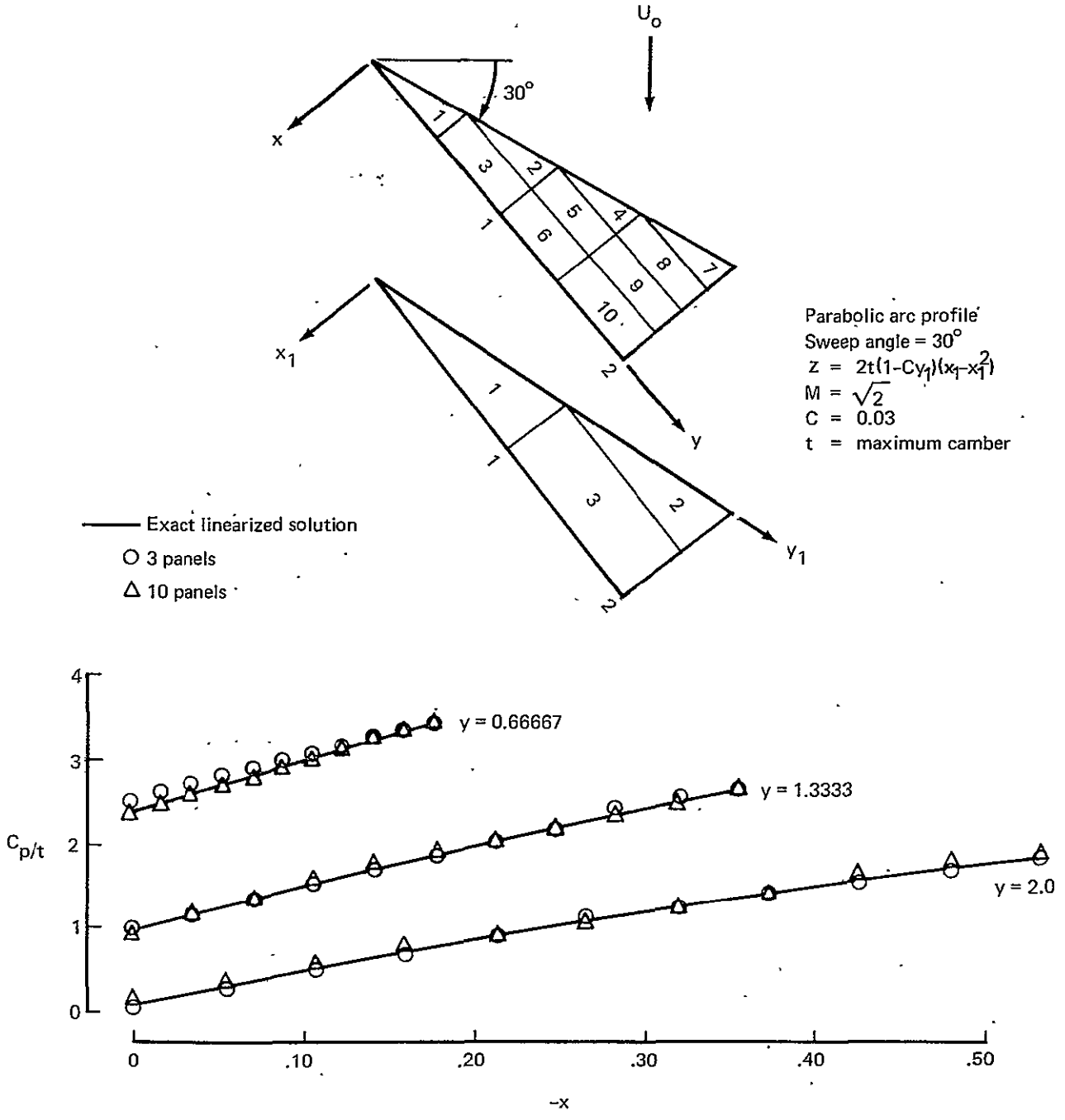

Figure 10.—Pressure Distributions on Portion of the Wing Behind Supersonic Leading Edge

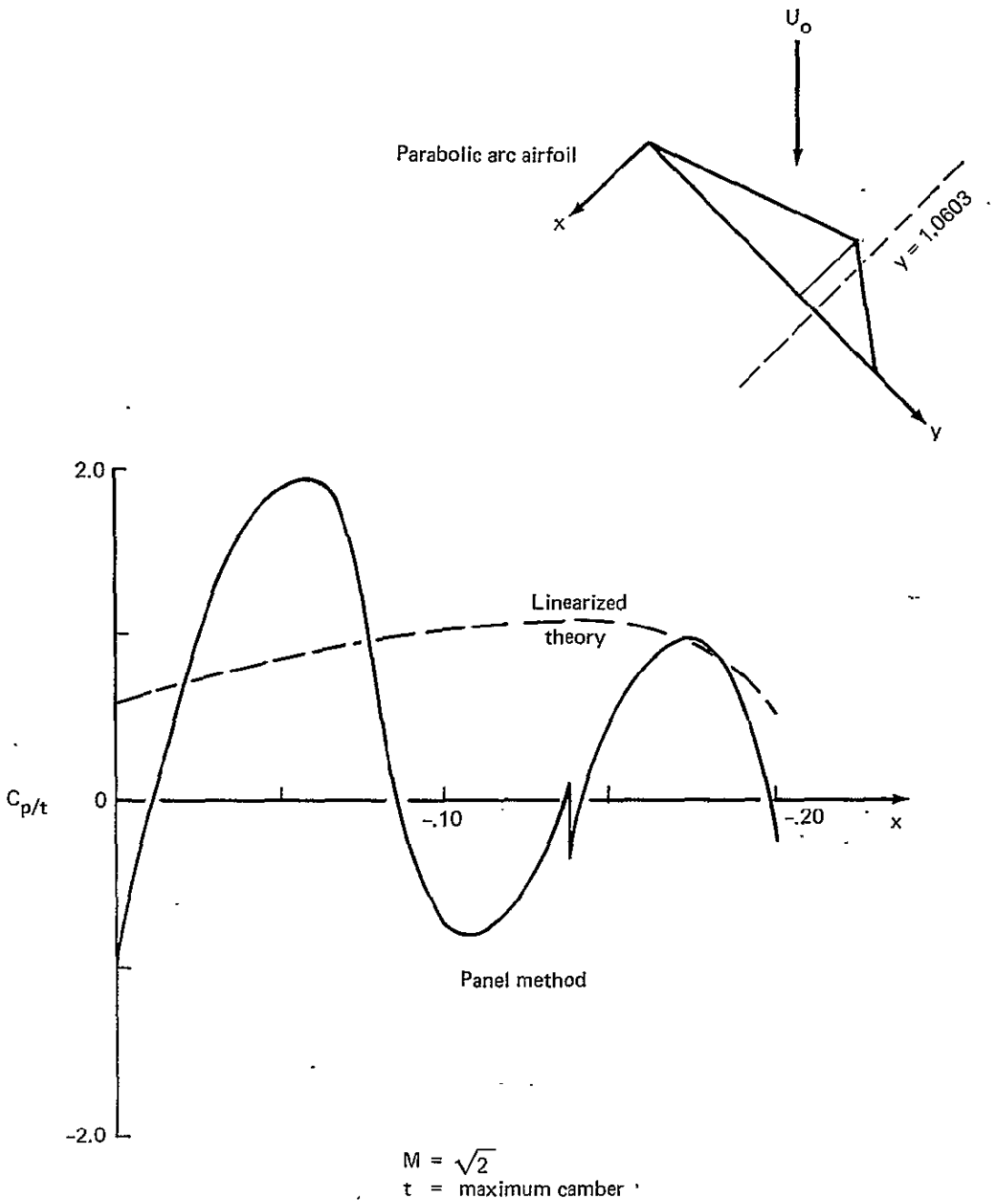

Figure 11.—Pressure Distributions on Portion of the Wing Behind Subsonic Leading Edge Along the Line y = 1.0603

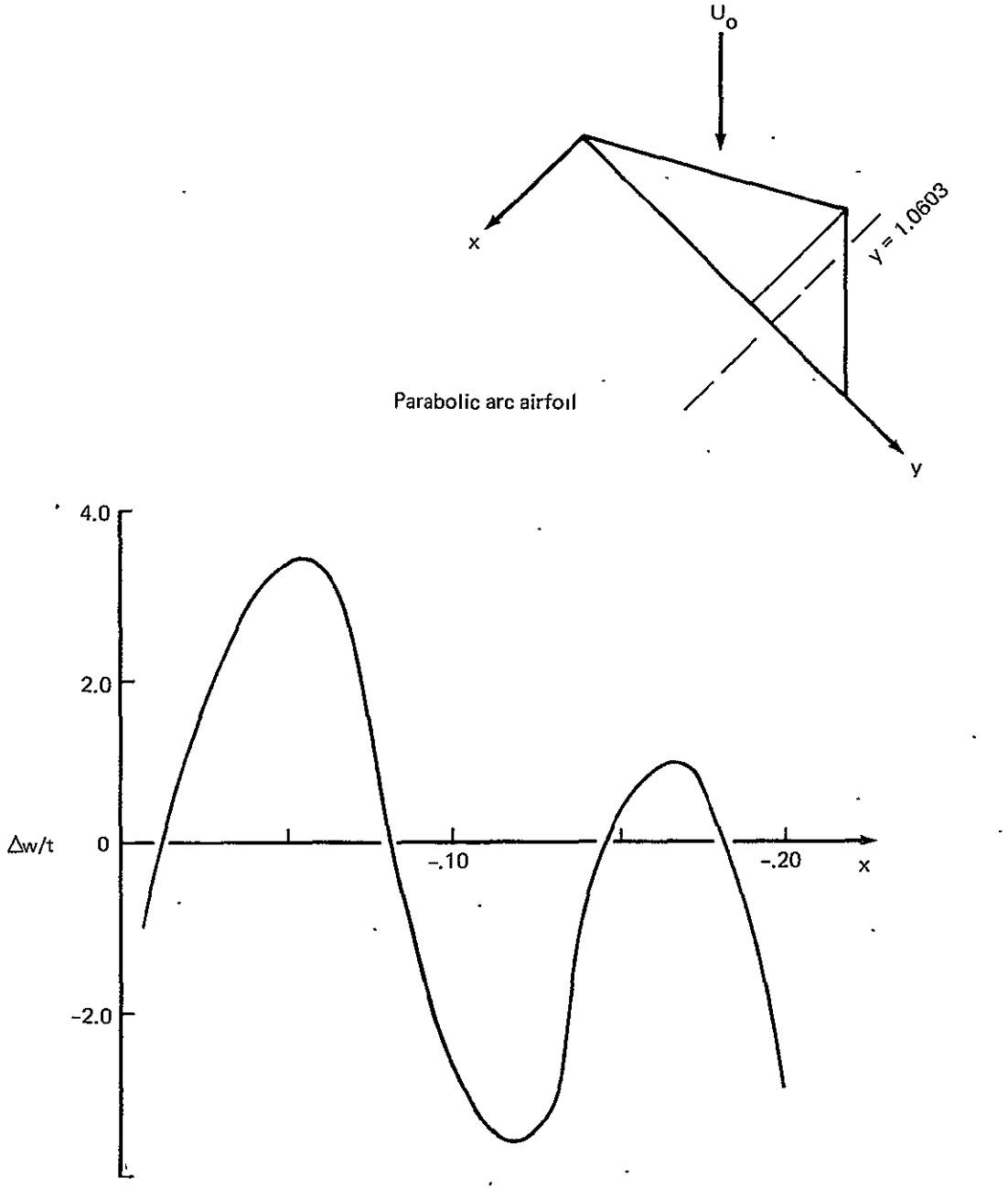

Figure 12.—Error in Downwash From Mach Line Doublet Panel Method Behind Subsonic Leading Edge Along the Line y = 1.0603

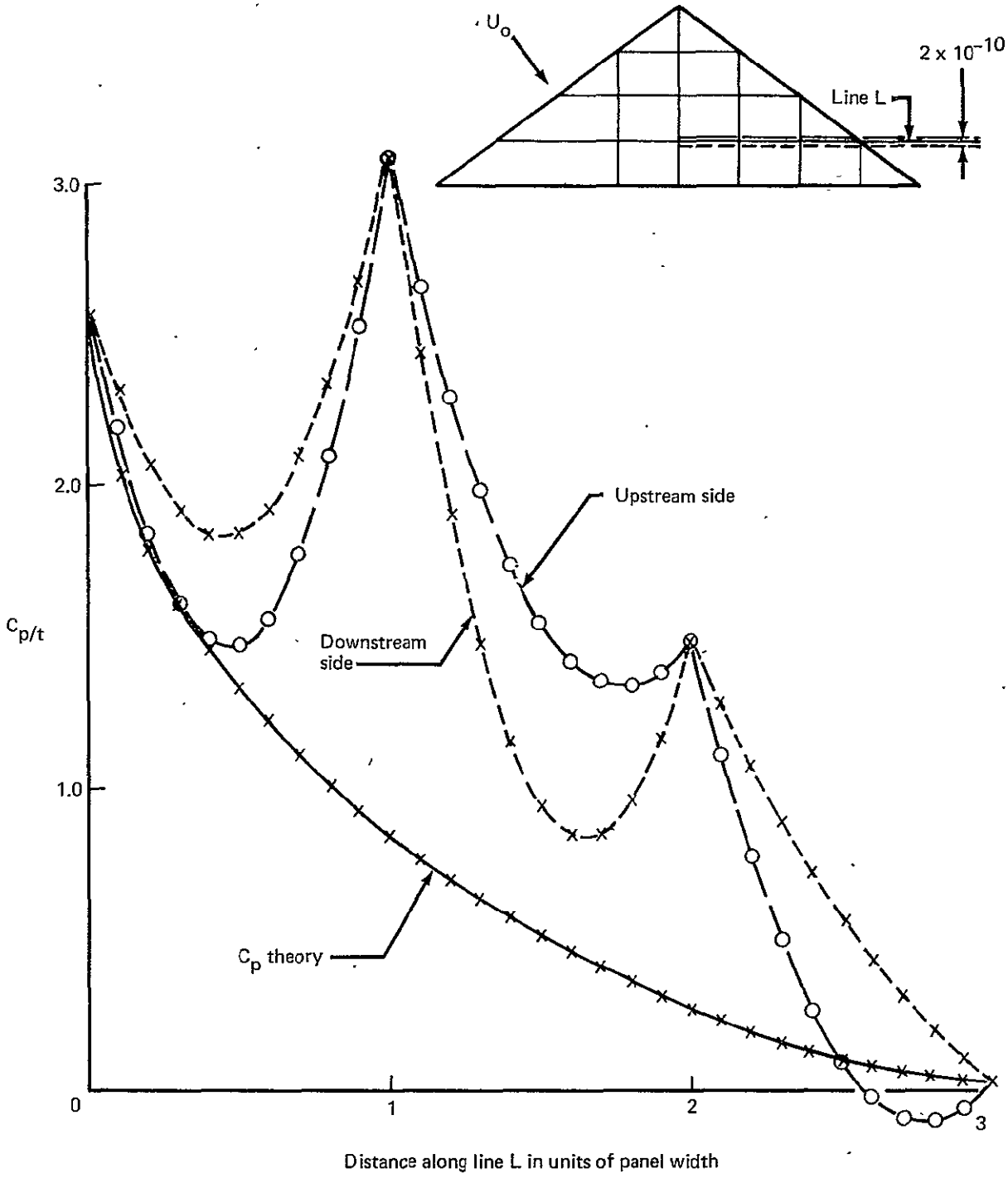

Figure 13.—Discontinuity in Pressure Coefficient Along Panel Edges of Mach Line Doublet Panels in the Region Behind Subsonic Leading Edge

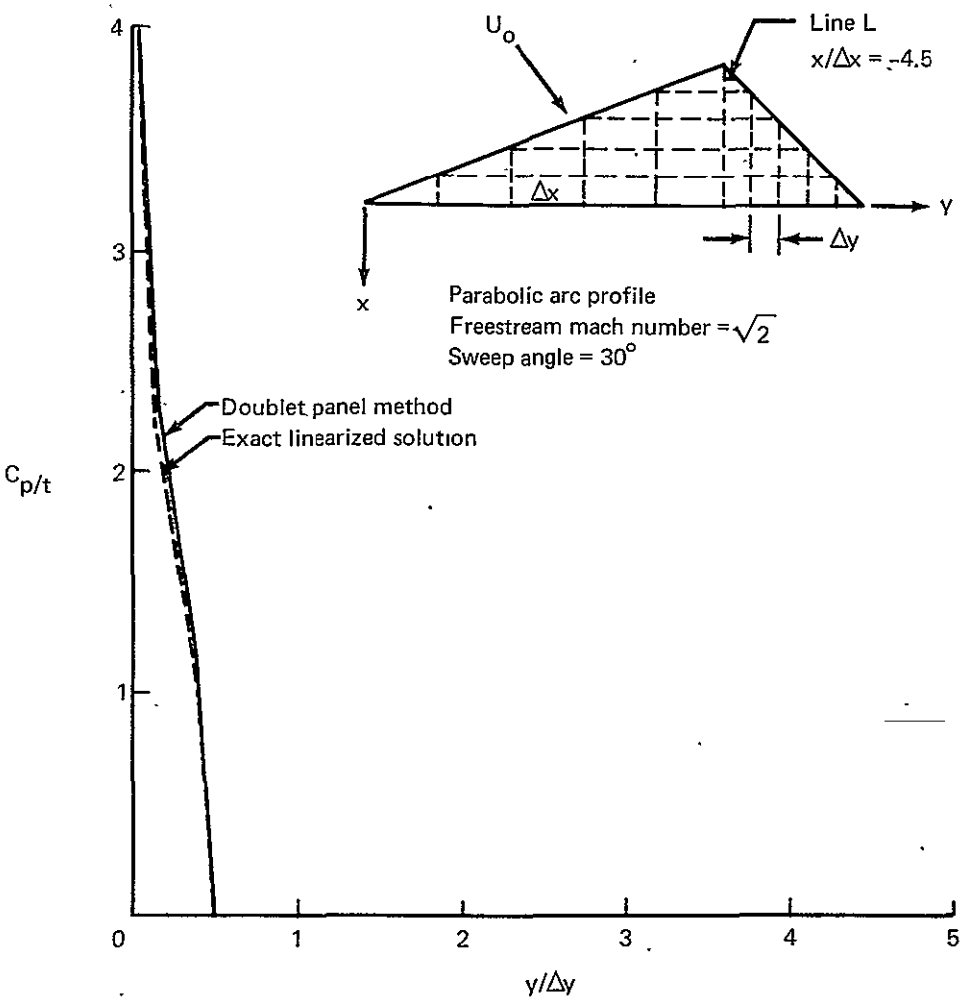

Figure 14.—Pressure Distribution Along Line L Downstream of Special Mach Line With Flat Plate Solution Superimposed on Doublet Panel Solution

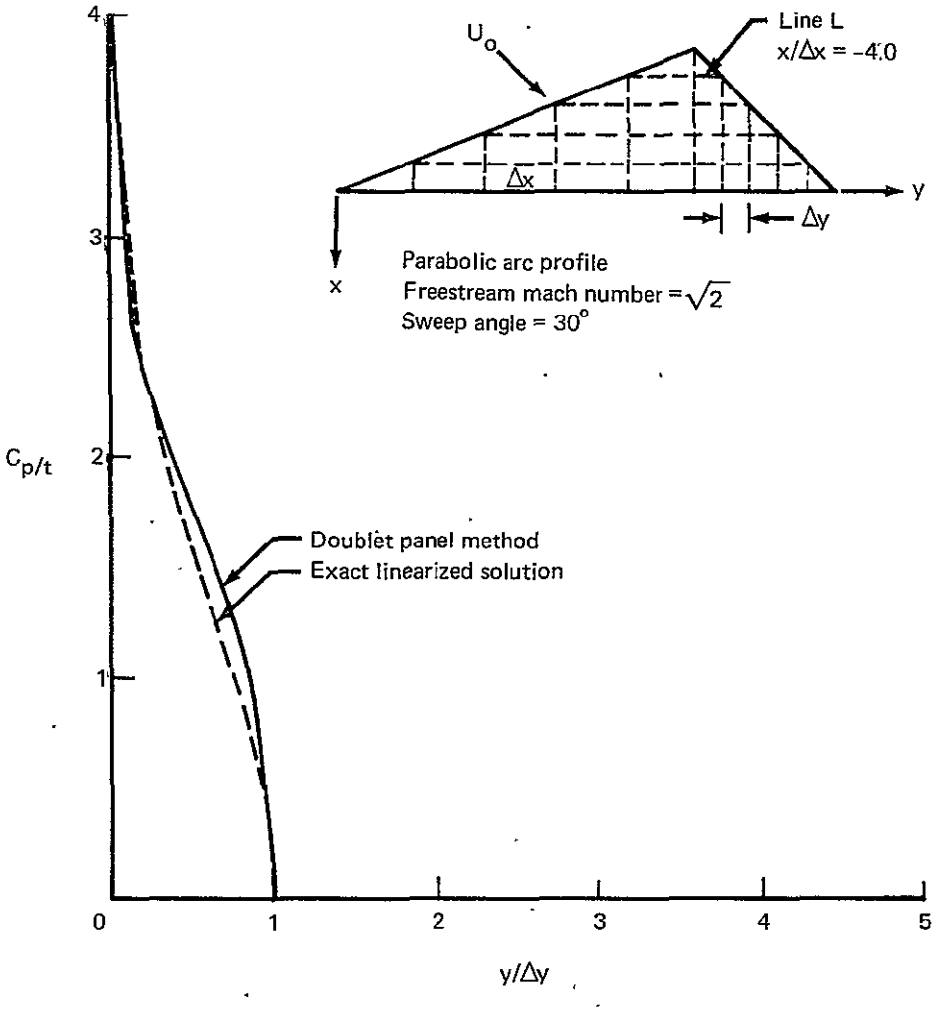

Figure 15.—Pressure Distribution Along Line L Downstream of Special Mach Line With Flat Plate Solution Superimposed on Doublet Panel Solution

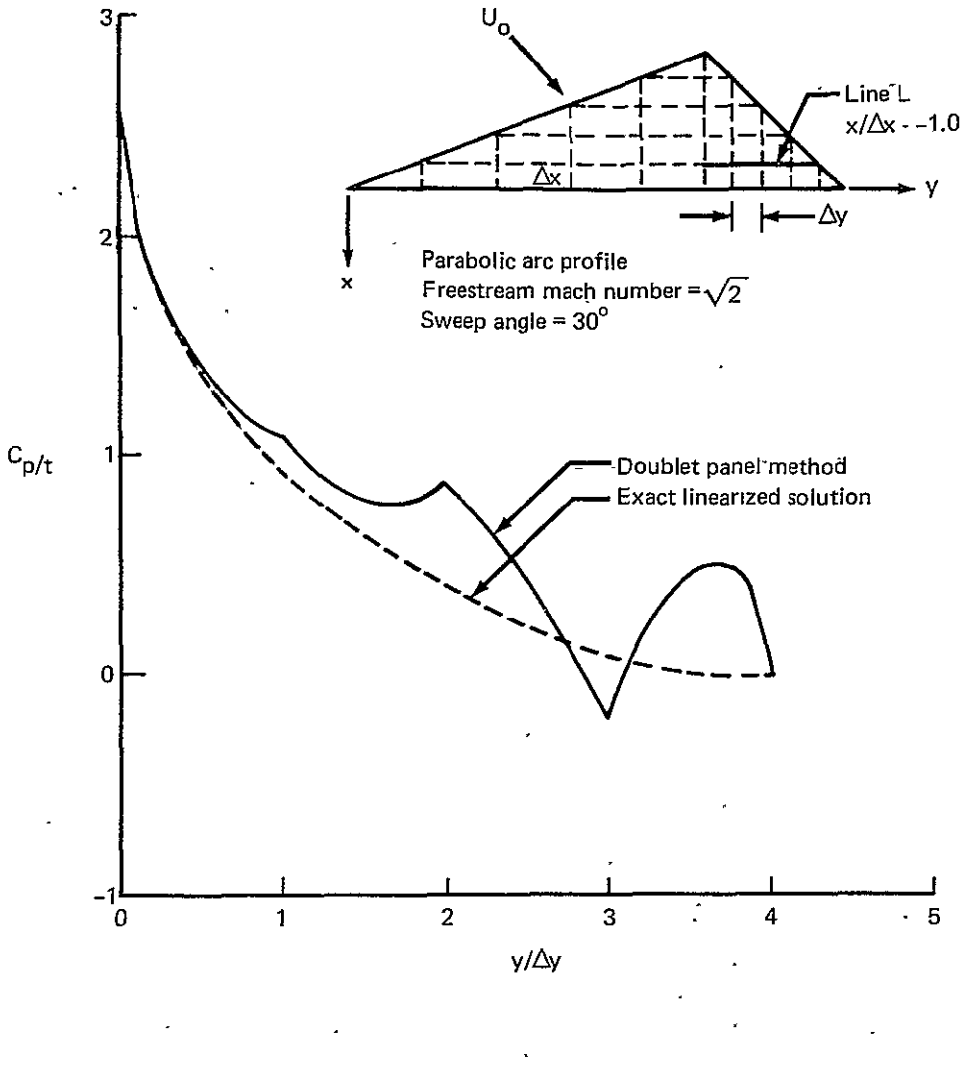

Figure 16.—Pressure Distribution Along Line L Downstream of Special Mach Line With Flat Plate Solution Superimposed on Doublet Panel Solution

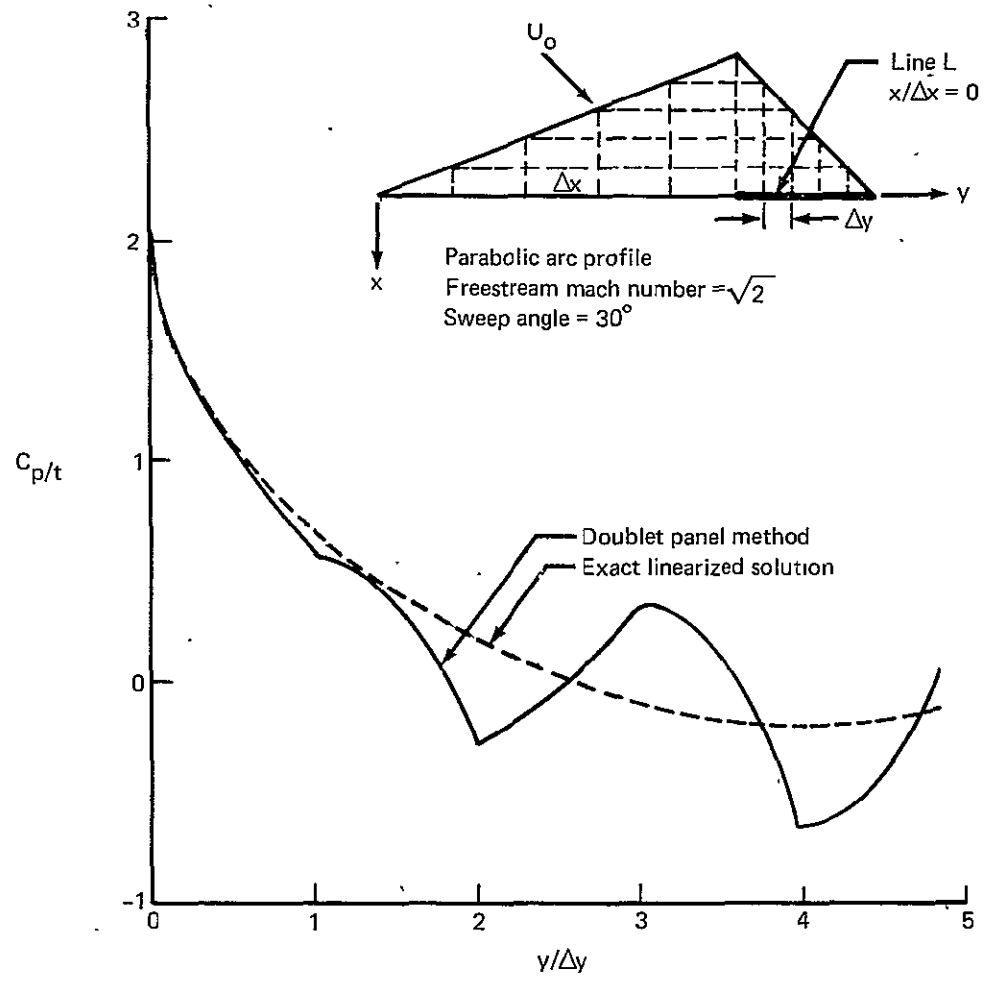

Figure 17.—Pressure Distribution Along Line L Downstream of Special Mach Line With Flat Plate Solution Superimposed on Doublet Panel Solution

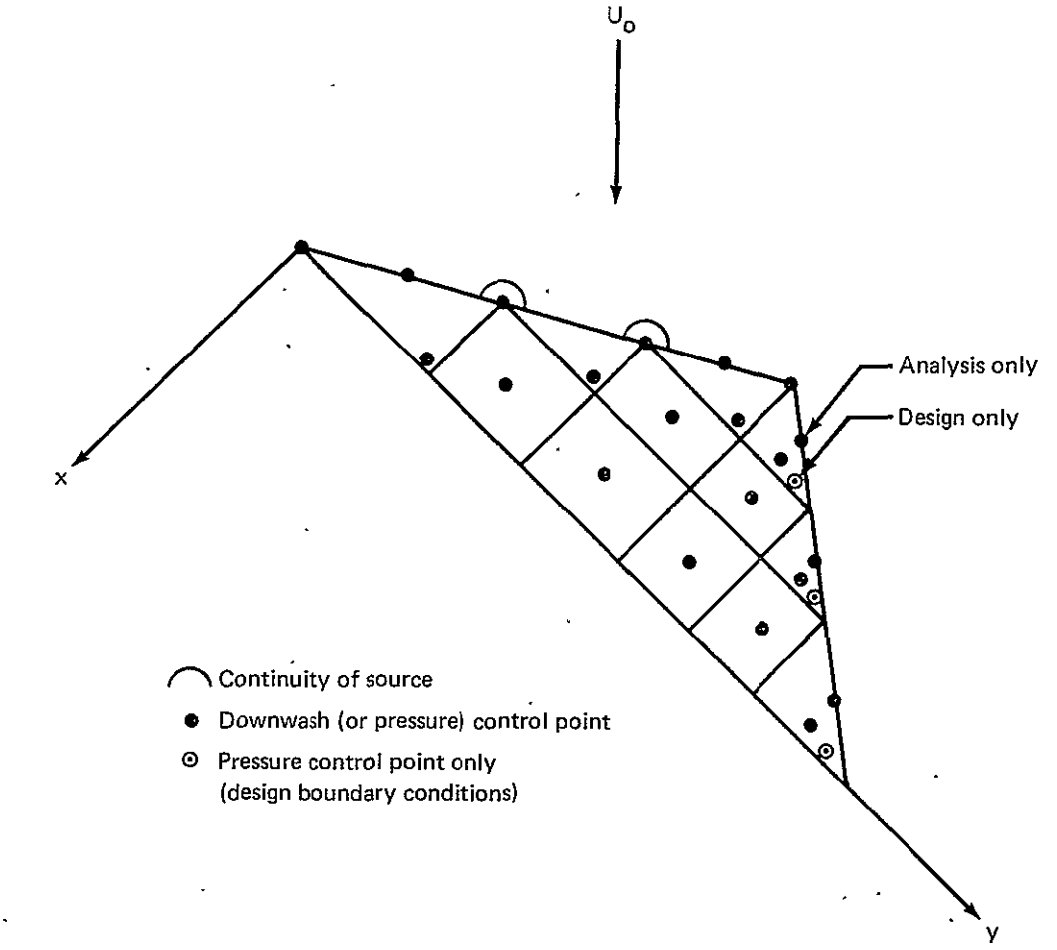

Figure 18.—Control Point Locations and Continuity Conditions for Source Mach Line Paneling

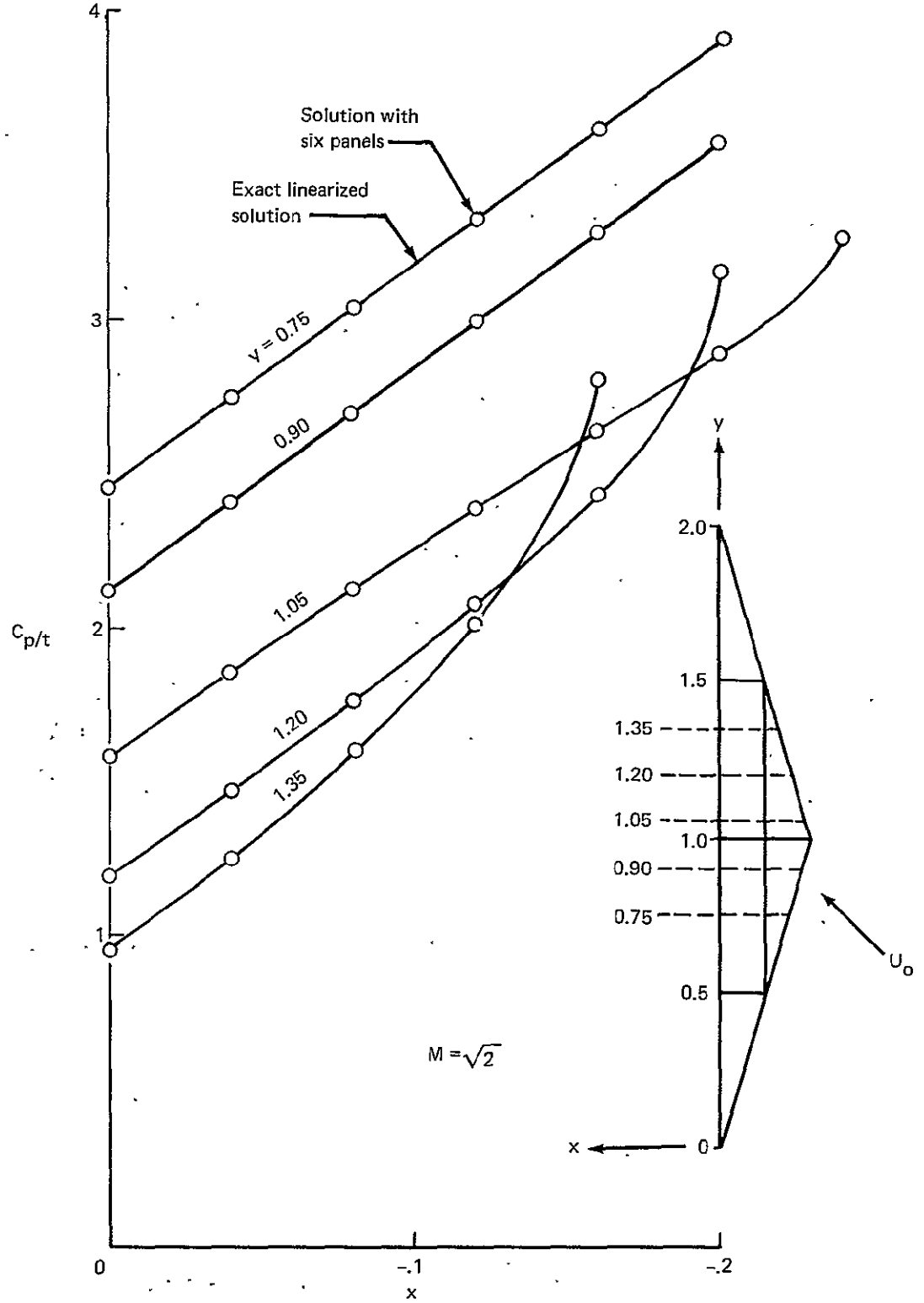

Figure 19.—Comparison of Pressure Distribution From the Source Mach Line Panel Method With the Exact Solution From Linearized Theory for Wing With Parabolic Arc Profile

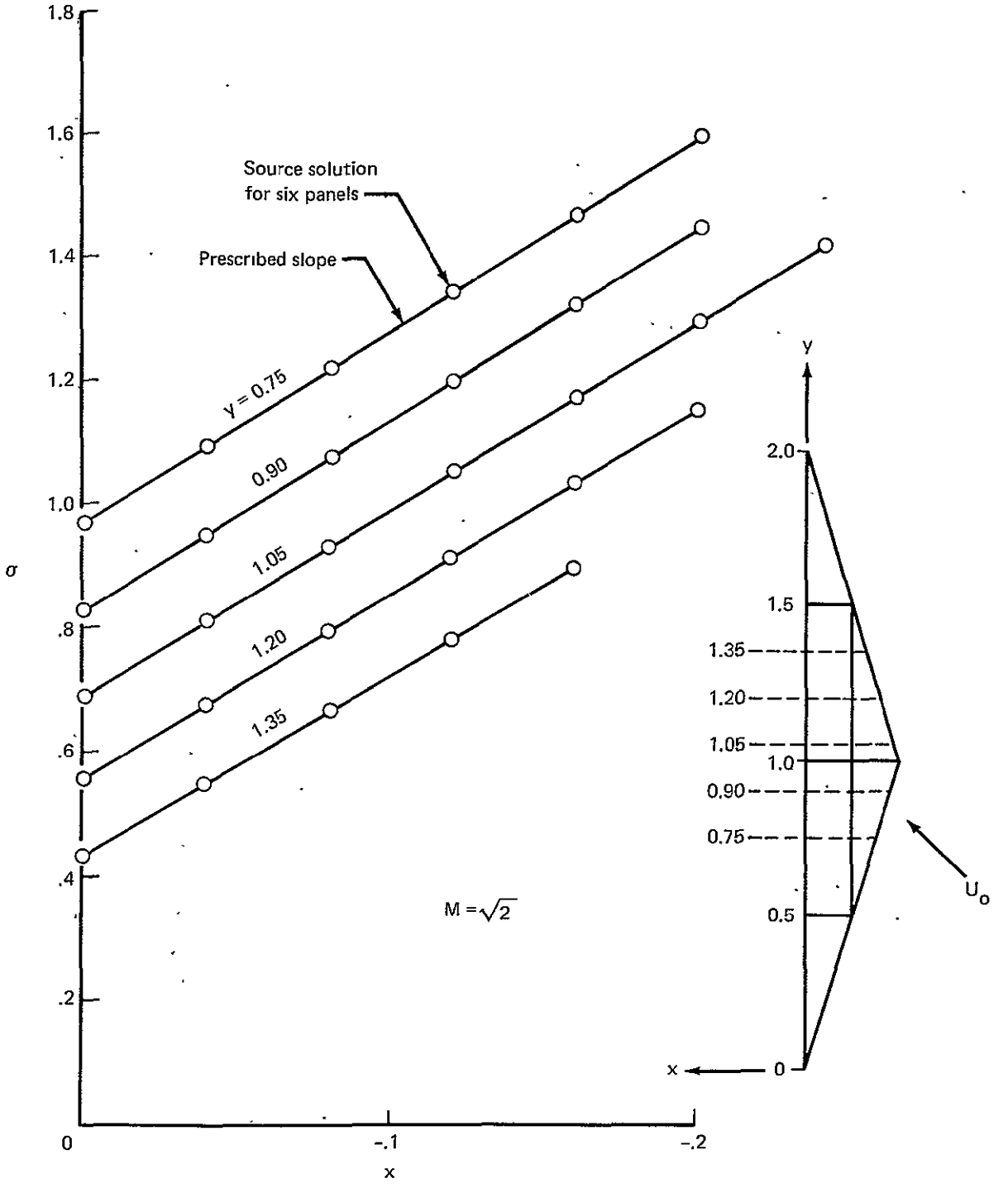

Figure 20.—Comparison of Source Distribution With Wing Slopes

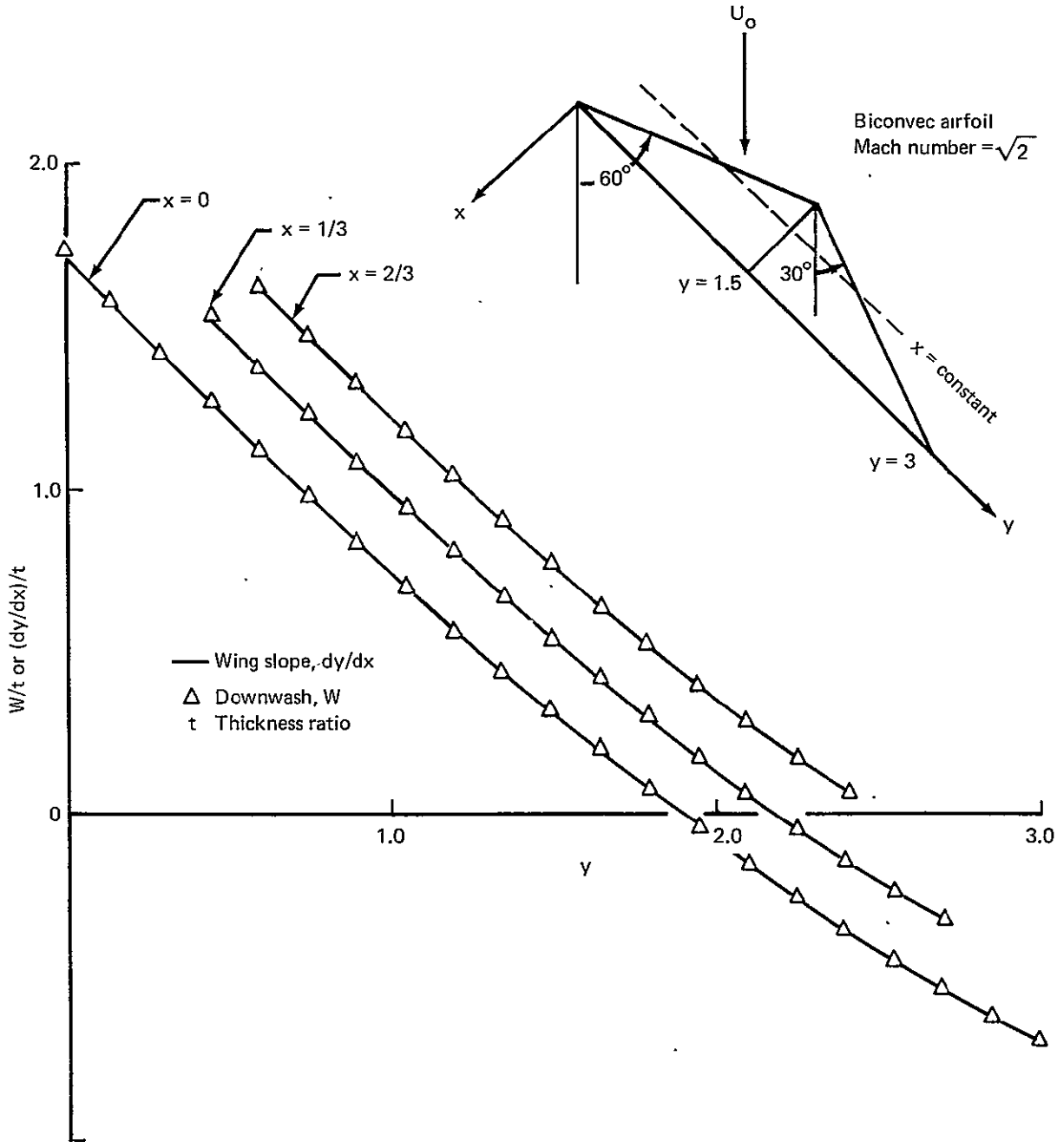

Figure 21.—Comparison of Downwash From Supersonic Source Design Panel Method With Actual Wing Slopes

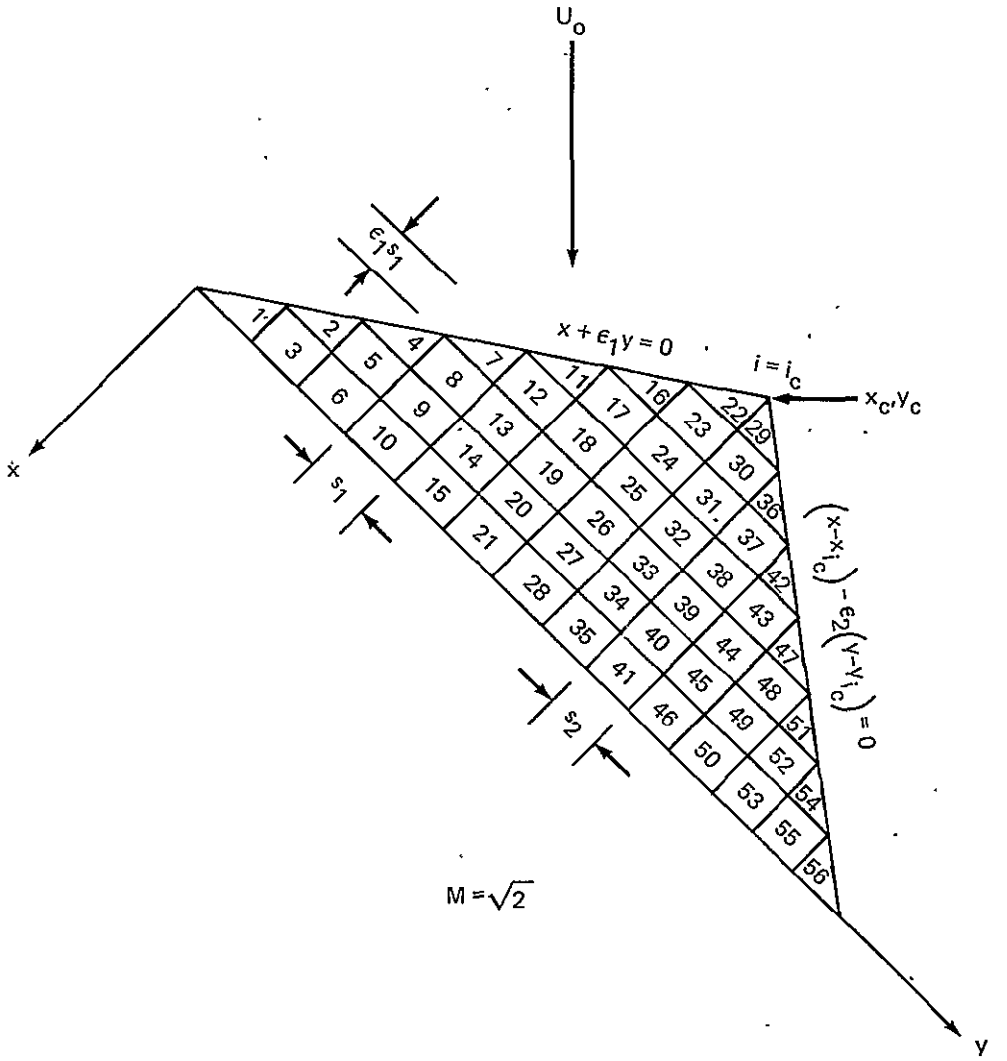

Figure 22.—Schematic Paneling on Wing Used to Test Mach Line Panel Methods

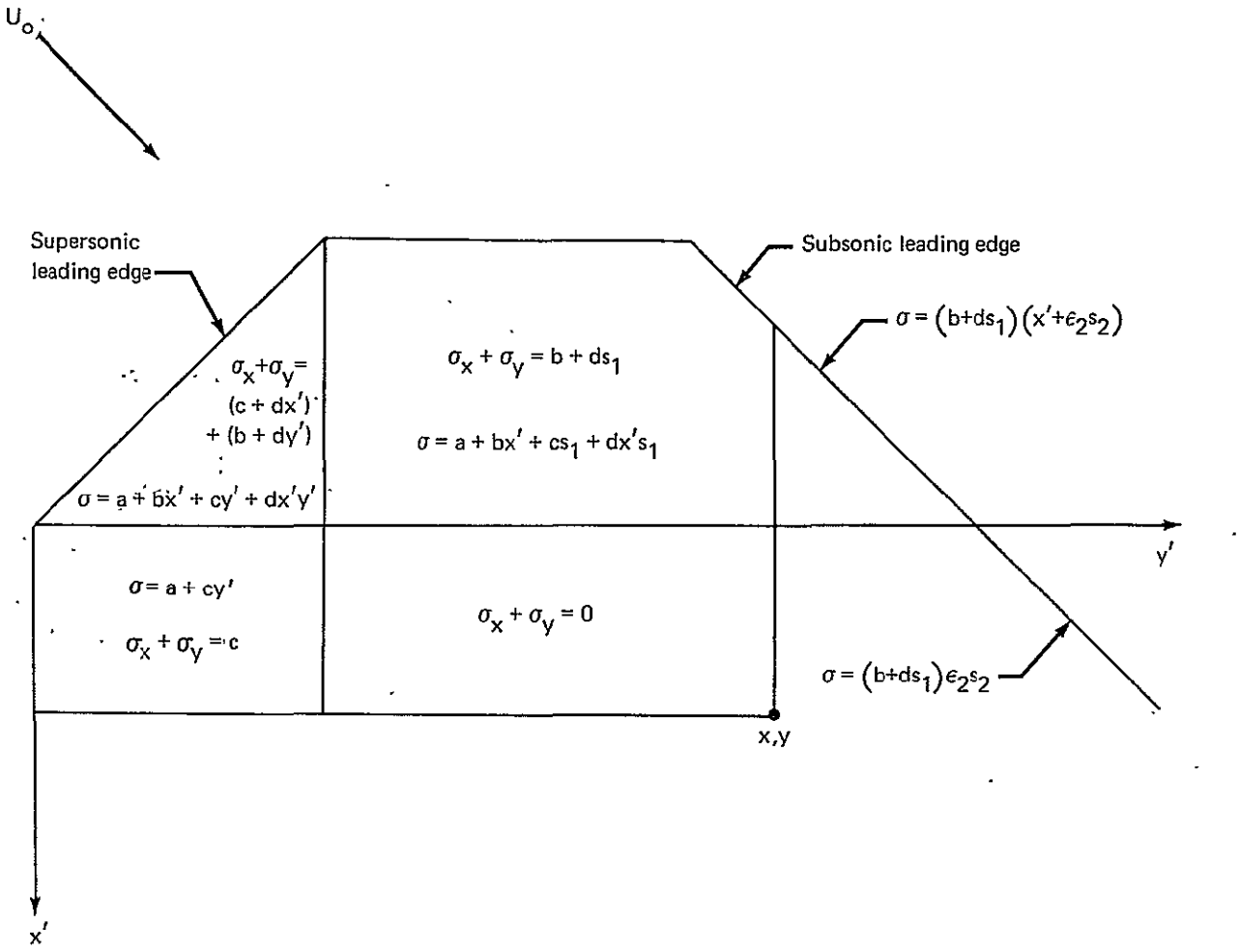

Figure 23.—Region of Integration for Leading Edge Source Panel With the Zone of Dependence Terminated by a Subsonic Leading Edge

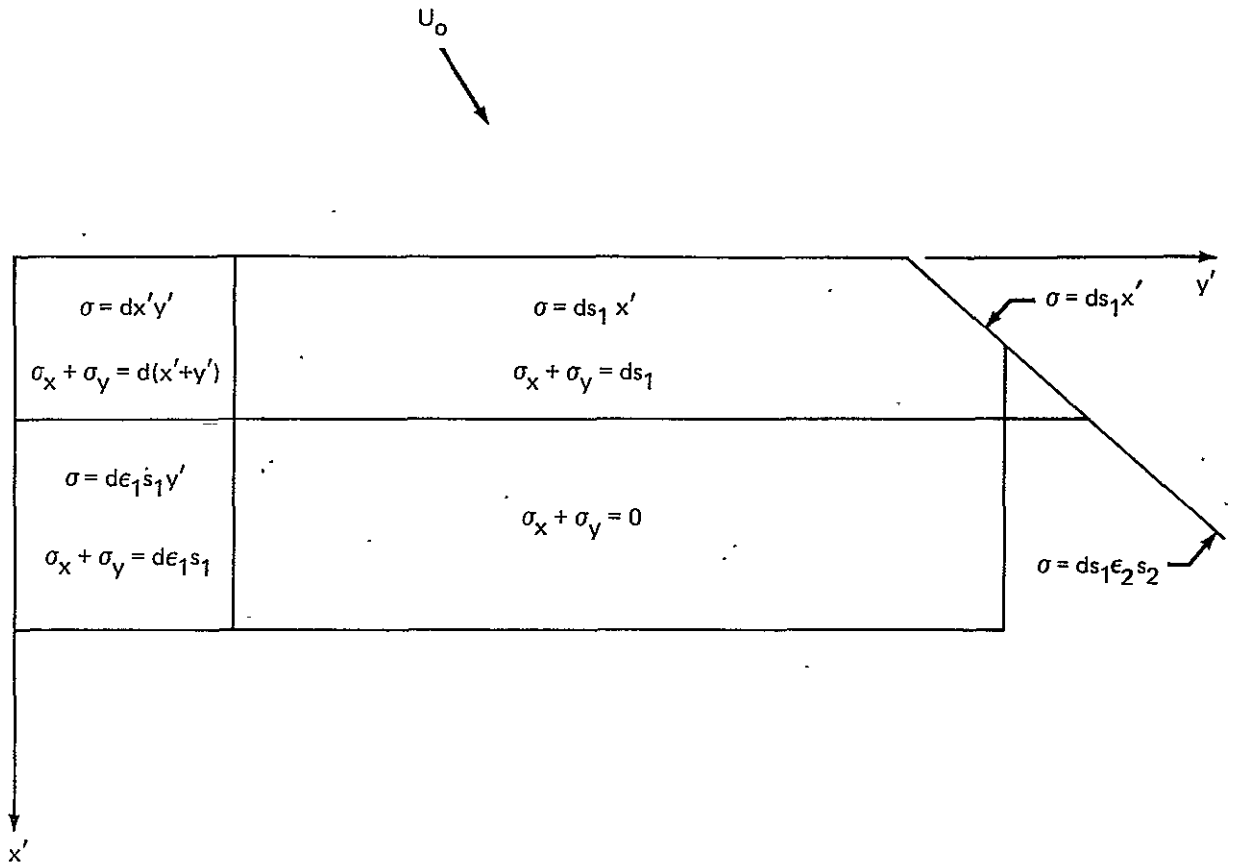

Figure 24.—Region of Integration for Interior Source Panel With the Zone of Dependence Terminated by a Subsonic Leading Edge